Tumor Microenvironmental Control of Metastasis: Effects of the Immune Cells and Physical Forces on Cell Migration

By

Ran Li

B.S.E. Chemical Engineering (2010), University of Michigan

Submitted to the Department of Biological Engineering on January 15, 2017
in Partial Fulfillment of the Requirements for the Degree of

Doctor of Philosophy in Biological Engineering

at the

MASSACHUSETTS INSTITUTE OF TECHNOLOGY

January 2017 [February 2017]

Author Signature redacted
Department of Biological Engineering

Certified by Signature redacted
Roger D. Kamm
Professor of Mechanical Engineering
Professor of Biological Engineering
Thesis Supervisor

Accepted by Signature redacted
Forest M. White
Professor of Biological Engineering
Graduate Officer

Tumor Microenvironmental Control of Metastasis: Effects of the Immune Cells and Physical Forces on Cell Migration

By

Ran Li

Submitted to the Department of Biological Engineering on January 15, 2017 in Partial Fulfillment of the Requirements for the Degree of Doctor of Philosophy in Biological Engineering

Abstract:
Metastasis, which accounts for 90% of cancer deaths, critically depends on the ability of cancer cells to migrate through the dense extracellular matrix (ECM) surrounding the solid tumor. Recent advances in cancer biology have revealed that non-cancerous cells and biophysical forces in tumor microenvironment can influence metastasis. Specifically, macrophage, one of the most abundant tumor-associated stromal cell types, has been shown to assist cancer cell invasion. However, exactly how macrophages affect the different aspects (e.g. speed and persistence) of cancer cell migration, especially in 3D ECM that mimics the *in vivo* tumor microenvironment, remains largely unknown. In addition to macrophages, elevated interstitial flow (the flow of tissue fluid) within the tumor tissue has been shown to influence cancer cell and fibroblast migration. Nevertheless, the effects of this tumor-associated biophysical force on macrophages are still unknown.

In this thesis, we first explored how macrophages control the subtle details (speed vs. persistence) of cancer cell migration. Using a microfluidic migration assay, we found that macrophage-released TNFα and TGFβ1 enhance cancer cell migration speed and persistence in 3D ECM in an MMP-dependent fashion via two distinct pathways. Specifically, macrophage-released TGFβ1 enhances cancer cell migration speed via the induction of MT1-MMP expression in cancer cells. In contrast, macrophage-released TNFα and TGFβ1 synergistically enhance cancer cell migration persistence via the induction of NF-κB-mediated MMP1 expression. Therefore, these results suggest that macrophages control different aspects of cancer cell migration in 3D differently, and both TNFα and TGFβ1 released by macrophages need to be simultaneously inhibited to effectively limit macrophage-assisted cancer cell metastasis.

In a separate study, we investigated how tumor-associated interstitial flow (IF) affects macrophage migration and protein expression. We discovered that IF promotes macrophage migration in 3D ECM via the flow-induced activation of FAK and Akt. Interestingly, IF also directs the preferential migration of macrophages against the direction of flow (upstream). Moreover, we show that IF polarizes macrophages toward a pro-metastatic M2 phenotype via integrin/Src-dependent STAT3/6 activation. Since IF emanates from tumor core to stromal tissue surrounding the tumor, these results suggest that IF can promote metastasis by not only recruiting macrophages from stroma into tumor, but also enhancing the M2 polarization of macrophages in the tumor microenvironment.

Keywords: Tumor Microenvironment, Macrophages, Interstitial Flow, Migration, and Polarization

Thesis Committee:
Thesis advisor: Roger D. Kamm, Professor of Mechanical and Biological Engineering, MIT
Thesis Chair: Douglas A. Lauffenburger, Professor of Biological Engineering, MIT
Michael T. Hemann, Professor of Biology, MIT

Acknowledgement

I would first like to acknowledge Professor Roger Kamm, my thesis advisor, for his continuous support and infinite patience. It has been truly a pleasure to work with Roger, who continues to inspire me with his dedication to research, commitment to teaching, and humility despite renown. Working with him, I learned not only how to be a good scientist, but also a member of the scientific community. He is a role model for me, and I hope I can use the lessons I learned from him in my future endeavors.

I would also like to thank my thesis committee members, Professor Douglas Lauffenburger and Professor Mike Hemann. Every discussion I had with them has enlightened me and pushed me to become a better researcher. They have helped me tremendously in shaping my thesis research. In addition, I would like to thank Professor Richard Hynes and Jess Hebert for their expertise with *in vivo* experiments.

I owe special thanks to Dr. Ioannis Zervantonakis and Dr. William Polacheck. Their works on cancer cell intravasation and migration had provided foundation for my thesis research. I could not have completed my dissertation without their training, helpful discussion, and scientific insights. I would also like to acknowledge Tara Lee and Hao Xing, two outstanding MIT BE undergraduate students whom I had privilege to work with. I cannot overstate how much their hard work has contributed to the completion of my Ph.D.

The completion of this Ph.D. thesis will not have been possible without the supports from the past and present members of the Kammsters. I especially like to thank Dr. Sebastien Uzel, Dr. Joy Rimchala, Dr. Jessie Jeon, Dr. Levi Wood, and Dr. Vernella Vickerman for introducing me to the lab and training me in the experimental and research techniques. Special gratitude is also extended to Jordy Whisler, Vivek Sivathanu, and Jean Carlos Serrano, my office-mates who have cheered me on and made NE47-315 a second home to me. I would also like to thank Dr. Emad Moeendarbary and Dr. Michelle Chen for the insightful discussion on science, experiments, and life in general. I have truly learned a lot from them. I would also like to express my gratitude to Professor Shuichi Takayama and Dr. Nicholas Douville, whom I had privilege to work with when I was an undergraduate student at the University of Michigan, for giving me opportunity to work in their lab and introducing me to the field of microfluidics.

Finally, I would like to thank my parents, who had sacrificed immensely to uproot themselves from China so that I can get the best education in the world. Without their constant encouragement and emotional supports, I could not have completed this thesis. I would also like to thank Jamin Liu, my girlfriend, for always standing with me and encouraging me through the tough times. Our frequent "food trips" to the NYC have been a welcome distraction and reality check.

This thesis work is supported by funding from National Science Foundation Graduate Research Fellowship and Koch Institute Graduate Research Fellowship.

Table of Contents

Chapter 1. Introduction

1.1: Tumor Microenvironment and Metastasis

Cancer represents a group of complex and systemic diseases that are characterized by uncontrollable growth and dissemination of abnormal, cancerous cells (1). Metastasis, which is the dissemination of cancer cells from the primary tumor site to a secondary tumor site, accounts for 90% of cancer deaths (1–3). Although various treatment strategies have been devised to control tumor growth, therapeutic targeting and management of metastasis remain elusive. Tumor metastasis includes a cascade of events that is widely thought to begin when epithelial-like cancer cells are transformed from an immobile, cobblestone-shaped, epithelial phenotype to a highly motile, spindle-shaped, mesenchymal phenotype. This transformation is called epithelial-to-mesenchymal transition (EMT), and it marks an important step in cancer cells gaining ability to migrate from the primary tumor site. Following EMT, cancer cells penetrate the basement membrane surrounding the tumor tissues, and migrate into the tumor-associated stroma. Once inside the stromal tissues, cancer cells can transmigrate through tumor-associated blood vessels, a process termed intravasation. Intravasation is a crucial step in metastasis, as it allows cancer cells to gain access to the circulation. In the blood vessels, cancer cells will disseminate throughout the body, and if they survive, extravasate, or transmigrate, through the blood vessels into the tissues of secondary organ. Following extravasation, these metastasized cancer cells can colonize the secondary sites and develop into a metastatic tumor (Fig. 1.1) (4).

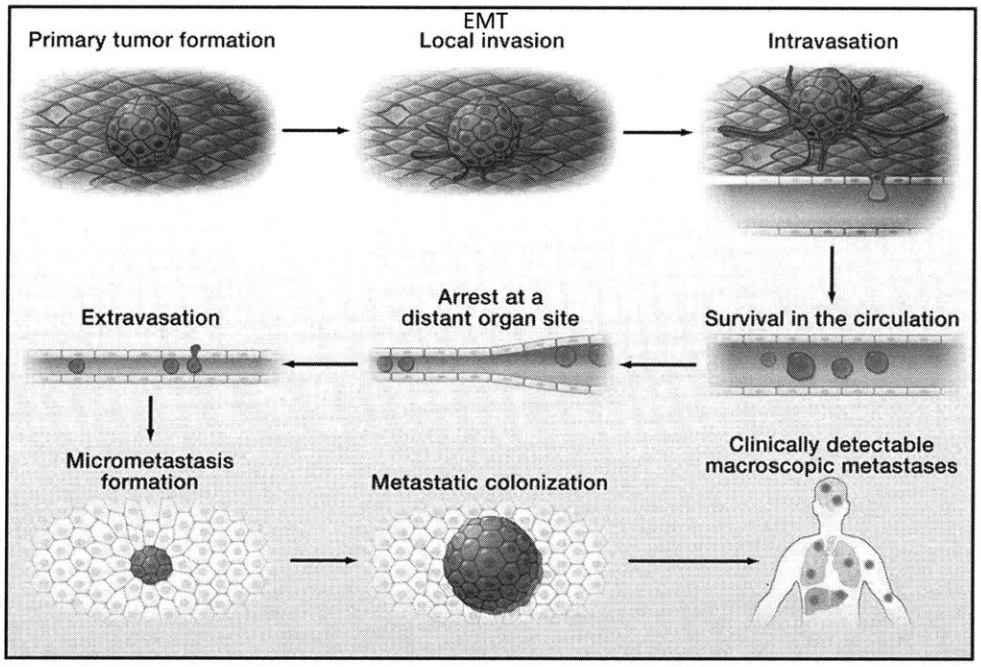

Fig.1.1: Schematic of the metastatic cascade. The cascade begins as the primary tumor forms. Cancer cells in the tumor can undergo EMT, leading to the invasion of cancer cells into the

stroma surrounding the tumor. As cancer cells migrate, they can enter the blood stream through intravasation. The cancer cells that survive in the blood stream can arrest at a distal organ and extravasate into the secondary organ site. After extravasation, these metastasized cancer cells colonize the secondary organ inside the body. Figure modified from (4).

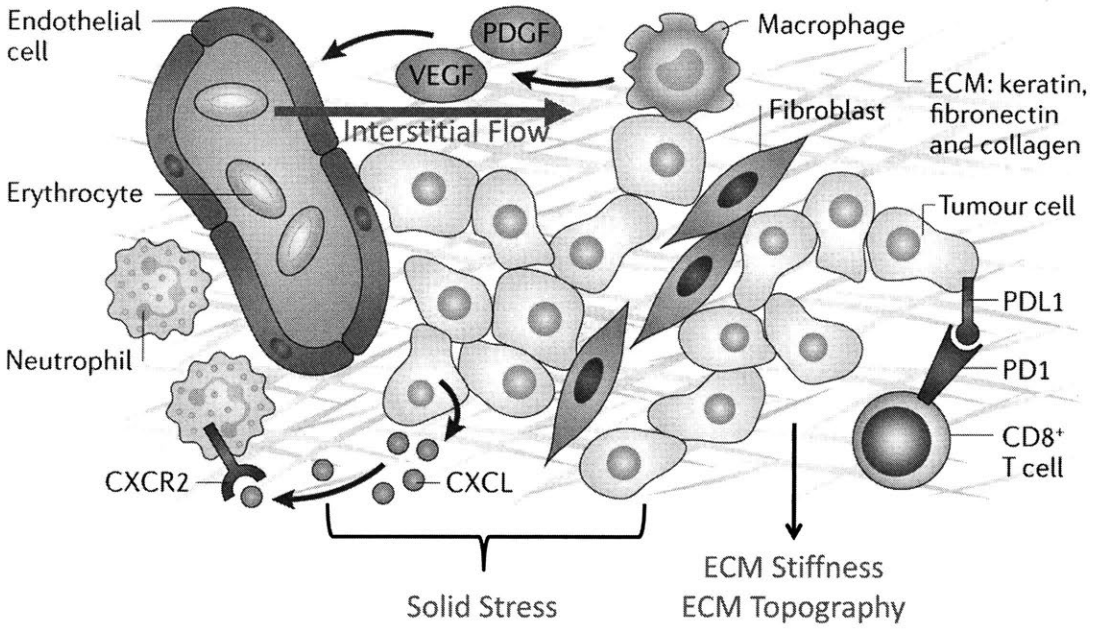

Fig. 1.2: Schematic of tumor microenvironment. The tumor microenvironment is complex. It includes tumor-associate stromal cells (e.g. endothelial cells, fibroblasts, macrophages, neutrophils, and T cells), tumor-associated ECM (e.g., fibronectin and collagen), and tumor-associated biophysical forces (e.g. elevated interstitial flow and increased matrix stiffness). All of these factors could affect tumor progression and metastasis. Modified from (5).

The reason that the development of anti-metastasis medicine remains challenging results from the fact that metastasis is a complex process that depends not only on cancer cells themselves, but also on the environment in which they reside. In fact, recent advances in cancer biology have revealed that the interaction between cancer cells and their surrounding environment, particularly at the primary tumor site, is crucial for tumor progression and metastasis (6–8). This environment, collectively called the tumor microenvironment, consists of tumor-associated stromal cells, extracellular matrix (ECM), and various biophysical forces (7, 9) (Fig. 1.2). It has been known that tumor-associated stromal cells, including fibroblasts, macrophages, and endothelial cells, contribute to malignancy (6–8). For example, tumor-associated blood vessels deliver nutrients to the cancer cells. In addition, these blood vessels also serve as a route of metastatic dissemination (10). Fibroblasts, on the other hand, have been shown to enhance cancer cell growth and migration. Tumor-associated fibroblasts can secrete stromal cell-derived factor-1 (SDF-1) to promote tumor growth, transforming growth factor-β (TGF-βs) to promote EMT, and hepatocyte growth factors (HGFs) to promote cancer cell drug resistance (11). Besides these stromal cells, a myriad of biophysical

forces in the tumor microenvironment can also promote tumor metastasis. For instance, tumor tissues are ~10-fold stiffer than the normal tissues due to the aberrant ECM homeostasis, a result of tumor-associated fibroblasts depositing an excess of collagen I (12, 13). This elevated tissue stiffness has been shown to promote EMT (14, 15), cell migration (16, 17), and proliferation (18). Moreover, bundling and alignment of ECM in the vicinity of the tumor tissue have been shown to create a matrix topography that favors cancer cell movement (19). Finally, elevated solid stress inside the tumor microenvironment, a result of the uncontrolled enlargement of tumor tissues, can affect cancer cell growth and metastasis (20).

Macrophages are one of the most abundant stromal cell types in the tumor microenvironment, especially in breast tumor tissue (21). These immune cells have been shown to promote carcinogenesis (22–24), cancer progression (25, 26), and cancer cell dissemination (26–28). Specifically, these macrophages could increase cancer cell invasion through the release of growth factors, cytokines, and matrix metalloproteases (MMPs) (26, 29, 30). Besides tumor-associated macrophages, one of the key biophysical forces that promotes metastasis is interstitial flow (31, 32). It has also long been documented that elevated interstitial flow exists inside many solid tumors such as breast carcinoma, colorectal carcinoma, and melanoma (33). This elevated interstitial flow is due to the increased permeability of tumor blood vessels and the collapse of tumor lymphatic vessels (33). Recent clinical data show that high interstitial flow correlates with poor prognosis (34, 35). Moreover, numerous *in vitro* data suggest that interstitial flow, via its effects on cancer cells and tumor-associated stromal cells, could enhance metastatic dissemination (36–38). Therefore, both tumor-associated macrophages and interstitial flow are significant factors in controlling the tumor microenvironment and metastasis. In the following sections, we will discuss these two key features of the tumor microenvironment in detail.

1.2: Role of macrophages in tumor metastasis

1.2.1: Macrophages in the tumor microenvironment

Macrophages are innate immune cells that reside in nearly every part of the body. These cells are incredibly plastic, able to adopt a diverse array of phenotypes based on the stimulus they encounter in their microenvironment. These functionally diverse cells are crucial in many important biological processes, including immunity against diseases, tissue homeostasis, and organ development. Moreover, different types of macrophages reside in different tissues. For instance, Kupffer cells are resident macrophages of liver, and they are functionally different from microglia, which are resident macrophages of the brain. These tissue resident macrophages maintain tissue homeostasis, and they are the first-line of defense against foreign bodies such as bacteria and viruses. In addition to the resident macrophages, additional macrophages can be called upon to the site of injury or infection in the form of monocytes. Once the monocytes are recruited to the tissue, they can differentiate into macrophages (39, 40).

Depending on their microenvironment, macrophages can polarize to a classically activated (M1) or an alternatively activated (M2) phenotype (Fig. 1.3) (41). M1 phenotype is pro-inflammatory, and macrophages adopt this phenotype in response to infection or injury to the tissues. These M1 macrophages secrete pro-inflammatory cytokines, such as interleukin-6 (IL-6), tumor necrosis factor-α (TNFα), and interleukin-1 (IL-1), to promote inflammation and immune responses. They also produce reactive nitrogen and oxygen species (RNS and ROS) to combat pathogens. *In vitro*, M1 macrophages can be obtained by treating naïve, unpolarized (M0) macrophages with lipopolysaccharide (LPS) or interferon-γ (IFN-γ). In contrast, M2 polarization results from stimulating M0 macrophages with cytokines IL-4, IL-10, or IL-13. Once adopting an M2 phenotype, macrophages will secrete anti-inflammatory cytokines, such as IL-10 and TGFβs. Indeed, M2 macrophages are found to participate in tissue repair, wound healing, and tissue hemostasis. Finally, it should be noted that while M1 and M2 classification of macrophage phenotypes is popular, it represents the extreme states of their polarization. As such, in realty, macrophages inside the body usually adopt a spectrum of phenotypes that is defined by these two extreme states (41–43) (Fig. 1.3).

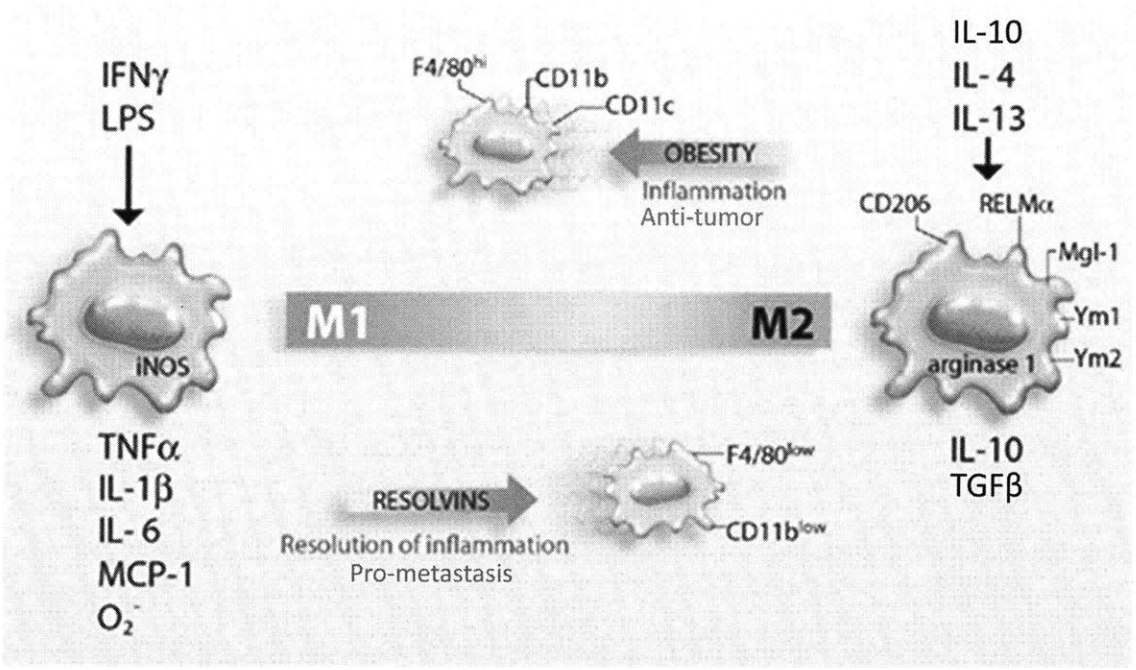

Fig. 1.3: Distinct polarization of macrophages. Macrophages can be polarized to a pro-inflammatory M1 state upon IFNϒ/LPS stimulation or anti-inflammatory M2 state upon IL-4/IL-13 treatment. M1 macrophages have enhanced expression of iNOS, and they secrete TNFα, IL-1β, and IL-6. In contrast, M2 macrophages have enhanced expression of CD206, Ym1, and arginase I. They secrete IL-10 and TGFβs. Modified from (44).

The presence of macrophages in primary tumor tissues has been documented for many years. However, only recently has the importance of macrophages in tumor malignancy been appreciated. Recent clinical data show that macrophages are the

predominant immune cells that reside in the tumor mass (9, 45, 46). In addition, macrophages in the tumor tissues generally adopt an M2 phenotype. Indeed, the presence of M2 macrophages in the primary tumor site has been demonstrated to correlate with poor prognosis in breast, prostate, and kidney cancer (47) (Fig. 1.4A). Macrophages are especially important to breast cancer malignancy since they could constitute about half of breast tumor tissue (48). The importance of macrophages in tumor progression has also been shown in mice studies. Significantly, polyoma middle T (PyMT) mice that were depleted of macrophages showed a delayed tumor progression and metastasis (47, 49). Conversely, overexpression of CSF-1 (a chemoattractant for macrophages) in mice tumor promoted the infiltration of macrophages and tumor progression (26). Finally, in contrast to M2 macrophages, M1 macrophages are generally thought to promote tumor suppression by activating anti-tumor immunity. Hence, the dual roles that macrophages (M1 vs. M2) play in tumor progression make them attractive targets for anti-tumor therapy.

A) Clinical outcome of macrophage infiltration

Favorable prognosis	Reference	Poor prognosis	Reference
Stomach	(59)	Breast*,†	(15, 37)
Colorectal	(72)	Prostate*	(35)
Melanoma	(73)	Endometrial*	(36)
		Bladder*,†	(34)
		Kidney*	(17)
		Esophageal Superficial†	(50)
		Squamous cell carcinoma*	(33)
		Malignant uveal melanoma*	(31)
		Follicular lymphoma	(75)

*Correlation with increased tumor angiogenesis.
†Correlation with increased involvement of local lymph nodes. No correlation with survival was found in colon carcinoma (70), high-grade astrocytomas (71), lung carcinoma (74), or cervical carcinoma (76).

B) Localization of Macrophage in tumor

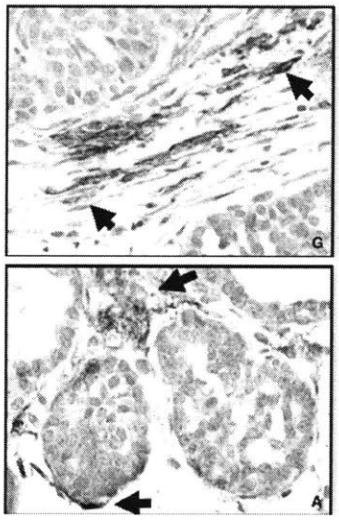

Fig. 1.4. Clinical outcomes of macrophage recruitment into tumor, and the localization of macrophages in the tumor microenvironment. (A) The recruitment of macrophages into tumor tissues results in poor prognosis for most types of tumors, including breast tumor, prostate tumor, and melanoma. (B) Tissue section staining (blue=cancer cells, brown=macrophages) obtained from mice showing that macrophages tend to reside in the tumor-associated stroma, especially at the tumor-stromal boundary. Modified from (47).

Macrophages in tumor microenvironment originate from blood monocytes (50, 51). Circulating blood monocytes are recruited to primary tumor by various growth factors (CSF-1) and chemokines (CCL-2, CCL-8, CXCL8) released by tumor cells (47, 50). At the primary tumor site, these monocytes will differentiate into macrophages. Moreover, cytokines secreted by cancer cells can educate these macrophages to adopt an M2 phenotype. Some *in vivo* studies have also reported that tumor-associated macrophages can proliferate at the tumor site (52, 53). Macrophages in primary tumor sites commonly reside in the area of tumor cell invasion, mostly at stromal-tumor

boundary (47, 54) (Fig. 1.4B). These macrophages secrete a variety of different growth factors, cytokines, reactive oxygen species, and MMPs that could promote malignancy. Specifically, macrophages secrete reactive oxygen and nitrogen species that enhance carcinogenesis (22, 26). In addition, macrophages release angiogenic factors (VEGFa, VEGFc, TNFα) that assist in the formation of tumor blood vessels, which provide cancer cells with nutrient and the route for escape from primary tumor site (26, 55, 56). Moreover, macrophages secrete proteases (MMP2, MMP9, MMP12, MMP7, uPA) that facilitate basement membrane breakdown. Furthermore, TGFβ released by macrophages can promote immune suppression by inhibiting the proliferation and activation of cytotoxic T cells, NK cells, and dendritic cells while enhancing the generation of anti-inflammatory T_{reg} cells (57). Finally, macrophages release various growth factors and cytokines (TNFα, EGF, FGF, HGF, TGFβs) (26, 29, 45). These macrophage-released growth factors and cytokines have been speculated to assist cancer cell migration and intravasation (Fig. 1.5). A few experiments have directly demonstrated that macrophage-released EGF could increase cancer cell invasion and intravasation (28, 30, 58). Indeed, an EGF/CSF-1 paracrine loop was recently identified as an important interaction between cancer cells and macrophages that contributes to metastasis. Specifically, it was discovered that in certain tumors, cancer cells secrete CSF-1 to attract macrophages, while macrophages secrete EGF to promote cancer cell invasion and intravasation (30). Despite this discovery, more studies are needed to gain a detailed understanding of how other macrophage-released molecules, such as TNFα and TGFβ1, affect cancer cell migration, especially the temporal dynamics of migration. In the next section, we will discuss the dynamics of cell migration in detail.

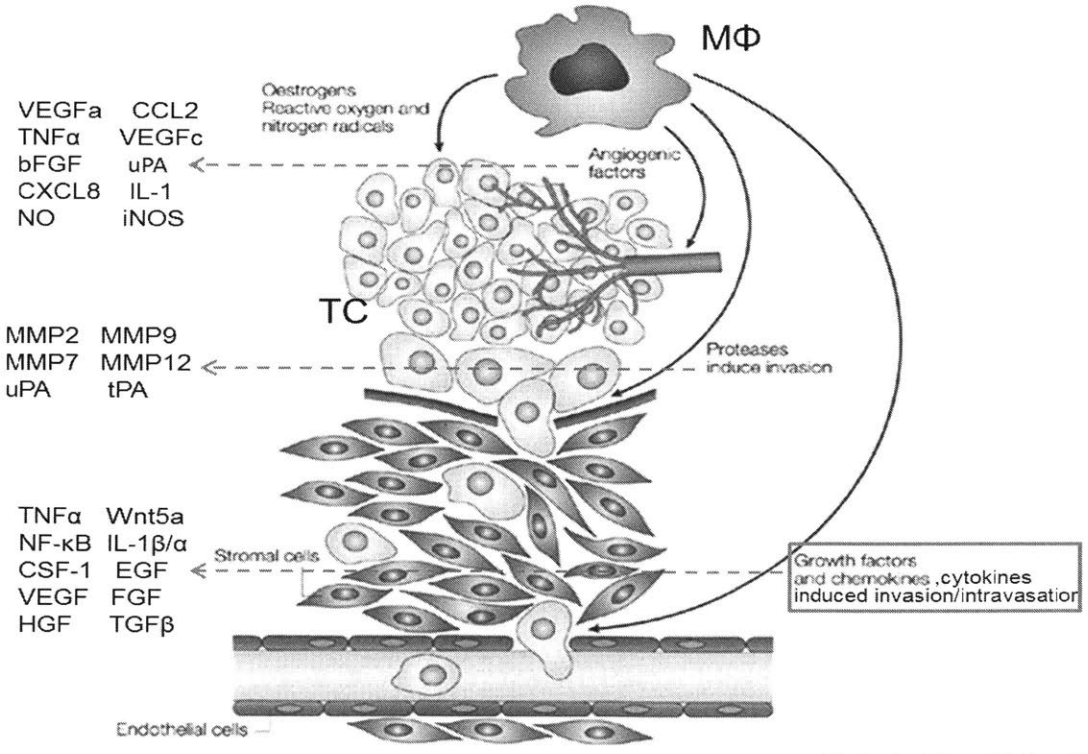

(Adapted from Pollard 2004)

Nature Reviews | Cancer

Fig. 1.5 Macrophages contribute to tumor progression and metastasis via various pathways. Macrophages release reactive oxygen and nitrogen species to enhance carcinogenesis, and secrete angiogenic factors (e.g. VEGF, TNFα) to promote tumor angiogenesis. Macrophages also produce a myriad of MMPs, growth factors, and cytokines to induce cancer cell invasion and intravasation. Modified from (59).

1.2.2: Cancer cell migration -- the importance of 3D migration and the dynamics of migration

The migration behavior of cancer cells is a key determinant of tumor metastasis. It dictates how cancer cells break through basement membrane and invade the tissue surrounding the primary tumor. It also determines how cancer cells transmigrate through the tumor endothelium and enter the blood stream. All these processes are important components of metastatic cascade (60). To study cancer cell migration, many researchers employ the transwell migration assay, an assay in which cancer cell motility is assessed as the number of cells that transmigrate through a plastic 2D membrane (60, 61). This 2D transwell assay cannot accurately mimic physiological conditions, as it fails to account for the existence of 3D ECM in the tumor microenvironment (62, 63). In addition, various reports indicate that there are differences between cancer cell movement in 2D and 3D (61, 63–65). For example, FAK is absolutely crucial for an effective 3D cell migration, while the defect in the migration of FAK-null cells on 2D substrate can be compensated by over-expressing other cell migration machineries (66). Moreover, it has been discovered that cell migration speed and persistence on 2D substrate do not correlate with the speed and persistence of migration in 3D ECM (64).

Transwell experiments also have the disadvantage of being an end-point assay. With this approach, only the end-point readout of the number of cancer cells that have transmigrated through the membrane can be obtained. Hence, the temporal dynamics of cell migration, such as how fast (speed) or how persistently (persistence) the cell moves, cannot be captured using this assay (63). These subtle details of migration dictate the metastatic potential of cancer cells. For example, a stimulus that increases both cancer cell migration speed and persistence can greatly enhance metastasis. More importantly, speed and persistence can be modulated independently of one another by a single stimulus. For example, inhibiting β1 integrin has been shown to decrease cancer cell migration speed but have no effect on persistence (67). On the other hand, interstitial flow can increase cancer cell migration persistence without altering the speed of migration (36). Finally, a stimulus can affect speed and persistence of migration differently when cells are cultured on 2D substrates compared to in 3D matrix. Specifically, EGF has been shown to increase cancer cell migration speed and decrease persistence when cells are migrating on 2D surfaces. However, this same growth factor enhances both cancer cell migration speed and persistence when cells are cultured in 3D ECM (68). Since these dynamics are important characteristics of cell migration and they could be influenced independently of one another, a detailed quantification of these dynamics is needed to gain a deeper insight into cancer cell migration (69–71).

Finally, it is now well-appreciated that cell heterogeneity is an important aspect of metastatic diseases (64, 71). It has been shown that different subpopulations of cancer

cells within the tumor contribute to tumor progression and metastasis differently. Indeed, cancer cell migratory behavior can vary greatly between different cells in the same population. Hence, transwell assays, which can only produce an averaged migration statistic for the entire population, often fail to reveal important subpopulation variation in cancer cell migration (69). Therefore, to address these disadvantages of the transwell assay, we have to assess 3D cancer cell migration dynamics and any heterogeneity in these dynamics by using a microfluidic 3D migration assay.

1.2.3: The effects of macrophages on cancer cell migration -- possible roles of TNFα and TGFβ1

Besides EGF, macrophages in the tumor microenvironment also secrete a large amount of TNFα and TGFβ1 that are speculated to affect cancer cell migration through a 3D ECM (26, 72). TNFα is a cytokine that is predominantly produced by monocytes/macrophages (73, 74), such as Raw 264.7 macrophages, primary murine bone marrow-derived macrophages (BMDM), and primary monocyte-derived macrophages (MDMΦ) (75, 76). In addition, previous reports have shown that co-culture of macrophages with cancer cells increases the macrophage expression of TNFα (72). TNFα is now known to be a major contributor of cancer inflammation and progression (77). Several *in vivo* studies have revealed that skin cancer cannot develop in mice lacking TNFα. Moreover, recombinant TNFα treatment could lead to liver metastasis in mice (78). These results have led researchers to speculate that TNFα can promote cancer cell growth and invasion. Indeed, *in vitro* studies revealed that exogenously supplied TNFα could increase the motility of many types of breast and colon cancer cells (79). Specifically, treating MDA-MB-231 breast carcinoma cells with recombinant TNFα can increase cell migration as measured by a 2D wound healing assay and transwell assays (80–82). Furthermore, TNFRI, a major TNFα receptor, is expressed on many cancer cell types such as MDA-MB-231 cells (77, 83). Several recent reports have also evaluated the importance of TNFα in the promotion of cancer cell invasion by macrophages. Hagemann et al. showed that co-culture of macrophages with MCF7 breast cancer cells led to a TNFα-dependent enhancement of macrophage MMP expression and cancer cell invasion (29). In subsequent papers, they also found that co-culture of macrophages with MCF7 cells led to TNFα-mediated increases in NF-κB activity in MCF7 cells and Wnt 5a expression in macrophages (84–86). These results demonstrate that TNFα plays a major role in the crosstalk between cancer cells and macrophages. However, since these studies were performed using an end-point transwell assay, they could not reveal any information on how macrophage-released TNFα affects 3D migration dynamics (speed and persistence) of cancer cells.

A major TGFβ isoform secreted by macrophages, such as Raw 264.7 macrophages, BMDM, and MDMΦ, is TGFβ1 (87–91). Previous reports have revealed that co-culture of macrophages and tumor cells can lead to an up-regulation of TGFβ1 in macrophages (26, 54, 72). TGFβ1 is thought to be a pro-tumorigenic growth factor, as the existence of TGFβ1 in the breast tumor tissue has been linked to metastasis and poor prognosis (88, 92). Indeed, TGFβ1 is believed to be responsible for the initiation of epithelial-to-mesenchymal transition (EMT) and cancer cell invasion in tumor (93, 94).

Exogenously supplied TGFβ1 can induce EMT in pre-transformed epithelial cells. Exogenously supplied TGFβ1 could also increase the motility of metastatic cancer cells, such as MDA-MB-231 breast cancer cells, as measured by 2D wound-healing and transwell assays (95–97). In recent years, several groups have evaluated whether tumor-associated macrophages play a role in the induction of EMT. Their experiments showed that macrophages could promote the EMT of pre-transformed epithelial cells through their release of TGFβ1 (98, 99). However, whether macrophage-released TGFβ1 affects the 3D migration dynamics of metastatic cancer cells remains to be investigated. To address these gaps in knowledge, we used a microfluidic 3D migration assay, in combination with time-lapse imaging, to assess how macrophages affect the temporal dynamics of cancer cell 3D migration. We also evaluated how macrophage-released TNFα and TGFβ1 affect cancer cell migration dynamics. We hypothesized that macrophages can alter the dynamics of cancer cell 3D migration, and that this macrophage-assisted cancer cell migration is controlled by TNFα and TGFβ1 released by macrophages.

1.3: Role of interstitial flow (IF) in tumor metastasis

1.3.1: The origin of elevated interstitial flow in tumor tissue

Interstitial flow is the movement of interstitial fluid from the blood vessels, through porous extracellular matrix (ECM), and into the lymphatic vessels (100). Recent discoveries have demonstrated that heightened interstitial flow occurs inside neoplastic lesions (101, 102). This elevated flow is a consequence of over-permeabilized tumor blood vessels, which allow excess blood plasma to leak into the interstitial space and increase the total volume of interstitial fluid inside tumor tissue. Excess interstitial fluid needs to be drained into the lymphatic vessels. However, the growth of solid tumor causes the collapse of tumor lymphatic vessels, blocking the lymphatic drainage of interstitial fluid. This blockage causes the buildup of interstitial fluid pressure inside tumors, leading to a high pressure gradient and interstitial fluid flow (1-4 μm/s compared to 0.1 μm/s in normal tissue) from the center of the tumor to tissue surrounding the neoplastic lesions (32, 63, 103) (Fig. 1.6). The interstitial flow velocity is believed to be highest near the tumor margin (33). Since this is where tumor-associated macrophages tend to reside, we expect that these macrophages will experience an elevated IF *in vivo*. Therefore, it is important to study how this tumor-associated physical factor affects macrophages to gain a detailed understanding of the tumor microenvironment.

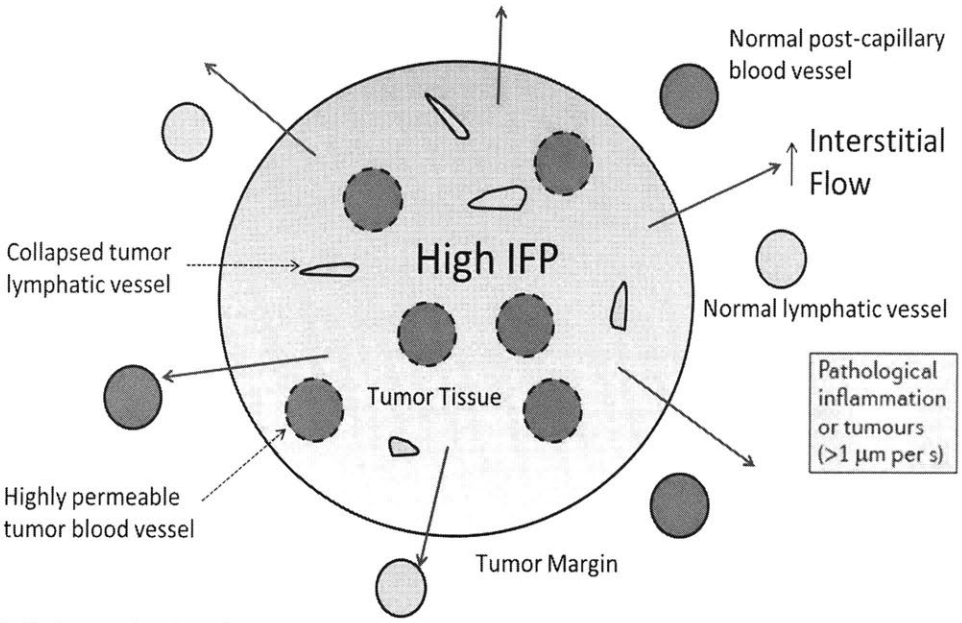

Fig. 1.6: Schematic showing the build-up of interstitial fluid pressure (IFP) inside the tumor tissue, resulting in the flow of interstitial fluid (blue arrow) from the center of the tumor tissue toward the tissue surrounding the neoplastic lesion. The interstitial fluid from the tumor will drain into normal post-capillary blood vessels and lymphatic vessels surrounding the tumor.

1.3.2: The effects of interstitial flow on cells

Much clinical data has demonstrated that elevated interstitial flow correlates with poor prognosis (34, 63). Recent studies have revealed that interstitial flow acts as a biomechanical factor that enhances progression of the neoplastic lesion by affecting the migration, morphology, and growth factor/cytokine expression of cancer cells and tumor-associated stromal cells. For example, Polacheck et al., using a microfluidic device, demonstrated that 3.0 μm/s interstitial flow leads to alignment and migration of MDA-MB-231 breast cancer cells against the direction of flow (upstream). They also found that this alignment and migration are mediated via the flow-induced phosphorylation of focal adhesion kinase (FAKs) (36). In a subsequent paper, the authors further demonstrated that this upstream migration results from the polarization of cancer cell migration machinery against the flow. Specifically, they show that interstitial flow produces a tension on the integrins located at the upstream face of the cells, which results in the activation of integrin and subsequent localization of vinculin, FAK, and paxillin at the upstream facing membrane (Fig. 1.7B). Besides this mechanotransduction pathway, interstitial flow was also shown to create a micro-gradient of cell-secreted CCL21, which directs the movement of cancer cells expressing CCR7 in the direction of flow (downstream) through autologous fashion (autologous chemotaxis) (37) (Fig. 1.7A). Furthermore, the responses of cancer cells to interstitial flow also depend on cell seeding density. Polacheck et al. discovered that when interstitial flow is applied to a population of cancer cells with low cell seeding density, cancer cells tend to move downstream through autologous chemotaxis mechanisms. However, when the same level of interstitial flow is applied to cancer cell population with high seeding density, the mechanotransduction pathway seems to be dominant and cells tend to migrate upstream. This phenomenon is attributed to the fact that high seeding density created an

unfavorable environment for the generation of the autocrine gradient, as the chemokines secreted by nearby cells can mask this gradient (36). Finally, a very recent study has revealed that tumor cells' responses to interstitial flow are also heterogeneous (69). Specifically, it shows that a subpopulation of cells that move in the direction of flow has low migration speed but high migration persistence. Conversely, the subpopulation of cells that move against the flow has high migration speed but low migration persistence (69). These results, which could not be obtained from an end-point transwell assay, highlight the importance of assessing the temporal dynamics of cell migration.

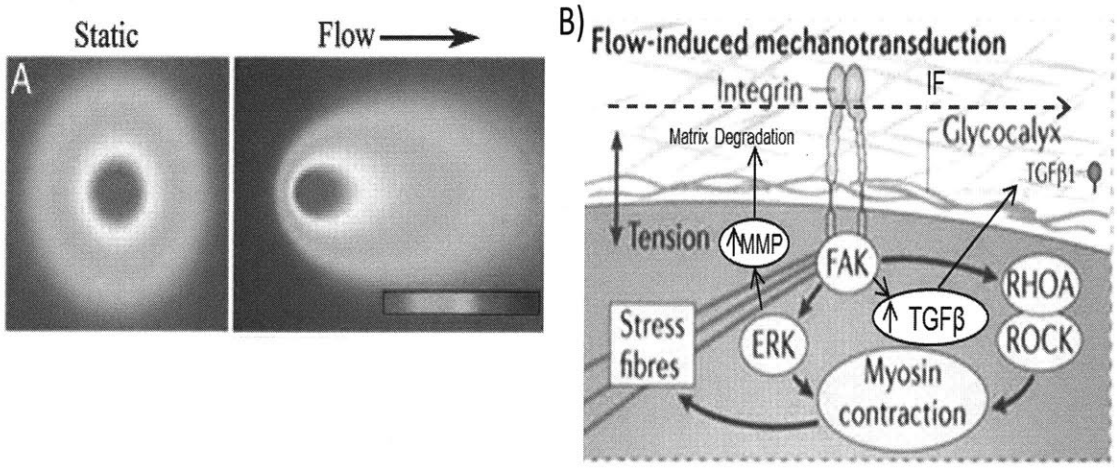

Fig. 1.7. Mechanisms of interstitial flow-induced cellular responses. (A) Interstitial flow can induce the migration of cancer cells in the direction of flow via autologous chemotaxis. Under static conditions (left image), chemokines released by a cell will distribute symmetrically around the cell. However, under the physiological interstitial flow condition (right image), the symmetric distribution of chemokine is altered to create a transcellular micro-gradient that can direct cell migration in the direction of flow. (B) Interstitial flow could also induce cellular responses through mechanotransduction pathways. Cells sense interstitial flow using integrin and glycocalyx. Interstitial flow (IF) stimulates integrin, which leads to the activation of FAK and downstream up-regulation of TGFβ. The activation of FAK could also lead to the activation of ERK, which further leads to the up-regulation of MMPs. Modified from (6, 37).

Interstitial flow could also affect stromal cells. Interstitial flow-induced sprouting of endothelial cells, which is mediated by integrin and Src, has been observed (104–106). Moreover, Ng et al. discovered that interstitial flow could increase the expression of TGFβ1 in fibroblasts (107). They further demonstrated that cells could sense this interstitial flow through β1 integrin. A later study performed by Shi et al. found that interstitial flow increased the migration of fibroblasts through the up-regulation of MMP1. Subsequent experiments demonstrated that this up-regulation of MMP1 expression was linked to interstitial flow-induced phosphorylation of ERK1/2 and expression of c-Jun. Recent study also introduces the possibility that glycocalyx, such as syndecan, are involved in cell sensing of interstitial flow (108–110) (Fig. 1.7B). Furthermore, interstitial flow has also been shown to affect the interaction between cancer cells and stromal cells. Interstitial flow was reported to induce the release of

proteases by tumor-associated fibroblasts. This led to priming of the ECM by fibroblasts, which allowed cancer cells to migrate through the matrix easily (38). In summary, all these studies suggest that many different types of cells can sense interstitial flow through β1 integrin and glycocalyx.

1.3.3: The effects of interstitial flow on macrophages and macrophage-cancer cell interaction – possible mechanisms

Despite the advances from the studies presented above, the effects of interstitial flow on tumor-associated macrophages, a key contributor to tumor malignancy, and their interaction with cancer cells, have not been investigated. Since many cellular pathways and molecules that are used by cells to sense and respond to interstitial flow are conserved in macrophages, we expect that interstitial flow can elicit responses from macrophages. Indeed, macrophages have been demonstrated to respond to their mechanoenvironment (111). They have also been shown to respond to different substrate stiffness, and their ability to phagocytose has been linked to the stiffness of the target (112, 113). Macrophages could also use podosomes, an adhesive structure with proteolysis activity, to sense the mechanical cues and transmit them inside the cell (115–117). Specifically, Raw 264.7 macrophages, which were used in our study, possess podosomes, and integrin is found in these podosomes (118–122). Integrins, which are important in cell sensing of interstitial flow, also play a pivotal role in macrophage migration (123) and the release of cytokines (124–126). Macrophages express abundant β1 integrin, which is in contrast to monocytes (127, 128). Specifically, the expression of both α1β1 (125, 129) and α2β1 (130–132) has been found on macrophages. Recent *in vivo* and *in vitro* reports have shown that macrophages adhere to collagen I gel (118, 130, 131) through β1 integrin such as α1β1 and α2β1 integrin. Indeed, Raw 264.7 cells can adhere to collagen I (118, 133), and they do so using either α1β1 or α2β1 integrin. Moreover, macrophages also use mesenchymal migration to navigate inside the dense collagen I matrix (123), and β1 integrin and podosomes are heavily involved in this process (131, 134). Macrophages also express glycocalyx, another possible sensor of interstitial flow. Macrophage is actually a main producer of heparin sulfate proteoglycans (HSPGs), a major component of glycocalyx (135). Macrophages have been shown to produce syndecan-1, syndecan-2, and syndecan-4 (135, 136). Specifically, Raw 264.7 macrophages have been reported to produce syndecan-1 (137, 138). All in all, these results point to the possibility that macrophages could sense interstitial flow since they express major flow sensors (integrin and glycocalyx).

Besides flow sensors, macrophages also express FAK and ERK1/2, which are the major transducers of cellular signals initiated by interstitial flow (121, 139, 140). It has long been known that β1 integrin and FAK co-localize inside the adhesive structure of macrophages (139). Additionally, Raw 264.7 macrophages express FAK, and the phosphorylation of FAK at tyrosine 397 has been observed (141). Macrophages lacking FAK have impaired ability to migrate and form protrusion (140, 142–144). ERK1/2 is another important molecule in macrophages, and it plays important roles in macrophage cytokine release. Many previous studies have reported that the crosslinking of β1 integrin promotes the release of cytokines by macrophages (124, 126, 145). Moreover, the

adhesion of macrophages to substrate is crucial for its cytokine production (124, 126). Indeed, blocking β1 integrin-mediated macrophage adhesion inhibits TNFα production (125, 146). Further research has revealed that ERK1/2 is involved in this integrin-assisted cytokine production, as artificially-induced integrin activation leads to the phosphorylation of ERK1/2 in macrophages (125, 147), and the inhibition of this ERK1/2 phosphorylation leads to a decreased cytokine production. Besides promoting the release of cytokines, ERK1/2 phosphorylation and activation could also lead to increased macrophage proliferation (148–150).

Finally, we hypothesized that the polarization of macrophages could be affected by interstitial flow, since kinases and transcription factors that control this process have been shown to be mechanosensitive in other cell types. It is well known that cytokines, such as IL-4 and IL-10, can induce the expression of M2 markers in macrophages through the transcription factors STAT3 and STAT6. Once IL-4 and IL-10 bind to their respective receptors on macrophage surface, they activate kinases such as JAK1, JAK3, and Tyk2. These kinases can further phosphorylate and activate STAT3 and STAT6, which, upon activation, translocate to the nucleus and initiate the production of M2 cytokines. In contrast, the activation of transcription factors STAT1 and STAT5 leads to the production of M1 markers in macrophages treated with LPS and IFN-γ (Fig. 1.8) (41). Recent reports suggest that the STAT and JAK pathways are mechanosensitive in cardiomyocytes and osteoblasts. Specifically, Pan et al. have shown that mechanical stretch could induce the phosphorylation (activation) of JAK1, JAK2, and Tyk2 in cardiomyocytes, leading to the downstream activation of STAT1 and STAT3 (151). Moreover, Zhou et al. reported that fluid shear stress can enhance the phosphorylation of STAT3 in osteoblasts (152). However, whether STAT and JAK pathways are mechanosensitive in macrophages has not been explored. All in all, it is important to understand how interstitial flow affects macrophage polarization, since it determines whether the macrophages are anti- or pro-metastatic in the context of tumor progression.

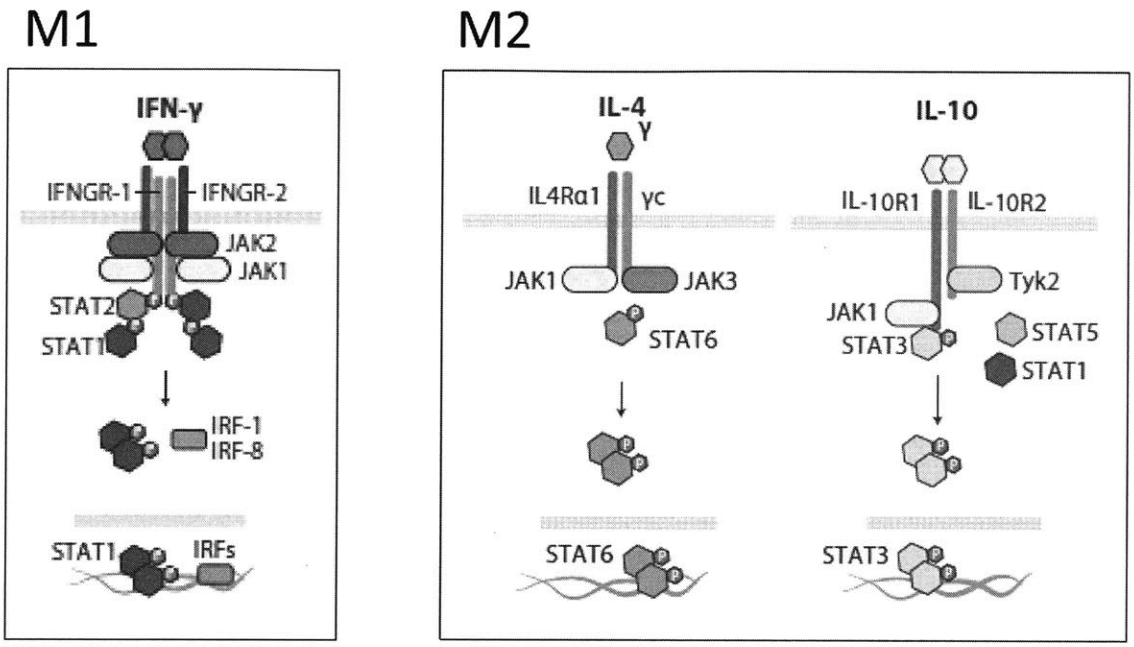

Fig. 1.8: JAK-STAT pathways in macrophages. (Left) The chemical induction of M1 polarization in macrophages starts with the binding of IFNγ to its receptors, leading to the downstream activation of kinases JAK1 and JAK2. These two kinases further activate transcription factors STAT2 and STAT1, which induce the production of M1 markers. (Right) M2 macrophages are produced by stimulating naïve macrophages with cytokines such as IL-4 and IL-10. These cytokines, when bind to their receptors, signal the downstream activation of JAK1, JAK3, and Tyk2, leading to the phosphorylation of transcription factors STAT6 and STAT3. These phosphorylated transcription factors then transmigrate into the nucleus, leading to the production of M2 markers. Modified from (41).

Based on current literature presented above, we hypothesized that macrophages in the tumor microenvironment could sense, through their surface expression of integrin or glycocalyx, the elevated interstitial flow in the tumor tissue. This could lead to the phosphorylation of FAKs and ERK1/2 in tumor-associated macrophages. Since integrin, FAK, and ERKs are involved in macrophage migration and cytokine production, we further hypothesized that interstitial flow could affect these important biological processes in macrophages. Specifically, we expected that interstitial flow could influence the polarization of macrophages, since molecules that are involved in this process, such as STATs and JAKs, have been shown to be mechanosensitive in other cell types. Finally, we speculated that the changes in macrophage phenotypes due to interstitial flow treatment could lead to changes in how macrophages interact with cancer cells, resulting in flow-induced changes in the tumor microenvironment.

1.4: Aims and Overview

1.4.1: Thesis Aims

Metastasis, which accounts for 90% of cancer death, critically depends on the ability of cells from the primary tumor to navigate through the dense extracellular matrix in and surrounding the tumor tissues. As discussed in the previous sections, it is now well established that multiple factors within the tumor microenvironment can influence tumor growth and metastasis. Specifically, non-cancerous tumor associated-stromal cells, such as macrophages, have been shown to assist cancer cell invasion. Moreover, biophysical forces within the tumor microenvironment, especially interstitial flow (IF), can modulate the behavior of cancer cells and tumor-associated fibroblasts. Nevertheless, there are still several shortcomings in our current understanding of how the tumor microenvironment controls cell migration and metastasis. Most importantly, a detailed characterization of the temporal dynamics of macrophage-assisted cancer cell migration (e.g. speed and persistence) in 3D ECM remains lacking. Furthermore, whether IF could affect macrophages, as well as their ability to promote metastasis, is still largely unknown.

To further fulfill our knowledge of the tumor micro-environmental control of metastasis, we established the following two aims:

Aim 1: Investigate the effects of macrophages on the dynamics of cancer cell migration under static (no-flow) conditions. The overall dissemination of a cancer cell population from a primary tumor site is influenced by the migratory speed and persistence of each individual cancer cell (67). These characteristics of cancer cell migration, collectively called migration dynamics, can be modulated independently of one another by a single stimulus (69). Hence, a detailed quantification of how macrophages affect these migration dynamics, especially in 3D ECM that closely mimics the *in vivo* tumor tissue, is needed to gain a deeper insight into cancer cell migration. To determine if macrophages can affect the distinct aspects (speed vs. persistence) of cancer cell migration in different ways, we employed a microfluidic 3D time-lapse migration assay to quantify the migration dynamics of cancer cells co-cultured with macrophages. The mechanisms of observed effects were also investigated.

Aim 2: Investigate the effects of interstitial flow on macrophages and their ability to promote metastasis. The growth of solid tumors often results in an elevated interstitial fluid flow from the center of the tumor to the surrounding stroma, where tumor-associated macrophages reside (33). Macrophages express integrin and FAK, which have been found to be activated by interstitial flow in other cell types (125, 153). Since these molecules are involved in macrophage migration and protein expression, we hypothesized that elevated interstitial flow could modulate macrophage phenotype. We developed microfluidic and transwell flow assays to assess the effects of interstitial flow on macrophage migration and polarization, as well as macrophage's ability to promote cancer cell migration. The mechanisms of observed effects were meticulously interrogated.

1.4.2: Thesis Overview

In Chapter 2, we discuss the assays and methodologies used to address the two aims of this thesis. We first review the complexity of cancer cell migration processes, as well as the limitation of traditional assays employed by scientists to study cell migration. We then introduce the microfluidic 3D migration assay, which we used to study the effects of macrophages on cancer cell migration dynamics. This microfluidic system addresses several key shortcomings of traditional cell migration assays. We also discuss the development and characterization of the microfluidic and transwell flow assays used to study the effects of interstitial flow on macrophage migration and protein expression.

In Chapter 3, we discuss the effects of macrophages on the temporal dynamics of cancer cell migration (Aim 1). We found that macrophages enhanced both cancer cell migration speed and persistence through 3D ECM in an MMP-dependent fashion. We further identified two independent pathways used by macrophages to promote cancer cell migration speed and persistence. Specifically, macrophage-released TNFα and TGFβ1 synergistically enhance cancer cell migration persistence, and this increase in persistence was due to the synergistic induction of NF-κB-dependent MMP1 expression in cancer cells. In contrast, macrophages enhance cancer cell migration speed primarily through TGFβ1-induced MT1-MMP expression.

In Chapter 4, we describe the effects of interstitial flow on macrophage migration and polarization (Aim 2). We report that macrophages, a key tumor-associated immune cell type, can sense and respond to interstitial flow (IF). Surprisingly, we discovered that IF enhanced the ability of macrophages to promote metastasis. Specifically, we demonstrated that IF promoted macrophage migration against the flow direction, thereby recruiting macrophages from stroma into tumor tissues. Additionally, we show that IF polarized macrophages to a pro-metastatic M2 phenotype via integrin/Src-mediated STAT3/6 activation. Finally, we revealed that macrophages treated with flow had an enhanced ability in promoting cancer cell migration.

In Chapter 5, we conclude this thesis by discussing the implications of our results. Based on the results presented in Chapter 3, we provide evidence that different aspects of cancer cell migration (speed vs. persistence) can be modulated independently of each other, and a careful quantification of the effects of a stimulus on these two metrics could improve our understanding of metastasis. We further argue, based on the results discussed in Chapter 4, that interstitial flow plays crucial roles in shaping the tumor immune environment and promoting metastasis. We end this chapter by discussing possible future studies that could further enhance our understanding of how the tumor microenvironment modulates cell migration and metastasis.

1.5: References

1. Chambers AF, Groom AC, MacDonald IC (2002) Dissemination and growth of cancer cells in metastatic sites. *Nat Rev Cancer* 2(8):563–72.
2. Mehlen P, Puisieux A (2006) Metastasis: a question of life or death. *Nat Rev Cancer* 6(6):449–58.
3. Steeg PS (2006) Tumor metastasis: mechanistic insights and clinical challenges. *Nat Med* 12(8):895–904.
4. Faltas B (2012) Cornering metastases: therapeutic targeting of circulating tumor cells and stem cells. *Front Oncol* 2:68.
5. Chen Z, Fillmore CM, Hammerman PS, Kim CF, Wong K-K (2014) Non-small-cell lung cancers: a heterogeneous set of diseases. *Nat Rev Cancer* 14(8):535–546.
6. Swartz M a, et al. (2012) Tumor microenvironment complexity: emerging roles in cancer therapy. *Cancer Res* 72(10):2473–80.
7. Joyce J a, Pollard JW (2009) Microenvironmental regulation of metastasis. *Nat Rev Cancer* 9(4):239–52.
8. Mantovani A, Allavena P, Sica A, Balkwill F (2008) Cancer-related inflammation. *Nature* 454(7203):436–44.
9. Gabrilovich DI, Ostrand-Rosenberg S, Bronte V (2012) Coordinated regulation of myeloid cells by tumours. *Nat Rev Immunol* 12(4):253–68.
10. Wong SY, Hynes RO (2006) Lymphatic or hematogenous dissemination: how does a metastatic tumor cell decide? *Cell Cycle* 5(8):812–7.
11. Madar S, et al. (2013) "Cancer associated fibroblasts"--more than meets the eye. *Trends Mol Med* 19(8):447–53.
12. Handorf AM, Zhou Y, Halanski MA, Li W-J (2015) Tissue Stiffness Dictates Development, Homeostasis, and Disease Progression. *Organogenesis* 11(1):1–15.
13. Cox TR, Erler JT (2011) Remodeling and homeostasis of the extracellular matrix: implications for fibrotic diseases and cancer. *Dis Model Mech* 4(2):165–78.
14. Wei SC, et al. (2015) Matrix stiffness drives epithelial-mesenchymal transition and tumour metastasis through a TWIST1-G3BP2 mechanotransduction pathway. *Nat Cell Biol* 17(5):678–88.
15. Weaver VM, Fischer AH, Peterson OW, Bissell MJ (1996) The importance of the microenvironment in breast cancer progression: recapitulation of mammary tumorigenesis using a unique human mammary epithelial cell model and a three-dimensional culture assay. *Biochem Cell Biol* 74(6):833–51.
16. Pathak A, Kumar S (2012) Independent regulation of tumor cell migration by matrix stiffness and confinement. *Proc Natl Acad Sci U S A* 109(26):10334–9.
17. Shukla VC, Higuita-Castro N, Nana-Sinkam P, Ghadiali SN (2016) Substrate stiffness modulates lung cancer cell migration but not epithelial to mesenchymal transition. *J Biomed Mater Res Part A* 104(5):1182–1193.
18. Wirtz D, Konstantopoulos K, Searson PC (2011) The physics of cancer: the role of physical interactions and mechanical forces in metastasis. *Nat Rev Cancer* 11(7):512–22.
19. Riching KM, et al. (2009) 3D collagen alignment limits protrusions to enhance breast cancer cell persistence. *Lab Chip* 4(9):15342–7.
20. Jain RK, Martin JD, Stylianopoulos T (2014) The role of mechanical forces in tumor growth and therapy. *Annu Rev Biomed Eng* 16:321–46.
21. Leek RD, Harris AL (2002) Tumor-associated macrophages in breast cancer. *J Mammary Gland Biol Neoplasia* 7(2):177–89.
22. Mann A, Breuhahn K, Schirmacher P (2001) Up- and Down-Regulation of Granulocyte / Macrophage-Colony Stimulating Factor Activity in Murine Skin Increase Susceptibility to Skin Carcinogenesis by Independent Mechanisms Up- and Down-Regulation of Granulocyte / Macrophage-Colony Stimulating Factor Ac.
23. Zaynagetdinov R, et al. (2011) A critical role for macrophages in promotion of urethane-induced lung carcinogenesis. *J Immunol* 187(11):5703–11.
24. Fulton AM, Loveless SE, Heppner GH, Ta S (1984) Mutagenic Activity of Tumor-associated Macrophages in Salmonella typhimurium Strains TA98 and TA100 Mutagenic Activity of Tumor-associated Macrophages in Salmonella. 4308–4311.

25. Leek RD, et al. (1996) Association of macrophage infiltration with angiogenesis and prognosis in invasive breast carcinoma. *Cancer Res* 56(20):4625–9.
26. Pollard JW (2004) and metastasis. 4(January):1–8.
27. Xue C, et al. (2006) Epidermal growth factor receptor overexpression results in increased tumor cell motility in vivo coordinately with enhanced intravasation and metastasis. *Cancer Res* 66(1):192–7.
28. Wyckoff JB, et al. (2007) Direct visualization of macrophage-assisted tumor cell intravasation in mammary tumors. *Cancer Res* 67(6):2649–56.
29. Hagemann T, et al. (2004) Enhanced invasiveness of breast cancer cell lines upon co-cultivation with macrophages is due to TNF-alpha dependent up-regulation of matrix metalloproteases. *Carcinogenesis* 25(8):1543–9.
30. Goswami S, et al. (2005) Macrophages promote the invasion of breast carcinoma cells via a colony-stimulating factor-1/epidermal growth factor paracrine loop. *Cancer Res* 65(12):5278–83.
31. Shieh AC, Swartz M a (2011) Regulation of tumor invasion by interstitial fluid flow. *Phys Biol* 8(1):015012.
32. Rutkowski JM, Swartz M a (2007) A driving force for change: interstitial flow as a morphoregulator. *Trends Cell Biol* 17(1):44–50.
33. Heldin C-H, Rubin K, Pietras K, Ostman A (2004) High interstitial fluid pressure - an obstacle in cancer therapy. *Nat Rev Cancer* 4(10):806–13.
34. Curti BD, et al. (1993) Interstitial Pressure of Subcutaneous Nodules in Melanoma and Lymphoma Patients : Changes during Treatment Advances in Brief Interstitial Pressure of Subcutaneous Nodules in Melanoma and Lymphoma Patients : Changes during Treatment1. 2204–2207.
35. Hofmann M, et al. (2006) Lowering of tumor interstitial fluid pressure reduces tumor cell proliferation in a xenograft tumor model. *Neoplasia* 8(2):89–95.
36. Polacheck WJ, Charest JL, Kamm RD (2011) Interstitial flow influences direction of tumor cell migration through competing mechanisms. *Proc Natl Acad Sci U S A* 108(27):11115–20.
37. Shields JD, et al. (2007) Autologous chemotaxis as a mechanism of tumor cell homing to lymphatics via interstitial flow and autocrine CCR7 signaling. *Cancer Cell* 11(6):526–38.
38. Shieh AC, Rozansky H a, Hinz B, Swartz M a (2011) Tumor cell invasion is promoted by interstitial flow-induced matrix priming by stromal fibroblasts. *Cancer Res* 71(3):790–800.
39. Wynn TA, Chawla A, Pollard JW (2013) Macrophage biology in development, homeostasis and disease. *Nature* 496(7446):445–55.
40. Hoeffel G, Ginhoux F (2015) Ontogeny of Tissue-Resident Macrophages. *Front Immunol* 6:486.
41. Martinez FO, Gordon S (2014) The M1 and M2 paradigm of macrophage activation: time for reassessment. *F1000Prime Rep* 6:13.
42. Italiani P, Boraschi D (2014) From Monocytes to M1/M2 Macrophages: Phenotypical vs. Functional Differentiation. *Front Immunol* 5:514.
43. Mantovani A, Sozzani S, Locati M, Allavena P, A S (2002) Macrophage polarization: tumor-associated macrophages as a paradigm for polarized M2 mononuclear phagocytes. *Trends Immunol* 23(11):549–555.
44. Clària J, González-Périz A, López-Vicario C, Rius B, Titos E (2011) New insights into the role of macrophages in adipose tissue inflammation and fatty liver disease: modulation by endogenous omega-3 fatty acid-derived lipid mediators. *Front Immunol* 2:49.
45. Condeelis J, Pollard JW (2006) Macrophages: obligate partners for tumor cell migration, invasion, and metastasis. *Cell* 124(2):263–6.
46. Wang B, et al. (2011) Transition of tumor-associated macrophages from MHC class II(hi) to MHC class II(low) mediates tumor progression in mice. *BMC Immunol* 12(1):43.
47. Lewis CE, Pollard JW (2006) Distinct role of macrophages in different tumor microenvironments. *Cancer Res* 66(2):605–12.
48. Solinas G, Germano G, Mantovani a, Allavena P (2009) Tumor-associated macrophages (TAM) as major players of the cancer-related inflammation. *J Leukoc Biol* 86(5):1065–73.
49. Lin EY, Nguyen a V, Russell RG, Pollard JW (2001) Colony-stimulating factor 1 promotes progression of mammary tumors to malignancy. *J Exp Med* 193(6):727–40.
50. Sica A, Schioppa T, Mantovani A, Allavena P (2006) Tumour-associated macrophages are a distinct M2 polarised population promoting tumour progression: potential targets of anti-cancer therapy. *Eur J Cancer* 42(6):717–27.

51. Shih J, Yuan A, Chen JJ, Yang P (2006) Tumor-Associated Macrophage : Its Role in Cancer Invasion and Metastasis. 101–106.
52. Bingle L, Brown NJ, Lewis CE (2002) The role of tumour-associated macrophages in tumour progression: implications for new anticancer therapies. *J Pathol* 196(3):254–65.
53. Jenkins SJ, et al. (2011) Local macrophage proliferation, rather than recruitment from the blood, is a signature of TH2 inflammation. *Science* 332(6035):1284–8.
54. Green CE, et al. (2009) Chemoattractant signaling between tumor cells and macrophages regulates cancer cell migration, metastasis and neovascularization. *PLoS One* 4(8):e6713.
55. Boudreau N, Myers C (2003) Breast cancer-induced angiogenesis: multiple mechanisms and the role of the microenvironment. *Breast Cancer Res* 5(3):140–6.
56. Lewis CE, De Palma M, Naldini L (2007) Tie2-expressing monocytes and tumor angiogenesis: regulation by hypoxia and angiopoietin-2. *Cancer Res* 67(18):8429–32.
57. Wrzesinski SH, Wan YY, Flavell RA (2007) Transforming growth factor-beta and the immune response: implications for anticancer therapy. *Clin Cancer Res* 13(18 Pt 1):5262–70.
58. Wang W, et al. (2002) Single cell behavior in metastatic primary mammary tumors correlated with gene expression patterns revealed by molecular profiling. *Cancer Res* 62(21):6278–88.
59. Pollard JW (2004) Tumour-educated macrophages promote tumour progression and metastasis. *Nat Rev Cancer* 4(1):71–8.
60. Yamaguchi H, Wyckoff J, Condeelis J (2005) Cell migration in tumors. *Curr Opin Cell Biol* 17(5):559–64.
61. Roussos ET, Condeelis JS, Patsialou A (2011) Chemotaxis in cancer. *Nat Rev Cancer* 11(8):573–87.
62. Shin Y, et al. (2012) Microfluidic assay for simultaneous culture of multiple cell types on surfaces or within hydrogels. *Nat Protoc* 7(7):1247–59.
63. Polacheck WJ, Zervantonakis IK, Kamm RD (2012) Tumor cell migration in complex microenvironments. *Cell Mol Life Sci*. doi:10.1007/s00018-012-1115-1.
64. Meyer AS, et al. (2012) 2D protrusion but not motility predicts growth factor-induced cancer cell migration in 3D collagen. *J Cell Biol* 197(6):721–9.
65. Fraley SI, et al. (2010) A distinctive role for focal adhesion proteins in three-dimensional cell motility. *Nat Cell Biol* 12(6):598–604.
66. Hsia DA, et al. (2003) Differential regulation of cell motility and invasion by FAK. *J Cell Biol* 160(5):753–67.
67. Maheshwari G, Lauffenburger D a (1998) Deconstructing (and reconstructing) cell migration. *Microsc Res Tech* 43(5):358–68.
68. Kim H-D, et al. (2008) Epidermal growth factor-induced enhancement of glioblastoma cell migration in 3D arises from an intrinsic increase in speed but an extrinsic matrix- and proteolysis-dependent increase in persistence. *Mol Biol Cell* 19(10):4249–59.
69. Haessler U, Teo JCM, Foretay D, Renaud P, Swartz M a (2012) Migration dynamics of breast cancer cells in a tunable 3D interstitial flow chamber. *Integr Biol (Camb)* 4(4):401–9.
70. Tayalia P, Mazur E, Mooney DJ (2011) Controlled architectural and chemotactic studies of 3D cell migration. *Biomaterials* 32(10):2634–41.
71. Quaranta V, et al. (2010) NIH Public Access. 6879(09). doi:10.1016/S0076-6879(09)67002-6.Trait.
72. Hagemann T, et al. (2006) Ovarian cancer cells polarize macrophages toward a tumor-associated phenotype. *J Immunol* 176(8):5023–32.
73. Miles DW, Naylor MS, Bobrow LG, Rubens RD, Balkwill FR (1994) EXPRESSION OF TUMOUR NECROSIS FACTOR (TNFa) AND ITS RECEPTORS IN BENIGN AND MALIGNANT BREAST TISSUE. 782:777–782.
74. Yarilina A, Xu K, Chen J, Ivashkiv LB (2011) TNF activates calcium-nuclear factor of activated T cells (NFAT)c1 signaling pathways in human macrophages. *Proc Natl Acad Sci U S A* 108(4):1573–8.
75. Huang C, Ho B, Pan T (2012) Modulation of Proinflammatory Cytokines by Red Mold Dioscorea Ethanol Extract in Radioactive Cobalt-60 Exposure. 20(2):516–523.
76. Hald A, Rønø B, Lund LR, Egerod KL (2012) LPS counter regulates RNA expression of extracellular proteases and their inhibitors in murine macrophages. *Mediators Inflamm* 2012:157894.
77. Balkwill F (2009) Tumour necrosis factor and cancer. *Nat Rev Cancer* 9(5):361–71.

78. Moore RJ, et al. (1999) Mice deficient in tumor necrosis factor-alpha are resistant to skin carcinogenesis. *Nat Med* 5(7):828–31.
79. Rosen EM, et al. (1991) Tumor Necrosis Factor Stimulates Epithelial Tumor Cell Motility Tumor Necrosis Factor Stimulates Epithelial Tumor Cell Motility1. 5315–5321.
80. Cho S-G, et al. (2009) KiSS1 suppresses TNFalpha-induced breast cancer cell invasion via an inhibition of RhoA-mediated NF-kappaB activation. *J Cell Biochem* 107(6):1139–49.
81. Wu Y, et al. (2009) Stabilization of snail by NF-kappaB is required for inflammation-induced cell migration and invasion. *Cancer Cell* 15(5):416–28.
82. Li T, et al. (2012) Daintain/AIF-1 promotes breast cancer cell migration by up-regulated TNF-α via activate p38 MAPK signaling pathway. *Breast Cancer Res Treat* 131(3):891–8.
83. Butt AJ, Dickson K a, Jambazov S, Baxter RC (2005) Enhancement of tumor necrosis factor-alpha-induced growth inhibition by insulin-like growth factor-binding protein-5 (IGFBP-5), but not IGFBP-3 in human breast cancer cells. *Endocrinology* 146(7):3113–22.
84. Hagemann T, et al. (2005) Macrophages induce invasiveness of epithelial cancer cells via NF-kappa B and JNK. *J Immunol* 175(2):1197–205.
85. Hagemann T, et al. (2008) "Re-educating" tumor-associated macrophages by targeting NF-kappaB. *J Exp Med* 205(6):1261–8.
86. Pukrop T, et al. (2006) Wnt 5a signaling is critical for macrophage-induced invasion of breast cancer cell lines. *Proc Natl Acad Sci U S A* 103(14):5454–9.
87. Letterio JJ, Roberts a B (1998) Regulation of immune responses by TGF-beta. *Annu Rev Immunol* 16(1):137–61.
88. Ikushima H, Miyazono K (2010) TGFbeta signalling: a complex web in cancer progression. *Nat Rev Cancer* 10(6):415–24.
89. El Gazzar M (2007) HMGB1 modulates inflammatory responses in LPS-activated macrophages. *Inflamm Res* 56(4):162–7.
90. Zamora R, et al. (2012) Identification of a novel pathway of TGF-β1 regulation by extracellular NAD+ in mouse macrophages: in vitro and in silico studies. *J Biol Chem* (2). doi:10.1074/jbc.M112.344309.
91. Bujak M, Frangogiannis NG (2007) The role of TGF-beta signaling in myocardial infarction and cardiac remodeling. *Cardiovasc Res* 74(2):184–95.
92. Akhurst RJ, Derynck R (2001) TGF-beta signaling in cancer--a double-edged sword. *Trends Cell Biol* 11(11):S44–51.
93. Morton DM, Barrack ER (1995) Modulation of Transforming Growth Factor β 1 Effects on Prostate Cancer Cell Proliferation by Growth Factors and Extracellular Matrix Modulation of Transforming Growth Factor ÃŸ1Effects on Prostate Cancer Cell Proliferation by Growth Factors and Extracell. 2596–2602.
94. Vitolo D, et al. (2001) Laminin a2 chain (merosin M chain) distribution and VEGF , FGF 2 , and TGFb1 gene expression in angiogenesis of supraglottic , lung , and breast carcinomas. 197–208.
95. Bandyopadhyay a, et al. (1999) A soluble transforming growth factor beta type III receptor suppresses tumorigenicity and metastasis of human breast cancer MDA-MB-231 cells. *Cancer Res* 59(19):5041–6.
96. Zheng Q, Safina A, Bakin A V (2008) Role of high-molecular weight tropomyosins in TGF-beta-mediated control of cell motility. *Int J Cancer* 122(1):78–90.
97. Bakin A V, Rinehart C, Tomlinson AK, Arteaga CL (2002) p38 mitogen-activated protein kinase is required for TGFbeta-mediated fibroblastic transdifferentiation and cell migration. *J Cell Sci* 115(Pt 15):3193–206.
98. Schäfer H, et al. (2012) TGF-β1-dependent L1CAM expression has an essential role in macrophage-induced apoptosis resistance and cell migration of human intestinal epithelial cells. *Oncogene* (January):1–10.
99. Bonde A-K, Tischler V, Kumar S, Soltermann A, Schwendener R a (2012) Intratumoral macrophages contribute to epithelial-mesenchymal transition in solid tumors. *BMC Cancer* 12(1):35.
100. Levick JR (1987) REVIEW ARTICLE FLOW THROUGH INTERSTITIUM AND OTHER FIBROUS MATRICES.
101. Miskin R, Ben-Ishai R (1981) Induction of plasminogen activator by UV light in normal and xeroderma pigmentosum fibroblasts. *Proc Natl Acad Sci U S A* 78(10):6236–40.

102. Dafni H, Israely T, Bhujwalla ZM, Albumin T (2002) Overexpression of Vascular Endothelial Growth Factor 165 Drives Peritumor Interstitial Convection and Induces Lymphatic Drain : Magnetic Resonance Imaging , Confocal Microscopy , and Histological Tracking of Triple-labeled Albumin Overexpression of Vascul.
103. Wirtz D, Konstantopoulos K, Searson PC (2011) The physics of cancer: the role of physical interactions and mechanical forces in metastasis. *Nat Rev Cancer* 11(7):512–22.
104. Vickerman V, Kamm RD (2012) Mechanism of a flow-gated angiogenesis switch: early signaling events at cell-matrix and cell-cell junctions. *Integr Biol (Camb)* 4(8):863–74.
105. Sudo R, et al. Transport-mediated angiogenesis in 3D epithelial coculture. *FASEB J*:2155–2164.
106. Song JW, Munn LL (2011) Fluid forces control endothelial sprouting. *Proc Natl Acad Sci U S A* 108(37):15342–7.
107. Ng CP, Hinz B, Swartz M a (2005) Interstitial fluid flow induces myofibroblast differentiation and collagen alignment in vitro. *J Cell Sci* 118(Pt 20):4731–9.
108. Shi Z-D, Ji X-Y, Qazi H, Tarbell JM (2009) Interstitial flow promotes vascular fibroblast, myofibroblast, and smooth muscle cell motility in 3-D collagen I via upregulation of MMP-1. *Am J Physiol Heart Circ Physiol* 297(4):H1225–34.
109. Shi Z-D, Ji X-Y, Berardi DE, Qazi H, Tarbell JM (2010) Interstitial flow induces MMP-1 expression and vascular SMC migration in collagen I gels via an ERK1/2-dependent and c-Jun-mediated mechanism. *Am J Physiol Heart Circ Physiol* 298(1):H127–35.
110. Shi Z-D, Wang H, Tarbell JM (2011) Heparan sulfate proteoglycans mediate interstitial flow mechanotransduction regulating MMP-13 expression and cell motility via FAK-ERK in 3D collagen. *PLoS One* 6(1):e15956.
111. Yang JH, Sakamoto H, Xu EC, Lee RT (2000) Biomechanical regulation of human monocyte/macrophage molecular function. *Am J Pathol* 156(5):1797–804.
112. Féréol S, et al. (2006) Sensitivity of alveolar macrophages to substrate mechanical and adhesive properties. *Cell Motil Cytoskeleton* 63(6):321–40.
113. Beningo K a, Wang Y (2002) Fc-receptor-mediated phagocytosis is regulated by mechanical properties of the target. *J Cell Sci* 115(Pt 4):849–56.
114. Rosenson-Schloss RS, Vitolo JL, Moghe P V (1999) Flow-mediated cell stress induction in adherent leukocytes is accompanied by modulation of morphology and phagocytic function. *Med Biol Eng Comput* 37(2):257–63.
115. Collin O, et al. (2008) Self-organized podosomes are dynamic mechanosensors. *Curr Biol* 18(17):1288–94.
116. Collin O, et al. (2006) Spatiotemporal dynamics of actin-rich adhesion microdomains: influence of substrate flexibility. *J Cell Sci* 119(Pt 9):1914–25.
117. Labernadie A, Thibault C, Vieu C, Maridonneau-parini I, Charrière GM (2010) Dynamics of podosome stiffness revealed by atomic force microscopy. doi:10.1073/pnas.1007835107/-/DCSupplemental.www.pnas.org/cgi/doi/10.1073/pnas.1007835107.
118. Juin A, et al. (2012) Physiological type I collagen organization induces the formation of a novel class of linear invadosomes. *Mol Biol Cell* 23(2):297–309.
119. Mersich AT (2010) NIH Public Access. *Cytoskeleton* 67(9):573–585.
120. Dovas A, et al. (2009) Regulation of podosome dynamics by WASp phosphorylation: implication in matrix degradation and chemotaxis in macrophages. *J Cell Sci* 122(Pt 21):3873–82.
121. Linder S (2007) The matrix corroded: podosomes and invadopodia in extracellular matrix degradation. *Trends Cell Biol* 17(3):107–17.
122. Guiet R, et al. (2012) Macrophage mesenchymal migration requires podosome stabilization by filamin A. *J Biol Chem* 287(16):13051–62.
123. Van Goethem E, Poincloux R, Gauffre F, Maridonneau-Parini I, Le Cabec V (2010) Matrix architecture dictates three-dimensional migration modes of human macrophages: differential involvement of proteases and podosome-like structures. *J Immunol* 184(2):1049–61.
124. Monick MM, Powers L, Butler N, Yarovinsky T, Hunninghake GW (2002) Interaction of matrix with integrin receptors is required for optimal LPS-induced MAP kinase activation. *Am J Physiol Lung Cell Mol Physiol* 283(2):L390–402.
125. Suzuki K, et al. (2007) Semaphorin 7A initiates T-cell-mediated inflammatory responses through alpha1beta1 integrin. *Nature* 446(7136):680–4.
126. Berton G, Lowell C a (1999) Integrin signalling in neutrophils and macrophages. *Cell Signal*

11(9):621–35.
127. Ballana E, et al. (2009) Cell adhesion through alphaV-containing integrins is required for efficient HIV-1 infection in macrophages. *Blood* 113(6):1278–86.
128. La Linn M, et al. (2005) An arthritogenic alphavirus uses the alpha1beta1 integrin collagen receptor. *Virology* 336(2):229–39.
129. Krieglstein CF, et al. (2002) Collagen-binding integrin α 1 β 1 regulates intestinal inflammation in experimental colitis. 110(12):1773–1782.
130. Sondag CM, Combs CK (2010) Adhesion of monocytes to type I collagen stimulates an APP-dependent proinflammatory signaling response and release of Abeta1-40. *J Neuroinflammation* 7:22.
131. Philippeaux M-M, et al. (2009) Culture and functional studies of mouse macrophages on native-like fibrillar type I collagen. *Eur J Cell Biol* 88(4):243–56.
132. Adiguzel E, Ahmad PJ, Franco C, Bendeck MP (2009) Collagens in the progression and complications of atherosclerosis. *Vasc Med* 14(1):73–89.
133. Hayashi S, et al. (2011) The type II collagen N-propeptide, PIIBNP, inhibits cell survival and bone resorption of osteoclasts via integrin-mediated signaling. *Bone* 49(4):644–52.
134. Van Goethem E, et al. (2011) Macrophage podosomes go 3D. *Eur J Cell Biol* 90(2-3):224–36.
135. Asplund A, Ostergren-Lundén G, Camejo G, Stillemark-Billton P, Bondjers G (2009) Hypoxia increases macrophage motility, possibly by decreasing the heparan sulfate proteoglycan biosynthesis. *J Leukoc Biol* 86(2):381–8.
136. Saphire ACS, et al. (2001) Syndecans Serve as Attachment Receptors for Human Immunodeficiency Virus Type 1 on Macrophages Syndecans Serve as Attachment Receptors for Human Immunodeficiency Virus Type 1 on Macrophages †. doi:10.1128/JVI.75.19.9187.
137. Belting M, et al. (2003) Glypican-1 is a vehicle for polyamine uptake in mammalian cells: a pivital role for nitrosothiol-derived nitric oxide. *J Biol Chem* 278(47):47181–9.
138. Larabee JL, et al. (2011) Glycogen synthase kinase 3 activation is important for anthrax edema toxin-induced dendritic cell maturation and anthrax toxin receptor 2 expression in macrophages. *Infect Immun* 79(8):3302–8.
139. Allen WE, Jones GE, Pollard JW, Ridley a J (1997) Rho, Rac and Cdc42 regulate actin organization and cell adhesion in macrophages. *J Cell Sci* 110 (Pt 6:707–20.
140. Owen K a, et al. (2007) Regulation of lamellipodial persistence, adhesion turnover, and motility in macrophages by focal adhesion kinase. *J Cell Biol* 179(6):1275–87.
141. Matsumoto Y, et al. (2012) This information is current as of September 5, 2012.
142. Stokes JB, et al. (2011) Inhibition of focal adhesion kinase by PF-562,271 inhibits the growth and metastasis of pancreatic cancer concomitant with altering the tumor microenvironment. *Mol Cancer Ther* 10(11):2135–45.
143. Abshire MY, Thomas KS, Owen K a, Bouton AH (2011) Macrophage motility requires distinct α5β1/FAK and α4β1/paxillin signaling events. *J Leukoc Biol* 89(2):251–7.
144. Schaller MD (2010) Cellular functions of FAK kinases: insight into molecular mechanisms and novel functions. *J Cell Sci* 123(Pt 7):1007–13.
145. Ammon C, et al. (2000) Comparative analysis of integrin expression on monocyte-derived macrophages and monocyte-derived dendritic cells. *Immunology* 100(3):364–9.
146. Kapetanovic R, et al. (2011) Mechanisms of TNF induction by heat-killed Staphylococcus aureus differ upon the origin of mononuclear phagocytes. *Am J Physiol Cell Physiol* 300(4):C850–9.
147. Kanayama M, et al. (2011) α9β1 integrin-mediated signaling serves as an intrinsic regulator of pathogenic Th17 cell generation. *J Immunol* 187(11):5851–64.
148. Saegusa J, et al. (2008) Pro-inflammatory secretory phospholipase A2 type IIA binds to integrins alphavbeta3 and alpha4beta1 and induces proliferation of monocytic cells in an integrin-dependent manner. *J Biol Chem* 283(38):26107–15.
149. Gangoiti P, et al. (2008) Ceramide 1-phosphate stimulates macrophage proliferation through activation of the PI3-kinase/PKB, JNK and ERK1/2 pathways. *Cell Signal* 20(4):726–36.
150. Yu W, et al. (2012) Macrophage proliferation is regulated through CSF-1 receptor tyrosines 544, 559, and 807. *J Biol Chem* 287(17):13694–704.
151. Pan J, et al. (1999) Mechanical stretch activates the JAK/STAT pathway in rat cardiomyocytes. *Circ Res* 84(10):1127–36.
152. Zhou H, et al. (2011) Osteoblast/osteocyte-specific inactivation of Stat3 decreases load-driven bone

formation and accumulates reactive oxygen species. *Bone* 49(3):404–411.
153. Park P-H, McMullen MR, Huang H, Thakur V, Nagy LE (2007) Short-term treatment of RAW264.7 macrophages with adiponectin increases tumor necrosis factor-alpha (TNF-alpha) expression via ERK1/2 activation and Egr-1 expression: role of TNF-alpha in adiponectin-stimulated interleukin-10 production. *J Biol Chem* 282(30):21695–703.

Chapter 2. Development of Methods

2.1: Introduction

We developed and optimized microfluidic and transwell assays to address the specific aims set out by this thesis. In particular, we utilized an existing microfluidic platform, which we called the "static platform", to quantify the effects of macrophages on cancer cell migration speed and persistence in an ECM that closely mimics the tumor tissues *in vivo*. We also optimized this microfluidic 3D assay for live-cell imaging. Furthermore, to quantify the effects of interstitial flow on macrophage migration, we developed a novel microfluidic flow platform that allows for the precise application of defined and quantifiable levels of interstitial flow to cells cultured in a 3D ECM. Finally, we developed a transwell assay to investigate the effects of interstitial flow on the protein expression of cells. In this chapter, we will discuss the development and optimization of methods used in this thesis.

2.2: The advantage of microfluidic assay in studying cell migration

In the primary tumor site, cancer cells and tumor-associated stromal cells are constantly migrating in respond to the chemical and physical stimuli they receive from their environment (1). The migration of cancer cells is the primarily driver of metastasis. In this process, cancer cells break down basement membrane surrounding the tumor, invade into the stromal tissues, and spread into lymphatic and blood vessels. In addition to cancer cell migration, the migration of tumor-associated stromal cells, such as macrophages and fibroblasts, can also contribute to metastasis (2). For example, the migration of fibroblasts in the tumor stromal tissues has been shown to create micro-tracks that could assist cancer cell invasion (3). Moreover, the migration of macrophages into the tumor tissues allows these immune cells to promote tumor progression and metastasis (4).

Cell migration in the tumor microenvironment is a complex process that is often difficult to model accurately in traditional *in vitro* systems (5). *In vivo*, cells are surrounded by a 3D extracellular matrix (ECM) comprised of mostly collagen I matrix (6). To migrate through the dense ECM that often characterizes the tumor and tumor-associated stromal tissues, cells must first breakdown this matrix. Indeed, ECM functions as an obstacle to cell migration, and many cells in the tumor microenvironment, especially cancer cells, have enhanced ability to move through this matrix. For example, cancer cells use kinases to form protrusions, matrix metalloproteases (MMPs) to breakdown ECM, and integrins to adhere to the matrix to generate movement (7) . The activities and expression of these migration-associated molecules are elevated in cancer cells compared to cells in normal tissues. Besides ECM, a myriad of chemical stimuli, such as cytokines released by tumor-associated stromal cells, and physical stimuli, such as the fluid force imparted on the cells by interstitial flow, can guide cell migration (8, 9). Adding to this complexity, as discussed in Chapter One, different aspects of cancer cell migration (such as speed vs. persistence) can be modulated independently of each other

by a single stimulus (10). Therefore, in order to study cell migration in a detailed, quantitative, and realistic fashion, we will need an *in vitro* system that:

1) Incorporates a 3D ECM to mimic the tissues *in vivo,*
2) Allows for the application of cellular, chemical, or mechanical stimuli in controlled fashion,
3) Allows for the simultaneous observation and quantification of different aspects of cell migration, such as speed and persistence.

Traditionally, a transwell assay is used to quantify cell migration. This assay incorporates a transwell insert in a standard cell culture well. The insert contains a polycarbonate membrane with micron-size holes. Cells are seeded on top of the membrane, and allowed to migrate through the holes in the membrane. To quantify cell migration, the total amount of cells that migrate through the membrane is measured after a given-period of time (11, 12). Although the transwell assay is pivotal in enhancing our understanding of cell migration, it has the following shortcomings (Fig. 2.1):

1) **It only provides an end-point readout of cell migration**. Transwell assay measures amount of cells passing through the membrane in a given period of time. It provides no information on how a stimulus affects the temporal details (dynamics) of cell migration, such as migration speed and persistence. For example, when a transwell assay is used to quantify migration, a stimulus that increases cell migration speed but decreases migration persistence will be indistinguishable from a stimulus that increases migration persistence but decreases migration speed.

2) **It only provides a population-average readout of cell migration**. When the transwell assay is used, a single averaged value of cell migration is reported for each sample. This value does not contain any information on the heterogeneity of cell migration behaviors. Hence, the transwell assay cannot be used to determine whether a subpopulation of cell adopts a different migration characteristic from the rest of the cells.

3) **It does not mimic the *in vivo* environment.** Most transwell assays do not incorporate ECM in the transwell insert. Hence, the cells only need to migrate through the transwell membrane to reach their destination. This does not accurately reflect the *in vivo* scenario, in which cells are surrounded by a dense extracellular matrix that hinders their movement. In recent years, some transwell assays have been upgraded so that cells need to migrate through a 10 μm Matrigel layer in addition to the membrane. However, this 10-μm layer is much thinner than the tissues inside the body. Moreover, type I collagen, a major component of stromal ECM *in vivo*, is missing in Matrigel (13).

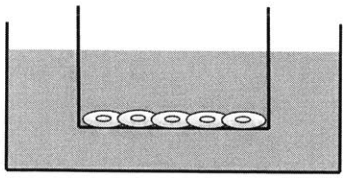

- End-point Readout
  - ↓ Speed; ↑ Persistence
  - =
  - ↑ Speed; ↓ Persistence
- Population Average Readout
  No info. on subpopulation of cells
- Do not mimic *in vivo* environment

Fig. 2.1: Shortcomings of transwell assays. Transwell assay provides an end-point, population-average read out. It does not give its user any information on the temporal dynamics of cell migration (e.g. speed and persistence), nor any information on whether a subpopulation of cells behaves differently from the rest. Finally, the transwell assay does not mimic the *in vivo* environment, since ECM is usually not incorporated in the insert of the transwell.

In recent years, the advent of live-cell imaging has allowed scientists to observe and quantify the temporal dynamics (speed and persistence) of cell migration. However, most of these migration experiments are performed with cells cultured on 2D petri dishes. These plastic petri dishes do not contain any ECM molecules present *in vivo*, and they are also much stiffer than the tissues in the body. Since ECM is a crucial barrier to cell migration *in vivo*, and substrate stiffness can affect cell migration (14), these 2D migration experiments produce results that often do not reflect the *in vivo* scenario.

The shortcomings in the traditional cell migration assays highlight the need for a sophisticated *in vitro* system that can mimic key aspects of *in vivo* conditions, while at same time allows its user to study the migration process in a controlled and reproducible manner. Microfluidic technology has recently emerged as a new tool to model cell migration processes, and many microfluidic cell migration assays have been developed to address the limitations of traditional assays. These microfluidic systems generally contain a cell culture micro-chamber connected to micro-channels containing growth media. These systems allow the users to apply a controlled chemical or mechanical stimulus to cells cultured in a physiologically relevant microenvironment. For example, user-defined fluid flow can be generated through the micro-channels to quantify the effects of fluid forces on cell migration (15). Moreover, spatially controlled complex chemokine gradients can be established to study how cells migrate in response to chemoattractants (16). Cells can also be seeded with extracellular matrix that mimics the *in vivo* tissues (17). Different cell types can also be arranged in the microfluidic devices in a configuration that mimics their organization within the body (18). Finally, since microfluidic systems are fabricated with polydimethylsiloxane (PDMS), a polymer that is transparent and gas permeable, live-cell imaging can easily be performed on samples

cultured within the microfluidic systems (19). Moreover, the small thickness (~microns) of the microfluidic system facilitates the high-resolution confocal imaging of 3D samples cultured within the device. All in all, microfluidic systems are perfect platforms for studying the complex processes of cell migration in a physiologically relevant environment with precise controls of experimental conditions.

2.3: Microfluidic Device Design and Fabrication

2.3.1: Microfluidic Static Platform Design

Two different microfluidic platforms (static platform and flow platform) were used in this thesis. To investigate the effects of macrophages on cancer cell migration dynamics under static (no-flow) conditions, we utilized the static platform previously developed by our laboratory (19) (Fig. 2.2). This microfluidic system is fabricated by plasma-bonding a PDMS slab with micro-features to a 0.16 mm glass coverslip. The device contains two microchannels that are 1.5 cm in length, 500 μm in width, and 120 μm in height. Each microchannel is connected to two media ports that are 3 mm in diameter. Growth media can be introduced into the microchannels through these ports. A cell culture chamber that is 1 cm in length, 1.3 mm in width, and 120 μm in height is positioned in between the microchannels. Collagen I gel can be introduced into the cell culture chamber through 1.2 mm gel-filling ports to mimic the ECM surrounding cancer cells, since Type I collagen is the most abundant component of ECM in the tumor microenvironment (20). Cancer cells and macrophages were suspended, in 3D fashion, in the collagen gel to mimic the *in vivo* condition. The microchannels are connected to the cell culture chamber, so growth media can be supplied to the cells seeded in the gel.

The cell culture chamber is lined with an array of 72 PDMS micro-posts, 36 on each side. These posts keep collagen I gel in the chamber during the gel filling process, and prevent the gel from leaking into the microchannels through surface tension. The geometries of the posts and the inter-post distance were design to maximize this surface tension. The height of cell culture chamber was designed to be only 120 μm to facilitate the imaging of the cells suspended in the 3D ECM by confocal microscopy. To further facilitate the imaging of the cell culture chamber, the coverslip used to fabricate the device is thin (0.16 mm). The cell culture chamber design, combined with the fact that PDMS is fully transparent and gas permeable, allows this PDMS microfluidic system to be used for high-resolution time-lapse observation of cancer cell-macrophage interactions and the quantification of the temporal dynamics of migration.

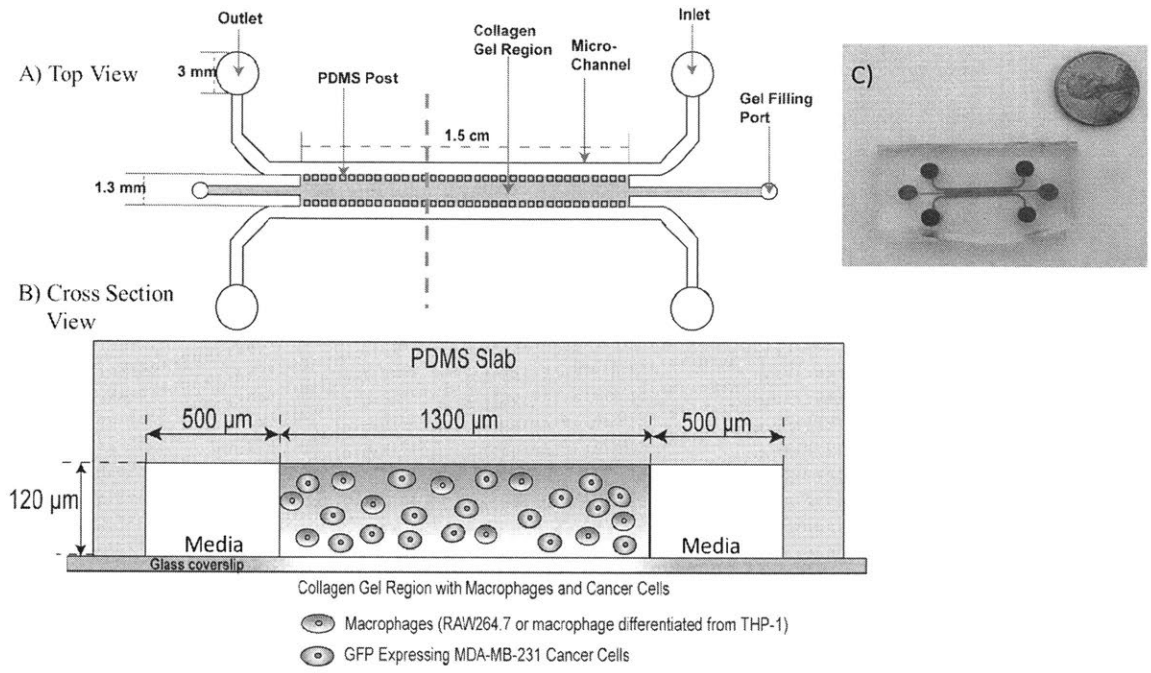

Fig. 2.2: Microfluidic static platform for studying macrophage-assisted cancer cell migration under static (no-flow) conditions. Schematics showing the top view **(A)** and cross sectional view **(B)** of the microfluidic device. This microfluidic device consists of a collagen I gel flanked by two micro-channels containing growth media (A). Cancer cells (green) and macrophages (red) were suspended in 3D collagen I ECM (orange) (B). **(C)** Photograph of the microfluidic static platform.

2.3.2: Microfluidic Flow Platform Design

To study the effects of interstitial flow (IF) on macrophage migration, we developed a novel PDMS microfluidic flow platform that allows for precise manipulation of interstitial fluid flow through a collagen I ECM seeded with macrophages. This system consists of a bottom layer containing a microfluidic device and a top layer containing two large media reservoirs (Fig. 2.3). The bottom layer of this system has similar design to the static platform. It contains a cell culture chamber sandwiched between two micro-channels connected to 3 mm media ports. However, the size of the cell culture chamber is drastically reduced compared to the static platform. Specifically, the micro-channel and the cell culture chamber are both 2.31 mm in length, 500 µm in width, and 200 µm in height. The chamber is separated from the micro-channels by an array of 10 PDMS micro-posts, five on each side. Macrophages suspended in the collagen I gel were introduced into the cell culture chamber through the gel-filling ports. Except for the micro-posts, the boundary of the collagen gel is in direct contact with the media in the micro-channels.

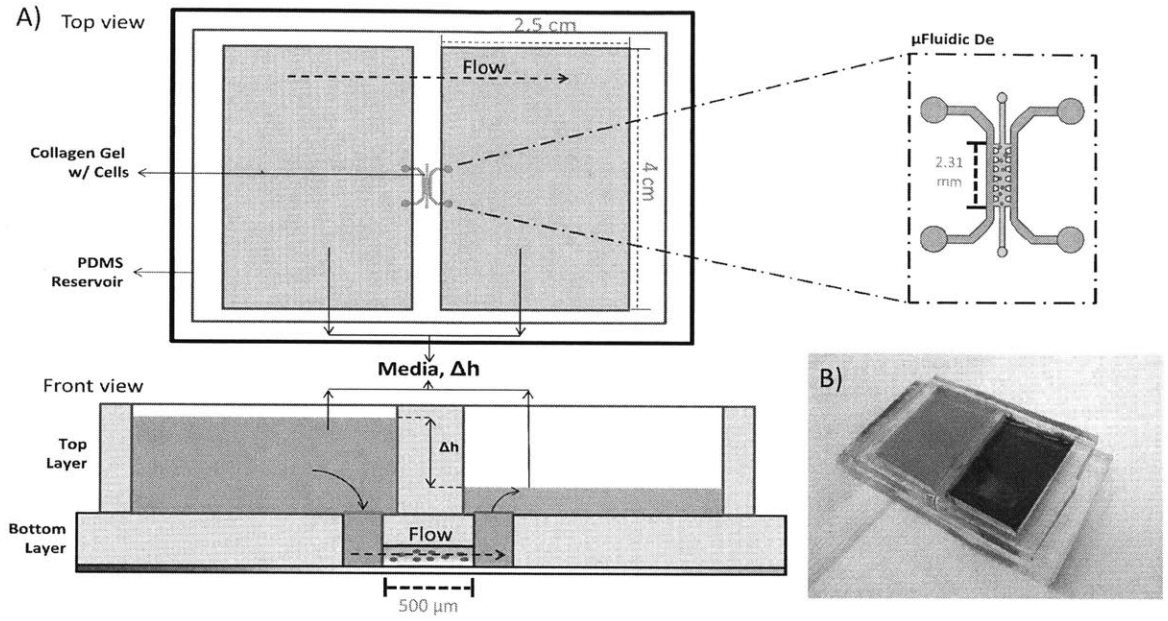

Fig. 2.3: Microfluidic flow platform for studying interstitial flow-directed macrophage migration. **(A)** Schematic of the two-layered microfluidic flow platform. The bottom layer consists of a microfluidic chamber containing 3D collagen I ECM seeded with macrophages. The top layer contains two media reservoirs, from which hydrostatic pressure gradient can be established by media-height differences. The hydrostatic pressure difference drives an IF of 3 μm/s through the ECM containing macrophages. (**B**) Photograph of the microfluidic flow platform.

The top layer of the flow platform is comprised of two large media reservoirs (2.5 cm x 4 cm), in which hydrostatic pressure gradient, generated by media-height difference, can be established between the reservoirs. Since the micro-channels are connected to the reservoirs through the 3 mm media ports, this pressure gradient can be transmitted through the collagen gel containing macrophages, resulting in an interstitial fluid flow through the gel. The velocity of this interstitial flow can be controlled by varying the media-height difference according to Darcy's law (see Eq. 1 in Section 2.6). Moreover, the cross-sectional area of the media reservoirs is designed to be 2000 times that of the collagen gel to ensure that no appreciable changes (~6%) in media-height difference and IF velocity were observed during the course of the experiment (see Eq. 2 in Section 2.6). Therefore, this PDMS flow platform allows us to precisely control the interstitial fluid flow through the 3D collagen ECM containing cells, while simultaneously monitor the migration dynamics of the cells through live-cell imaging. All in all, both static and flow platforms satisfy the criteria, outlined in previous section, for excellent experimental systems to study cell migration.

2.3.3: Microfluidic Platform Fabrication

The static platform, as well as the bottom layer of the flow platform, was assembled according to previously described methods using soft lithography (21, 15). Briefly, PDMS pre-polymer (Dow Corning) was mixed with curing agent (Dow Corning) at a ratio of 10:1. The mixture was poured over a silicon wafer containing the features of the microfluidic devices and cured overnight at 80 °C. The cured PDMS slab containing the features was removed from the silicon wafer. The media reservoirs and gel filling ports were subsequently fabricated using 3 mm and 1.2 mm biopsy punches, respectively. The PDMS slabs were autoclaved and dried overnight in an 80 °C oven. The microfluidic device was assembled by treating the sterile PDMS slab with plasma (Harrick Plasma) for 90 secs before binding it to a sterile coverslip (Corning). The device was then coated with 1 mg/mL poly-D-Lysine (PDL), washed, and dried in the 80 °C oven overnight. The positively charged PDL enhances the binding of negatively charged collagen I ECM to the surfaces of the cell culture chamber. Moreover, overnight drying helps the device to recover its hydrophobicity so that collagen I gel can be contained within the cell culture chamber during the gel filling process.

2.4: Cell Seeding in the Microfluidic Devices

In order to set up the microfluidic assays, macrophages and/or cancer cells have to be incorporated into the collagen I ECM embedded in both static and flow platforms. Considerable effort has been made to optimize the cell seeding protocol. Briefly, cancer cells or macrophages were harvested from tissue culture plates with 0.05% trypsin or a cell lifter, respectively. Cancer cells and/or macrophages were suspended in 2.5 mg/mL rat-tail collagen I ECM (BD Bioscience), and the collagen gel containing cells was carefully injected into the cell culture chamber through the gel filling port. The collagen gel was allowed to polymerize for 30 min at 37 °C and pH of 8-8.5. During the polymerization process, the device was flipped to prevent cells from settling to the bottom of the device, thus ensuring all cells were distributed evenly along the z-axis in the 3D ECM. After polymerization, fresh growth media were introduced into the micro-channels through the media reservoirs. The cells were incubated at 37 °C and 5% CO_2 overnight. To study the effects of macrophages on cancer cell migration, $2.3x10^6$ cells/mL of cancer cells and/or $0.92x10^6$ cells/mL of macrophages treated with Cell Tracker Red CMTPX (Invitrogen) were seeded in the static platform. In contrast, $1.3x10^6$ of macrophages were seeded in the flow platform to study the effects of interstitial flow on macrophage migration.

Multiple types of cancer cells and macrophages were used in our study to ensure that our results can be generalized. GFP expressing MDA-MB-231 (MDA231) human breast carcinoma cells (gift from Dr. Frank Gertler, MIT), PC3 human prostate carcinoma cells (ATCC), Du145 human prostate carcinoma cells (ATCC), and MDA-MB-435S (MDA435) human melanoma cells (ATCC) were used as model cancer cells. For macrophages, Raw 264.7 (Raw) mouse macrophages (ATCC), as well as primary murine

bone marrow-derived macrophages (BMDM) and human monocyte-derived macrophages (MDMΦ), were used. MDA231, MDA435, and Raw cells were cultured in DMEM. PC3 and Du145 cells were cultured in RPMI. Media were supplemented with 10% fetal bovine serum (FBS, invitrogen) and 100 U/mL penicillin/streptomycin (Sigma). Cell lines were authenticated using Short Tandem Repeat profiling (Promega).

To generate primary bone marrow-derived macrophages (BMDM), bone marrow cells were first isolated from freshly dissected femurs of C57BL/6 mice. These cells were then differentiated in RPMI supplemented with 10% FBS, 100 U/mL penicillin/streptomycin, 1% HEPES (Invitrogen), 40 ng/mL MCSF (Peprotech) and 50 μM β-Mercaptoethanol (Sigma) for 7 days to produce BMDM. Primary human monocyte-derived macrophages (MDMΦ) were generated from monocytes isolated from whole blood (Research Blood Component) using a Ficoll-Paque gradient (GE). Monocyte population was enriched using the EasySep™ Monocyte Enrichment Kit (StemCell Tech.), and cultured with IMDM (Lonza) supplemented with 2% L-glutamine (Invitrogen) and 2% AB serum (Sigma) for 7 days to generate MDMΦ. All cells were cultured in a humidified incubator at 5% CO_2 and 37 °C. The primary macrophages were used immediately for experiments.

2.5: Microfluidic Cell Migration Assay

Microfluidic cell migration assay was performed using the static platform to evaluate the effects of macrophages on cancer cell migration dynamics. Briefly, after overnight incubation, live-cell imaging was performed on the cells cultured in the static platform. A glass coverslip was first gently placed on top of the microfluidic device. This is performed to ensure that the microfluidic device will not dry out during the live-cell imaging process. The device was then moved onto a fluorescent microscope (Zeiss) fitted with a humidified environmental chamber operating at 37 °C and 5% CO_2. Time-lapse microscopy was employed to record cell movement in the collagen I ECM. Fluorescent and phase contrast images were taken every 15 mins for 18 hrs with a focus at the mid-plane of the gel along the z-axis. This is to ensure all the cells that were tracked for analysis were truly migrating in 3D ECM, not on the glass bottom or PDMS top surface. Cancer cells were distinguished from macrophages either by the GFP signal in the cytosol of cancer cells (when MDA231 cells were used) or by the CMPTX signal in macrophages. Images obtained from time-lapse microscopy were saved for later analysis (See Section 2.7).

To evaluate the effects of macrophages on cancer cell migration, we set up two experimental groups using the microfluidic migration assay. The control group, which contains cancer cells cultured in collagen I ECM alone, was compared to the treatment group with cancer cells and macrophages co-cultured in the collagen I ECM. To study the molecular mechanisms of the observed effects, we treated cells with various neutralizing antibodies, small molecule inhibitors, and growth factors. A detailed list of these reagents can be found in Appendix A.

2.6: Microfluidic Interstitial Flow Migration Assay

We used the flow platform described previously to perform microfluidic interstitial flow experiments. This flow assay was carried out to investigate the effects of interstitial flow on macrophage migration. In this section, we will describe the methods to model interstitial flow using Darcy's law, establish interstitial flow, validate interstitial flow velocity, and monitor cell migration.

2.6.1: Interstitial Flow Calculation and Hydraulic Permeability Estimation

As discussed in Section 2.3.2, the interstitial fluid flow was induced through the collagen I ECM containing macrophages by establishing and maintaining a media-height difference across the top layer of the flow platform. The media-height difference needed to induce a desirable velocity of interstitial flow can be determined by Darcy's law. This law describes the relationship between pressure drop *(ΔP)* and volumetric flow rate *(Q)* across a collagen gel scaffold:

$$\frac{Q(t)}{A} = \frac{K}{\mu}\frac{\Delta P(t)}{W} \quad (Eq.1)$$

where hydraulic permeability is K, viscosity is μ, surface area of the gel is A, and length of the gel scaffold in the direction of the flow is W (22). Since hydrostatic pressure gradient is related to media-height differences (Δh) in the microfluidic system, Darcy's law can be transformed and integrated to describe the change in interstitial flow velocity (v) over time in the microfluidic device (22):

$$v(t) = \frac{\rho g K \Delta h_0}{\mu W} e^{-\frac{2K\rho g A}{\mu W A_r}t} \quad (Eq.2)$$

where ρ is density of the media, A_r is the cross-sectional area of the reservoirs, and Δh_0 is the initial media height difference of the reservoirs (22). From this equation, we can calculate media-height difference (Δh_0) required to establish the pressure gradient to drive a desirable interstitial flow velocity in the device:

$$\Delta h_0 = \frac{v\mu W}{K\rho g} \quad (Eq.3).$$

However, as shown in Eq. 3, we need hydraulic permeability to calculate the media-height difference. Hydraulic permeability is an intrinsic property of a hydrogel that depends on the pore size and fiber density of the gel. This property needs to be empirically determined.

Darcy's law was used to estimate the hydraulic permeability of the 2.5 mg/mL collagen I ECM according to protocols described previously. Briefly, plastic media reservoirs were connected to the microfluidic device, and a media-height difference (Δh) of 1.5 cm was established to introduce a pressure drop across the 2.5 mg/mL collagen I gel scaffold. As the media flowed through the collagen gel, the drop in the media level in the high-pressure reservoir was monitored over time. Since Darcy's law can be re-written to show the change in volume of media in the reservoir (ΔV) over time:

$$\frac{2K\rho gA}{\mu W A_r}t = -\ln\left(1 - \frac{2\Delta V(t)}{A_r \Delta h_0}\right) \quad (Eq.4)$$

, we plotted "$-\ln\left(1-\frac{2\Delta V(t)}{A_r\Delta h_0}\right)$" versus time. Hydraulic permeability (K) was subsequently calculated from the slope of the plot. Based on the measured change in media level and the geometry of the microfluidic device, the hydraulic permeability of the 2.5 mg/mL of collagen I gel scaffold was determined to be **~7x10^{-14} m^2**.

According to the geometry of the gel scaffold in the microfluidic device, as well as the measured hydraulic permeability, the media-height difference needed to induce a ~3 μm/s interstitial flow in the microfluidic flow platform was estimated to be 1.5 mm. The change in the interstitial flow velocity over time was calculated using Eq. 2. We estimated that since the area of media reservoirs (A_r) is ~2000 times that of collagen gel (A), the change in IF velocity should be negligible (6%) in an 18-hr experiment. We tested this hypothesis by empirically measuring the changes in interstitial flow velocity over time, as shown in the following section.

2.6.2: Establishing and Measuring Interstitial Flow

After seeding macrophages into the bottom layer of the flow platform, the microfluidic device was incubated at 37 °C and 5% CO_2 overnight. Subsequently, this bottom layer was sealed against a PDMS layer containing two large (2.5 cm x 4 cm) media reservoirs (top layer) that were surface activated by plasma for 10 minutes. A media-height difference of 1.5 mm was established between the two reservoirs to generate a hydrostatic pressure gradient (~15 Pa) across the gel region, which we estimated, based on the measured collagen gel hydraulic permeability of 7x10^{-14} m^2, to drive interstitial fluid flow with a mean velocity of ~3 μm/s through the collagen gel containing macrophages. We chose the velocity of 3 μm/s to match the level of IF in the tumor tissues measured *in vivo* (23). In addition, the media-height difference of 1.5 mm was established by supplying 6.5 mL of growth media to one reservoir and 5 mL of growth media to the other. Since the cross-sectional area of the reservoirs is 10 cm^2, the media-volume difference of 1.5 mL created a media-height difference of 1.5 mm.

The velocity of the interstitial flow was also experimentally measured. To quantify the velocity of the IF, 200 nm FITC-conjugated micro-beads (Invitrogen) were introduced to the upstream reservoir (reservoir with higher pressure). The media-height

difference of 1.5 mm was established as previously described. The movement of the micro-beads through the collagen I ECM was recorded using a fluorescent microscope (Nikon). Image J (NIH) was used to track the bead movement, and Ibidi Chemotaxis and Migration software (Ibidi) was used to quantify the velocity of beads flowing in the 3D ECM. Using this method, we verified that interstitial flow velocity established in our experiments was indeed ~3 μm/s. Moreover, we determined that even after 18-hr of interstitial flow treatment, interstitial flow velocity remains at ~3 μm/s (Fig. 2.4).

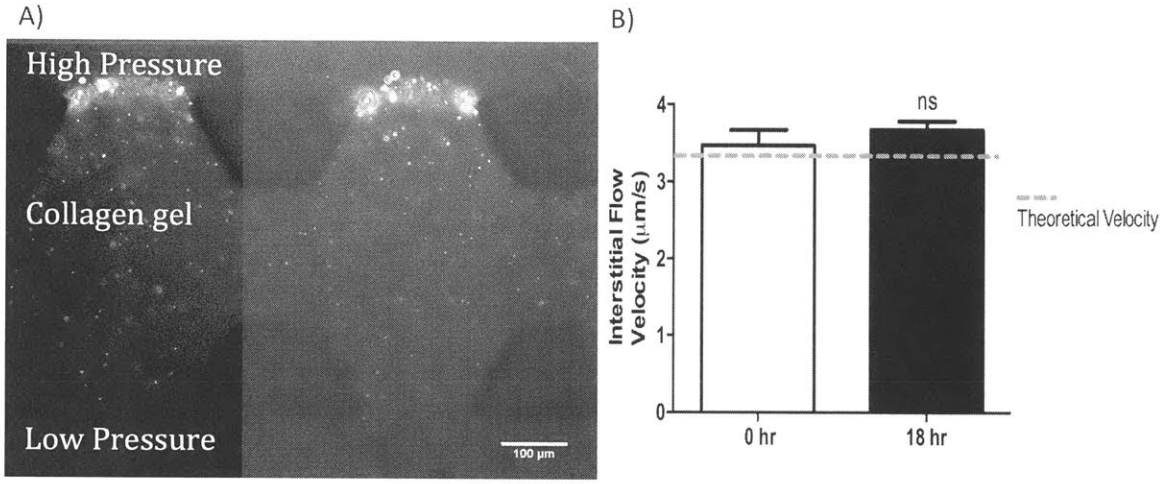

Fig. 2.4: Interstitial flow velocity measurement. (A) To validate the interstitial flow velocity used in the microfluidic flow assay, time-lapse microscopy was used to track the movement of fluorescent micro-beads (200 nm) through the collagen gel in the device. The micro-beads were introduced into the media in the high-pressure channel. **(B)** Quantification of micro-beads movement shows that a media-height difference of 1.5 mm resulted in an IF velocity of 3.47 μm/s, similar to theoretical velocity obtained from Darcy's law (red line; 3.34 μm/s). After 18 hours of the flow treatment, the movement of fluorescent micro-beads was tracked again, and the flow velocities of the beads were again quantified. The interstitial flow velocity measured after 18-hr flow treatment remains around 3.47 μm/s. Bars represent mean ± SEM of data (n=3, n=# of independent experiments; ns=not significant).

2.6.3: Monitor Cell Migration

Immediately after the establishment of the flow, the microfluidic flow system was transferred to a light microscope (Zeiss) fitted with a humidified environmental chamber operating at 37 °C and 5% CO_2. A microscope slide was placed on top of the media reservoirs to prevent the evaporation in the humidified chamber. The macrophages were treated with IF for a total of 18 hrs. Time-lapse microscopy was used to record the movement of macrophages in the 3D ECM. Phase contrast images were taken every 2 mins for 18 hrs with a focus at the mid-plane of the gel along the z-axis. To ensure that macrophages had enough time to respond to the IF, only the last 10 hrs of the 18 hrs movie were used for analysis.

2.7: Quantification of Cell Migration

For both microfluidic migration assays, Image J (NIH) was used to track the movements of the cells in the 3D ECM to produce cell trajectory plots. For Aim 1 of the thesis, cancer cell migration was tracked and quantified. In contrast, macrophage migration was quantified for Aim 2 of the thesis. From the cell trajectory plots, we quantified cell migration total speed (total distance cell travelled divided by migration time) and migration directedness (ratio between displacement and total distance travelled) using Ibidi Chemotaxis and Migration software (Ibidi) (Fig. 2.5). Migration total speed

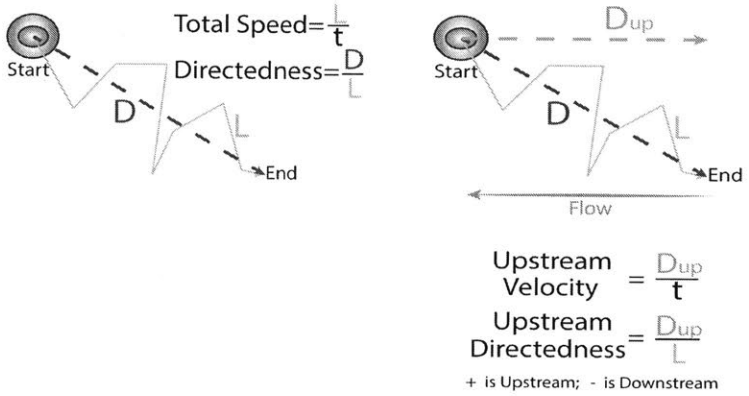

determines how fast a cell moves, while directedness determines the persistence of cell movement.

Fig. 2.5: Definition of Migration Dynamics. (Left) Definition of cell migration total speed and directedness. L represents total migration distance; D represents net displacement; t represents time. Total speed is L/t, while directedness, a measure of persistence, is D/L. **(Right)** Definition of upstream velocity and upstream directedness (+ upstream, - downstream, 0 no preference) used to quantify the upstream migration of macrophages. Upstream velocity is defined as the displacement of cell against flow direction (D_{up}) divided by the migration time (t). Upstream directedness is defined as D_{up} divided by the total distance (L).

For interstitial flow study, additional migration metrics were used to quantify the migration of macrophages under flow. For instance, we calculated upstream velocity (length of the displacement vector against the direction of flow divided by migration time) and upstream directedness (ratio between the length of the displacement vector against the direction of flow and total distance travelled), which quantify the directional migration of macrophages (Fig. 2.5). Numbers of the cells that travelled upstream (against flow direction) and downstream (with flow direction) were also quantified. Finally, the angle of the displacement vector of each cell was quantified to generate Rose plots.

2.8: Transwell Flow Assay

To study the effects of interstitial flow on macrophage protein expression, we need to perform Western blot analyses on cell lysates. For an accurate detection of protein expression level with Western blot, a large volume of cell lysate, usually collected from around a million cells, is required. Since each microfluidic device only contains a few thousand cells, the microfluidic flow assay is not suitable for studying the effects of interstitial flow on macrophage protein expression. To circumvent the problem of low cell number, we developed a transwell flow chamber. This chamber consists of a large transwell insert (diameter=24 mm, Falcon) situated in a well of the six-well plate. Macrophages were suspended inside the collagen I ECM in the transwell insert. A media-height difference was established between the inside and the outside of the insert, which created a hydrostatic pressure gradient (fluid pressure inside the insert is higher than outside the insert) that drove an interstitial flow through the gel seeded with macrophages. To maintain this media-height difference, a positive displacement pump is connected to the transwell system that re-circulates media from the outside to the inside of the insert (Fig. 2.6).

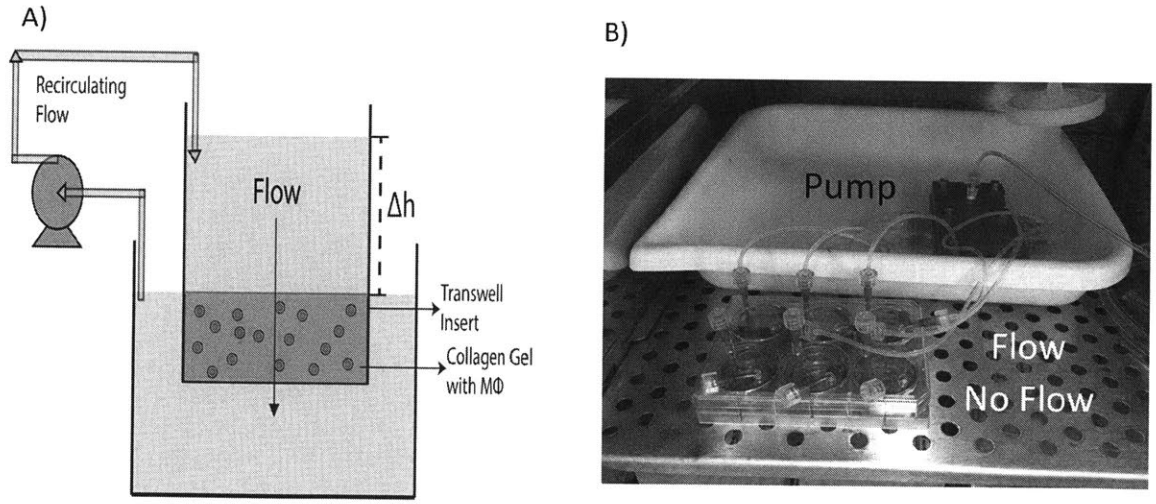

Fig. 2.6: Transwell flow chamber. **(A)** Transwell flow chamber used to study the effects of IF on macrophage protein expression. This chamber consists of a transwell system that is connected to a re-circulating pump, maintaining a media-height difference and hydrostatic pressure gradient that drives IF through a collagen gel containing macrophages. **(B)** Photograph of transwell flow chamber connected to the pump. Six flow chambers can be placed into one six-well plate. Flow was introduced in three of the six chambers, while the other three chambers serve as no-flow control.

We calculated the media-height difference that is required to produce 3 μm/s interstitial flow in the transwell system. Since the flow of interstitial fluid through collagen I ECM situated in the transwell insert is again governed by Darcy's law, Eq. 3 was used to calculate the media-height difference (Δh_0) necessary to achieve a desirable interstitial flow velocity (v) in the transwell flow chamber. Based on this equation, as well as the previously measured hydraulic permeability (K) and the length of the collagen gel in the transwell, the media-height difference needed to establish a 3 μm/s interstitial flow in the transwell flow chamber is ~10 mm.

We also tested the ability of the re-circulatory pump to maintain the media-height difference. As shown in Fig. 2.7, without media recirculation, the height difference between inside and outside of the insert is reduced to zero in an hour. However, when the transwell system is connected to the pump, the media-height difference, and thus interstitial flow, can be maintained for 360 mins. Subsequent experiments demonstrate that this media-height difference can be maintained for at least 48 hours in the transwell flow chamber. Furthermore, we verified that fluid pressure inside the insert did not significantly compress the collagen I ECM, as collagen I gel treated with flow has similar height and fiber density as that of the gel that was not treat with flow (Fig. 2.8). This result suggests that forces due to compression do not significantly affect macrophages seeded in our system.

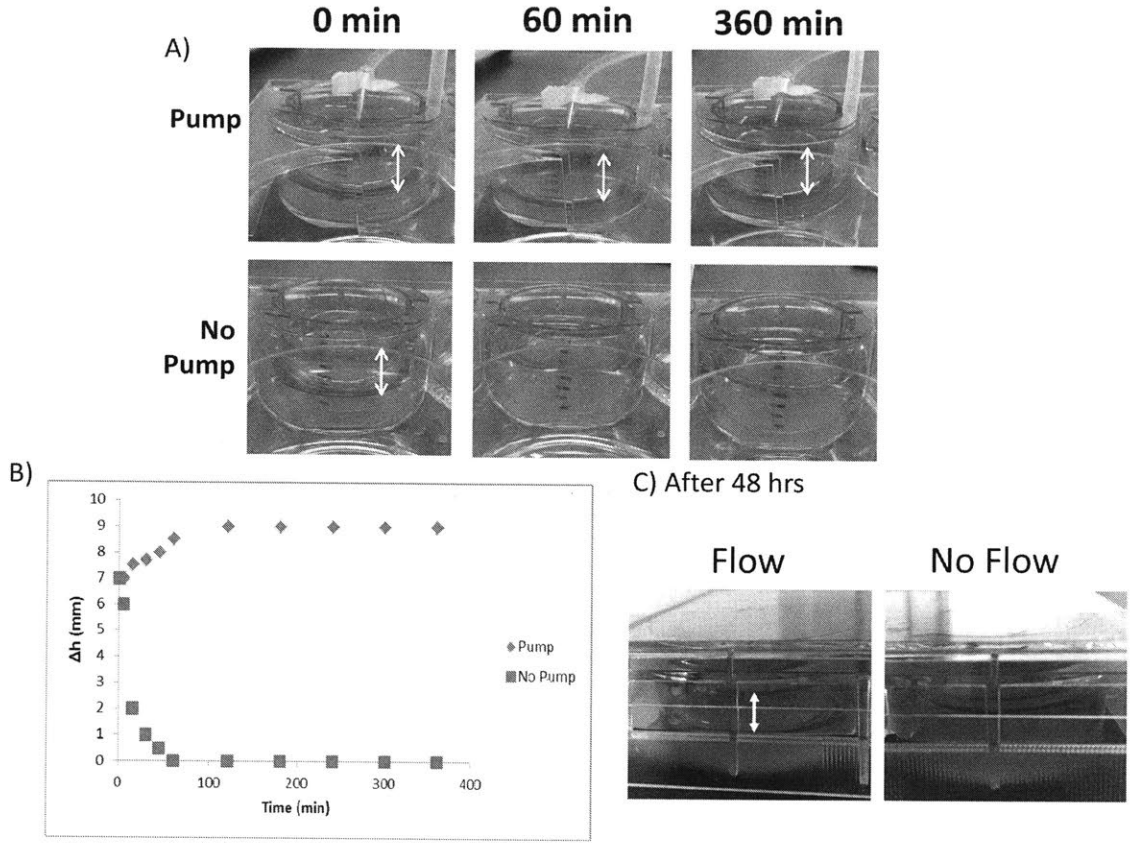

Fig. 2.7: Recirculating pump maintains the media-height level differences. **(A)** Pictures showing that recirculating pump maintains a media-height level difference in the transwell chambers. **(B)** Quantification of media-height level differences over time showing that when the transwell system was connected to the pump, media-height difference was maintained at 9 mm for at least 360 mins. However, when the transwell system was not connected to the pump, the height difference dropped to zero in 60 mins. **(C)** After 48 hours of interstitial flow treatment with the transwell flow chamber, the media-height difference in the chamber is still maintained.

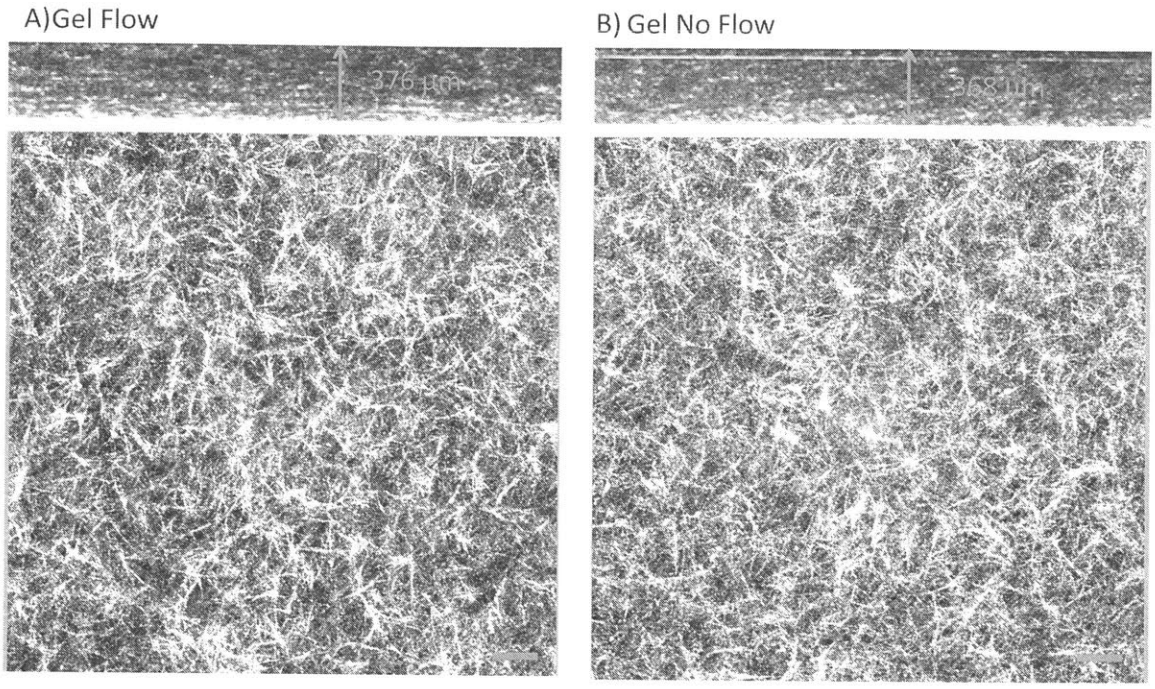

Fig. 2.8: High fluid pressure inside the transwell insert does not compress the collagen gel in the transwell flow system. A 10 mm media-height difference was maintained over a 2.5 mg/mL collagen gel in the transwell flow chamber for 48 hours. Confocal reflectance images (scale bars=50 µm) of the collagen gel were taken to compare the height, as well as the structures, of the collagen I gel treated with interstitial flow **(A)** with that of the gel not treated with flow **(B)**. No significant change in the height of collagen I gel (top) or the fiber density of the gel (bottom) was observed when the gels were treated with interstitial flow for 48 hours. This indicates that the method we used to induce interstitial flow through the collagen gel does not compress the gel.

To set up the transwell flow assay, 800,000 cells/mL of Raw 264.7 macrophages were seeded in a 2.5 mg/mL collagen I gel contained inside the transwell insert (Falcon). The collagen scaffold containing the cells was allowed to polymerize in a humidified incubator for 30 mins at 37 °C and pH of 8. Following the polymerization, transwell inserts were placed into a six-well plate and supplied with growth media. The cells were cultured for 24 hrs in a humidified incubator at 5% CO_2 and 37 °C.

To treat macrophages with IF, growth media were added to the inside of the transwell insert to establish a media-height difference of 10 mm between the inside and outside of the insert. This media-height difference contributes to a hydrostatic pressure difference that drives a flow of 3 µm/s through the collagen gel containing macrophages. To maintain the hydrostatic pressure difference, a pump was connected to the transwell system that continuously re-circulated media from the outside of the insert back into the inside of the insert. For the no-flow control group, same amount of media as the flow treatment group was added into the transwell system. However, instead of introducing the media only into the inside of the insert, the media was distributed equally between outside and the inside of the transwell insert so that no media-height difference was established. This procedure is done to ensure that although flow treatment and no-flow control groups receive same amount of growth media, media-height difference will only

be established in the control group. For the experiments that evaluated the effects of IF on protein expression, cells were treated with flow for 48 hrs. On the other hand, for experiments that evaluated the effects of IF on phosphorylation, cells were treated with flow for 15 min~60 min. With this transwell flow chamber, approximately two million cells per condition can be collected for western blotting analysis. When appropriate, macrophages in the transwell chamber were treated with various inhibitors and blocking antibodies to investigate the molecular mechanisms of the observed effects. A detailed list of these reagents, as well as concentrations used, can be found in Appendix B.

Finally, the microfluidic assays and transwell assay described here were used in combination with various other traditional techniques and assays. For a detailed description of the methodology used in this thesis, as well as a complete list of all the reagents, please see Appendix A and B.

2.9: References

1. Witz IP (2009) The tumor microenvironment: the making of a paradigm. *Cancer Microenviron* 2 Suppl 1:9–17.
2. Faltas B (2012) Cornering metastases: therapeutic targeting of circulating tumor cells and stem cells. *Front Oncol* 2:68.
3. Shieh AC, Rozansky HA, Hinz B, Swartz MA (2011) Tumor Cell Invasion Is Promoted by Interstitial Flow-Induced Matrix Priming by Stromal Fibroblasts. *Cancer Res* 71(3):790–800.
4. Lewis CE, Pollard JW (2006) Distinct role of macrophages in different tumor microenvironments. *Cancer Res* 66(2):605–12.
5. Polacheck WJ, Zervantonakis IK, Kamm RD (2012) Tumor cell migration in complex microenvironments. *Cell Mol Life Sci.* doi:10.1007/s00018-012-1115-1.
6. Wolf K, et al. (2013) Physical limits of cell migration: control by ECM space and nuclear deformation and tuning by proteolysis and traction force. *J Cell Biol* 201(7):1069–84.
7. Friedl P, Wolf K (2003) Tumour-cell invasion and migration: diversity and escape mechanisms. *Nat Rev Cancer* 3(5):362–74.
8. Goswami S, et al. (2005) Macrophages promote the invasion of breast carcinoma cells via a colony-stimulating factor-1/epidermal growth factor paracrine loop. *Cancer Res* 65(12):5278–83.
9. Polacheck WJ, Charest JL, Kamm RD (2011) Interstitial flow influences direction of tumor cell migration through competing mechanisms. *Proc Natl Acad Sci U S A* 108(27):11115–20.
10. Haessler U, Teo JCM, Foretay D, Renaud P, Swartz M a (2012) Migration dynamics of breast cancer cells in a tunable 3D interstitial flow chamber. *Integr Biol (Camb)* 4(4):401–9.
11. Tayalia P, Mazur E, Mooney DJ (2011) Controlled architectural and chemotactic studies of 3D cell migration. *Biomaterials* 32(10):2634–41.
12. Polacheck WJ, Zervantonakis IK, Kamm RD (2013) Tumor cell migration in complex microenvironments. *Cell Mol Life Sci* 70(8):1335–56.
13. Frantz C, Stewart KM, Weaver VM (2010) The extracellular matrix at a glance. *J Cell Sci* 123(24).
14. Shukla VC, Higuita-Castro N, Nana-Sinkam P, Ghadiali SN (2016) Substrate stiffness modulates lung cancer cell migration but not epithelial to mesenchymal transition. *J Biomed Mater Res Part A* 104(5):1182–1193.
15. Polacheck WJ, German AE, Mammoto A, Ingber DE, Kamm RD (2014) Mechanotransduction of fluid stresses governs 3D cell migration. *Proc Natl Acad Sci U S A* 111(7):2447–52.
16. Mosadegh B, et al. (2007) Generation of stable complex gradients across two-dimensional surfaces and three-dimensional gels. *Langmuir* 23(22):10910–2.
17. Chung S, et al. (2009) Cell migration into scaffolds under co-culture conditions in a microfluidic platform. *Lab Chip* 9(2):269–275.
18. Shin Y, et al. (2012) Microfluidic assay for simultaneous culture of multiple cell types on surfaces or within hydrogels. *Nat Protoc* 7(7):1247–59.
19. Zervantonakis IK, et al. (2012) Three-dimensional microfluidic model for tumor cell intravasation and endothelial barrier function. *Proc Natl Acad Sci* 109(34):13515–13520.
20. Fisher KE, et al. (2006) Tumor cell invasion of collagen matrices requires coordinate lipid agonist-induced G-protein and membrane-type matrix metalloproteinase-1-dependent signaling. *Mol Cancer* 5:69.
21. Polacheck WJ, Charest JL, Kamm RD (2011) Interstitial flow influences direction of tumor cell migration through competing mechanisms. *Proc Natl Acad Sci* 108(27):11115–11120.
22. Sudo R, et al. (2009) Transport-mediated angiogenesis in 3D epithelial coculture. *FASEB J* 23(7):2155–64.
23. Hompland T, et al. (2012) Interstitial fluid pressure and associated lymph node metastasis revealed in tumors by dynamic contrast-enhanced MRI. *Cancer Res* 72(19):4899–908.

Chapter 3: Effects of Macrophages on Cancer Cell Migration Dynamics

3.1: Abstract

This chapter contains contents from a manuscript entitled "**Macrophage-secreted TNFα and TGFβ1 Influence Migration Speed and Persistence of Cancer Cells in 3D Tissue Culture via Independent Pathways**" with authors *Ran Li, Jess Hebert, Tara Lee, Hao Xing, Alexandra Boussommier-Calleja, Richard Hynes, Douglas Lauffenburger, and Roger Kamm*. This manuscript is recently published in *Cancer Research*.

The ability of a cancer cell to migrate through the dense extracellular matrix (ECM) within and surrounding the solid tumor is a critical determinant of metastasis. Macrophages enhance invasion and metastasis in the tumor microenvironment but the basis for their effects is not fully understood. Using a microfluidic 3D cell migration assay, we found that the presence of macrophages enhanced the speed and persistence of cancer cell migration through a 3D extracellular matrix in a matrix metalloproteinases (MMP)-dependent fashion. Mechanistic investigations revealed that macrophage-released TNF α and TGF β 1 mediated the observed behaviors by two distinct pathways. These factors synergistically enhanced migration persistence through a synergistic induction of NF- κ B-dependent MMP1 expression in cancer cells. In contrast, macrophage-released TGF β 1 enhanced migration speed primarily by inducing MT1-MMP expression. Taken together, our results reveal new insights into how macrophages enhance cancer cell metastasis, and they identify TNF α and TGF β 1 dual blockade as an anti-metastatic strategy in solid tumors.

3.2: Introduction and Cancer Cell Migration Dynamics

As discussed in Chapter One, tumor microenvironment is a complex system that contains cancer cells, non-cancerous tumor-associated stroma cells, tumor-associated ECM, and tumor-associated biophysical factors. Within this microenvironment, ECM acts as a barrier to metastasis, and cancer cells have enhanced capabilities to navigate through the dense 3D collagen ECM surrounding the tumor (1). To migrate through the ECM, cancer cells employ proteases such as matrix metalloproteinases (MMPs) to degrade ECM, kinases to assist in forming protrusions, and integrins to adhere to the matrix to enable movement (2). Indeed, the activities and/or expressions of these molecules have been shown to be elevated in cancer cells (3–5).

Tumor-associated macrophages have recently emerged as a key regulator of tumor growth and metastasis. Various clinical data have revealed that the infiltration of macrophages in tumor tissues correlates with poor prognosis in cases of breast cancer, prostate cancer, and melanoma (6, 7). Moreover, *in vivo* and *in vitro* studies have shown that macrophages enhance cancer cell intravasation (8, 9) and invasion through various

signaling pathways (10, 11). However, many of these *in vitro* migration studies were performed on 2D tissue culture substrates, which fail to capture the 3D microenvironment present *in vivo*. In addition, the majority of these studies were carried out using transwell assays, which only yield an end-point readout of cell behaviors (12) and thereby provide little information on how macrophages affect different aspects of cancer cell migration, such as how fast or how persistently the cancer cell moves. These distinct features of migration (speed vs. persistence) describe cell migration dynamics, and they can be quantified using metrics such as total speed and directedness. Total speed (the total distance that cell migrated divided by the migration time) defines how fast a cancer cell migrates. In contrast, directedness (the ratio of cell displacement to the total distance that the cell travelled) measures the persistence of the cell movement (12, 13).

Cell migration dynamics, the subtle details of cell migration behaviors, are important, but frequently overlooked, concepts. Recently, it has become increasingly clear that migration dynamics, such as speed and persistence, determine the metastatic potential of a cancer cell (14), and stimuli that increase both of these factors can greatly enhance metastasis. More importantly, speed and persistence can be modulated independently of one another by a single stimulus. For example, inhibiting integrin has been shown to decrease cancer cell migration speed but has no effect on persistence (14). On the other hand, interstitial flow can increase cancer cell migration persistence without altering the speed of migration (15). Lending further complexity, a stimulus can affect speed and persistence of migration differently when cells are cultured on 2D substrates compared to in 3D matrix. Specifically, EGF has been shown to increase cancer cell migration speed and decrease persistence when cells are migrating on 2D surfaces. However, this same growth factor enhances both cancer cell migration speed and persistence when cells are cultured in 3D ECM (16). **Collectively, these results highlight the importance of characterizing how a stimulus affects different aspects of cancer cell migration (i.e. speed and persistence) in 3D ECM to gain a detailed and quantitative understanding of metastasis. However, to our knowledge, the effects of macrophages on the dynamics (speed and persistence) of cancer cell migration in 3D ECM have not been explored.**

In the present study, we employed a microfluidic 3D migration assay to examine how macrophages affect different aspects (speed and persistence) of cancer cell migration. This microfluidic assay allows us to perform real-time high-resolution imaging of cancer cells migrating in 3D collagen I ECM in the presence of macrophages, which recapitulates key aspects of their interactions in the primary tumor sites *in vivo*. By tracking the movement of cancer cells within the 3D ECM, we can evaluate the effects of macrophages on the dynamics of cancer cell migration in a more physiologically relevant environment than 2D *in vitro* assays. In addition, this microfluidic assay is better suited for the detailed mechanistic study of macrophage-assisted cancer cell migration than *in vivo* assays (such as intravital imaging), as it is easier to operate and offers a tightly controlled experimental environment. Using this microfluidic assay, we show that macrophages release TNFα and TGFβ1 that increase both migration speed (total speed) and persistence (directedness) of cancer cells in 3D ECM. Interestingly, macrophage-released TNFα and TGFβ1 were found to promote cancer cell migration speed and

persistence through two different mechanisms. Specifically, macrophages enhance cancer cell migration speed mainly through TGFβ1-induced MT1-MMP expression in cancer cells. In comparison, macrophage-released TNFα and TGFβ1 synergistically enhance cancer cell migration persistence via NF-κB-dependent MMP1 expression. These results demonstrate, for the first time, that speed and persistence of cancer cell migration in 3D can be modulated by macrophages via different pathways, which strongly suggests that both of these pathways need to be targeted to effectively mitigate macrophage-induced metastasis.

3.3: Methods

To study the effects of macrophages on cancer cell migration speed and persistence, we utilized the microfluidic 3D migration assay discussed in the Chapter Two. Cancer cells (MDA-MB-231 GFP breast carcinoma cells, MDA-MB-435S melanoma cells, and PC3 prostate cancer cells) were seeded with or without macrophages (Raw 264.7 macrophages, primary murine bone marrow-derived macrophages, and primary human monocyte-derived macrophages) inside a 2.5 mg/mL collagen I ECM embedded in the microfluidic devices. The migration of cancer cells was tracked over time (18 hrs) to produce migration trajectory. From the trajectory, cancer cell migration total speed and directedness were computed. Total speed measures how fast a cancer cell migrates, while directedness measures the persistence of cell migration. The mechanisms behind macrophages' effects on cancer cell migration were investigated using various biochemical assays. For a detailed description of the experimental procedures and assays used in this study, please see Chapter Two and the Appendix A.

All statistical analyses were performed using GraphPad Prism with a P-value of <0.05 considered statistically significant. The difference between groups was evaluated by two-tailed student t-test or one-way ANOVA. In all figures, ns represents not significant, * represents $p<0.05$, ** represents $p<0.01$, and *** represents $p<0.001$. For cell migration quantification, bars represent mean ± standard error of mean (SEM) of data from 40-100 cells from 3 independent experiments. For western blot and qRT-PCR quantification, bars represent mean ± SEM of data (fold increase relative to no-treatment or mono-culture control) from at least 3 independent experiments.

3.4: Macrophages enhance cancer cell migration total speed and directedness in 3D ECM

To determine the effects of macrophages on the dynamics of cancer cell migration in 3D matrix, we tracked the movement of cancer cells inside the collagen I ECM in the microfluidic devices. We chose to use collagen I ECM to mimic the tumor matrix since collagen I has been shown to be the major component of tumor-associated stromal tissue (1, 17) and it has also been implicated in metastasis (18). From the cell tracking, we quantified cancer cell migration total speed and directedness (defined in Fig. 2.5), and we compared the migration dynamics of cancer cells cultured alone with that of cancer cells co-cultured with Raw macrophages (Fig. 3.1). We found that Raw macrophages significantly enhanced cancer cell migration total speed and directedness (Fig. 3.2A) in

3D ECM for MDA-MB-231, PC3, and MDA-MB-435S cells. Similar to Raw macrophages, primary macrophages such as human MDMΦ and murine BMDM were also observed to increase cancer cell migration total speed and directedness (Fig. 3.2B) in 3D ECM. These results indicate that macrophages allow cancer cells to move faster and more persistently, contributing to increases in cancer cell invasion rate (ratio between the displacement of cell and migration time), which is an end-point measurement of cell invasiveness (Fig. 3.3). These results are in stark contrast to results obtained from a 2D migration assay, where we found that macrophages only slightly enhanced cancer cell migration total speed but markedly reduced cancer cell migration directedness (Fig. 3.4). Moreover, the abilities of macrophages to enhance cancer cell migration dynamics in 3D ECM were not affected by the seeding ratio of the cells or the addition of Matrigel into the collagen I ECM (Fig. 3.5). Hence, these results suggest that there are fundamental differences in how macrophages affect cancer cell migration on 2D substrates versus in 3D ECM.

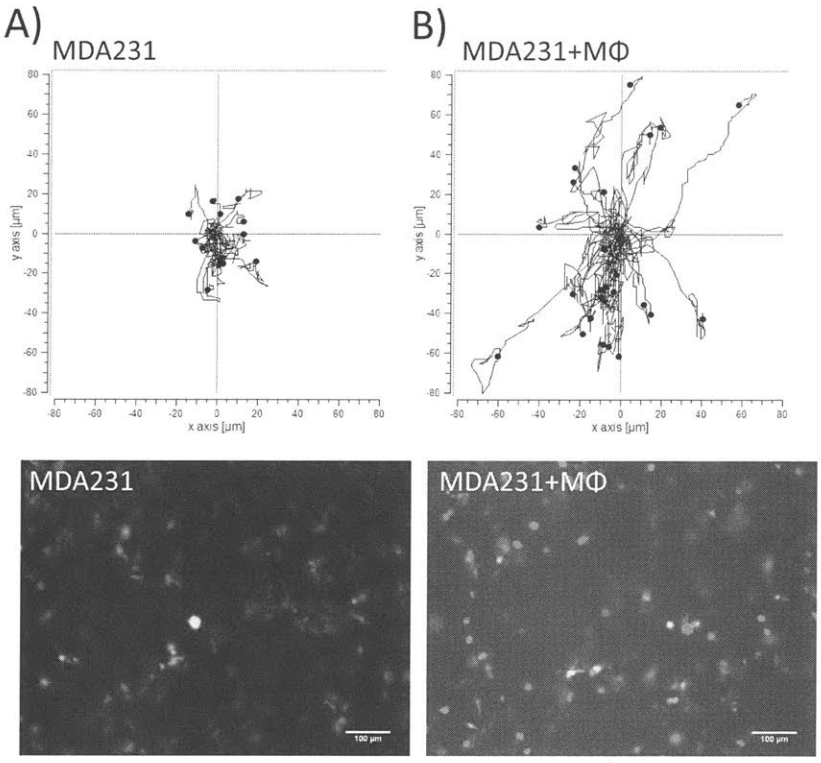

Fig. 3.1: Macrophages assist cancer cell migration in the microfluidic devices. Cancer cells and macrophages were suspended in a 3D collagen I ECM encased in the microfluidic device. **(A)** Representative cancer cell migration trajectories (top) and fluorescent micrograph (bottom) for GFP-expressing MDA231 cancer cell monoculture (green, MDA231). **(B)** Representative cancer cell migration trajectories (top) and fluorescent micrograph (bottom) for co-culture of GFP-expressing MDA231 cancer cell and cell-tracker-red treated Raw 264.7 macrophages (MΦ) (green, MDA231; red, Raw 264.7).

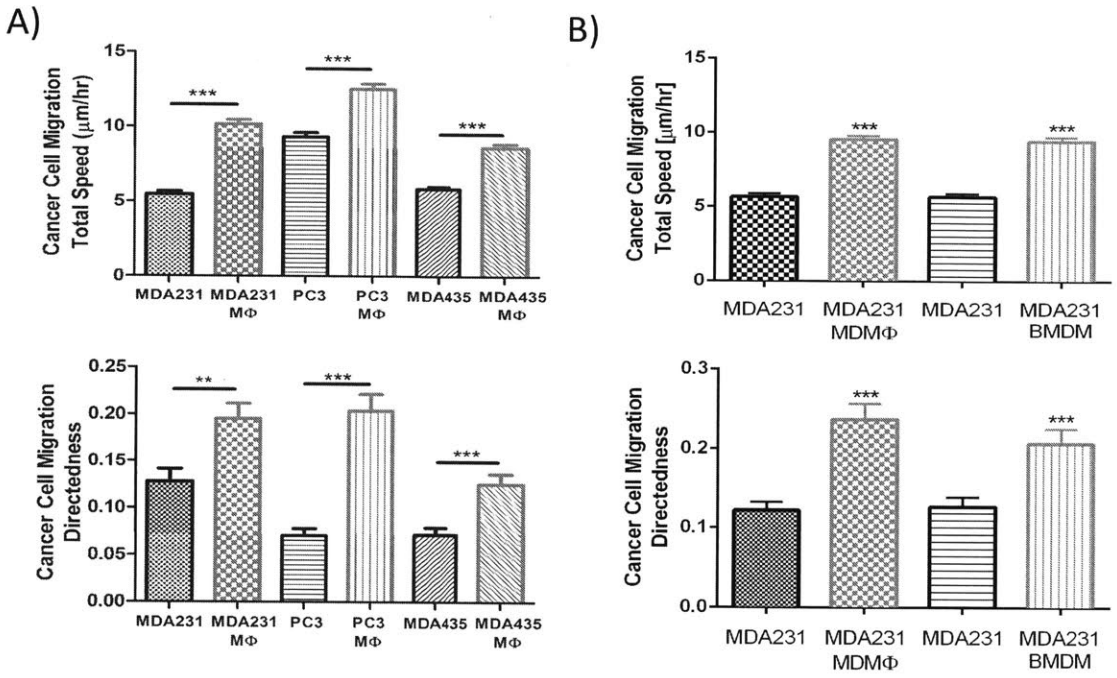

Fig. 3.2: Macrophages enhance cancer cell migration total speed and directedness in 3D ECM. (A) Co-culture of Raw macrophages (MΦ) with cancer cells significantly enhanced cancer cell migration total speed (top) and directedness (bottom) for MDA231 cells, PC3 prostate cancer cells, and MDA-MB-435S melanoma cells (MDA435). **(B)** Co-culture of primary human monocyte-derived macrophages (MDMΦ), as well as murine bone marrow-derived macrophages (BMDM), with MDA231 cells enhanced migration total speed (top) and directedness (bottom) of MDA231 cells. Bars represent mean +/- SEM of data from 40-100 cells from at least 3 independent experiments. (**: $p<0.01$; ***: $p<0.001$).

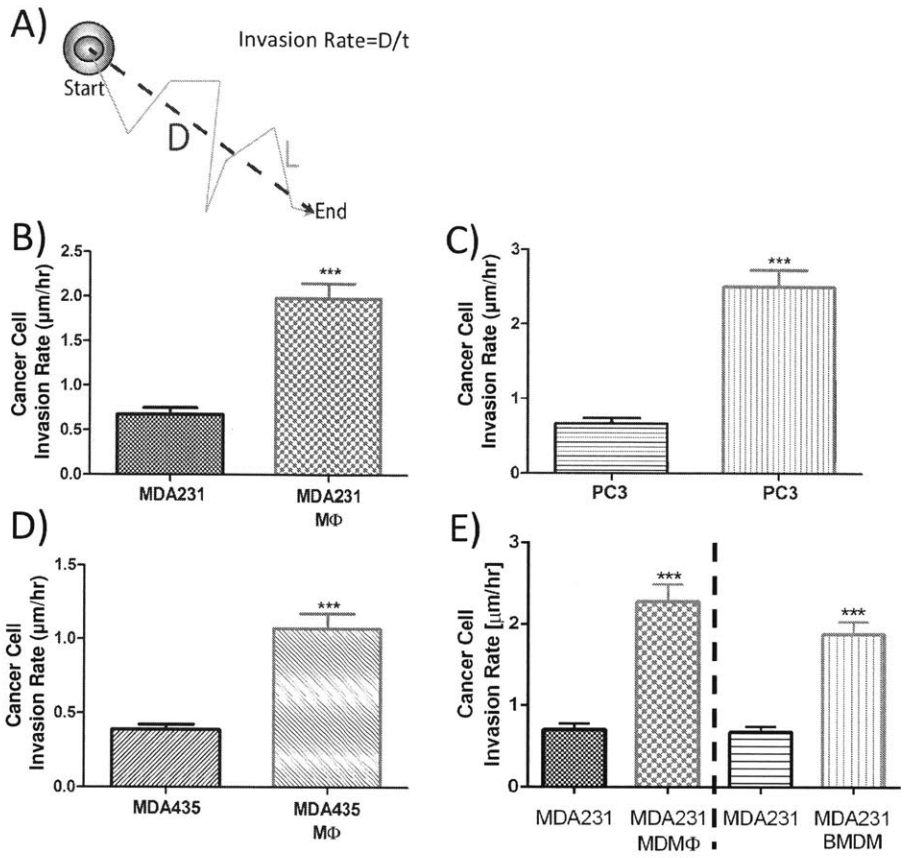

Fig. 3.3: Macrophages increase cancer cell invasion rate in 3D ECM. (**A**) Cancer cell invasion rate, an end-point migration measurement, is defined as the displacement of a cell divided by migration time (D/t, t=18 hrs). (**B-D**) Raw macrophages (MΦ) enhanced cancer cell invasion rate for MDA-MB-231 breast cancer cells (B), PC3 prostate cancer cells (C), and MDA-MB-435S melanoma cells (D). Invasion rate is an end-point measurement of cancer cell migration and invasiveness. **(E)** Primary human monocyte-derived macrophages (MDMΦ) and murine bone marrow-derived macrophages (BMDM) enhanced MDA231 cell invasion rate, similar to Raw macrophages. Bars represent mean +/- SEM of data from 40-100 cells from at least 3 independent experiments. (***: $p<0.001$).

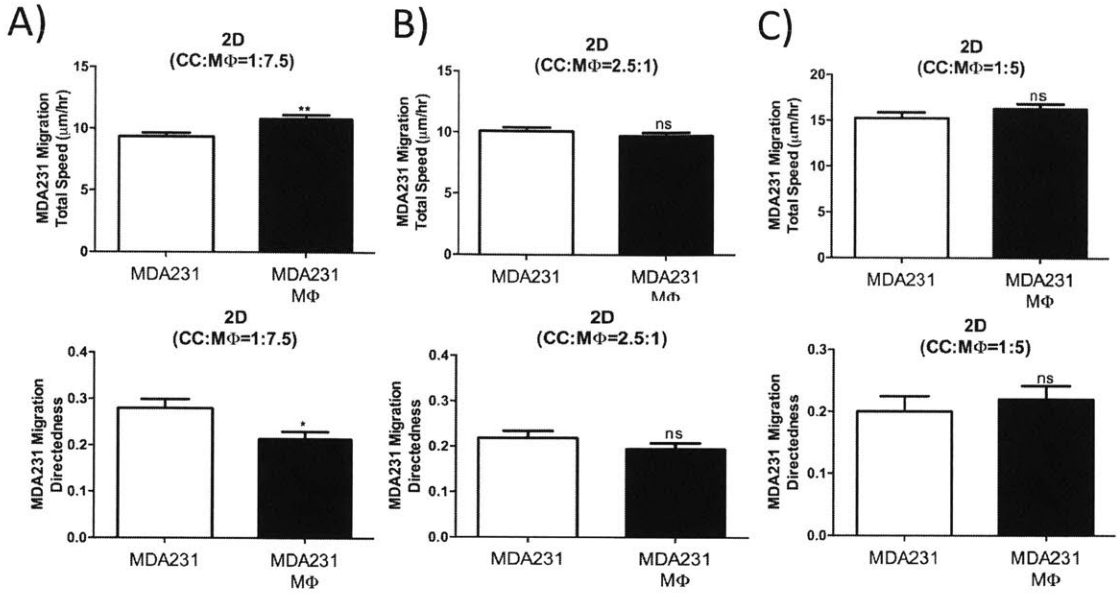

Fig. 3.4: macrophages increase cancer cell migration total speed but decrease directedness on 2D substrates. The effects of Raw 264.7 macrophages (MΦ) on cancer cell migration dynamics are different in 3D compared to 2D. **(A)** On 2D substrates, macrophages led to a slight increase in cancer cell migration total speed (top), but a decrease in cancer cell migration directedness (bottom) when cancer cells were co-cultured with macrophages at high macrophage seeding density (ratio of cancer cells to macrophages = 1:7.5). **(B-C)** No changes in cancer cell migration total speed and directedness were observed when cancer cells were co-cultured with macrophages on 2D substrate at low macrophage seeding density (ratios of 2.5:1 or 1:5). Bars represent mean +/- SEM of data from 40-100 cells from at least 3 independent experiments. (ns: not significant; *: $p<0.1$; **: $p<0.01$).

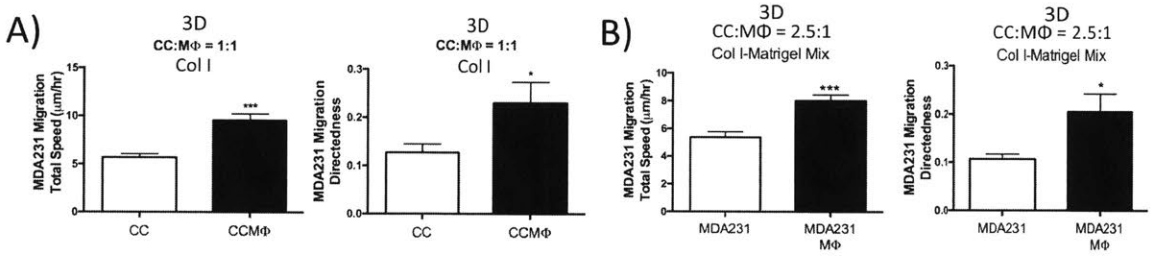

Fig. 3.5: Effects of seeding ratio and complex ECM on macrophages' ability to enhance cancer cell migration dynamics in 3D. (A) Macrophages increased cancer cell migration total speed and directedness in 3D collagen I ECM when cancer cells were co-cultured with macrophages at a seeding ratio of 1-to-1. Similar results were obtained when cancer cells were cultured with macrophages at a seeding ratio of 2.5-to-1 in 3D ECM. **(B)** Macrophages enhanced cancer cell migration total speed and directedness when both cells were cultured in a complex ECM containing collagen I and the Matrigel. Bars represent mean +/- SEM of data from 40-100 cells from at least 3 independent experiments. (*: $p<0.05$; ***: $p<0.001$).

3.5: Macrophage-induced cancer cell migration in 3D ECM is mediated via cancer cell MMP expression

Next, we investigated the molecular mechanisms that control how fast and how persistently the cancer cell migrates in 3D ECM. We hypothesized that MMPs produced by cancer cells are involved, since the migration of cells in the dense 3D matrix critically depends on their ability to degrade ECM (2, 16). To test this hypothesis, we treated MDA231 cancer cells with a pan-MMP inhibitor GM6001. We found that inhibiting MMP activities in cancer cells significantly reduced cancer cell migration total speed and directedness (Fig. 3.6B and C). Further evidence for the role of MMPs was obtained using confocal reflectance microscopy, which revealed that the migration of MDA231 cells in ECM produced micro-tracks of empty space (Fig. 3.6A). However, when these cells were treated with GM6001, the formation of cell protrusions, as well as the ability of cells to degrade ECM, was reduced compared to control samples (Fig. 3.7). These results illustrate that cancer cells migrate in our experimental system in an MMP-dependent fashion, and the production of MMPs is a critical determinant of cancer cell migration dynamics (total speed and directedness) in 3D ECM.

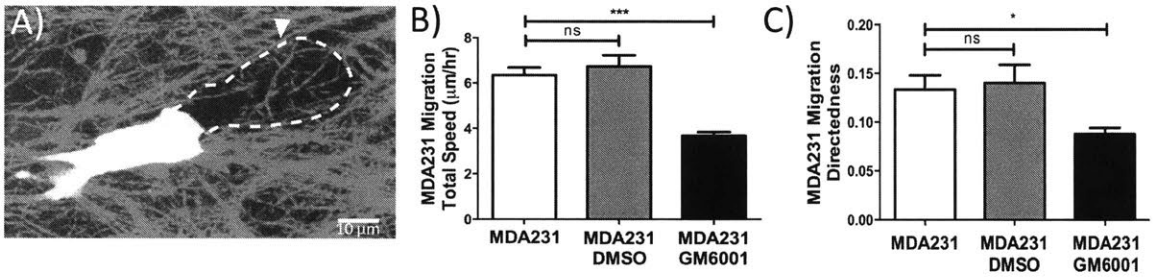

Fig. 3.6. Cancer cell migration speed and directedness are MMP-dependent. **(A)** Representative confocal image showing MDA231 cells (green) migrating through dense collagen I ECM (magenta) by degrading the matrix, leaving behind a micro-track (arrow). **(B and C)** Compared to the untreated and DMSO controls, inhibition of MMP activity by GM6001 significantly reduced MDA231 migration total speed (B) and directedness (C). Bars represent mean +/- SEM of data from 40-100 cells from at least 3 independent experiments. (ns: not significant; *: $p<0.05$; ***: $p<0.001$).

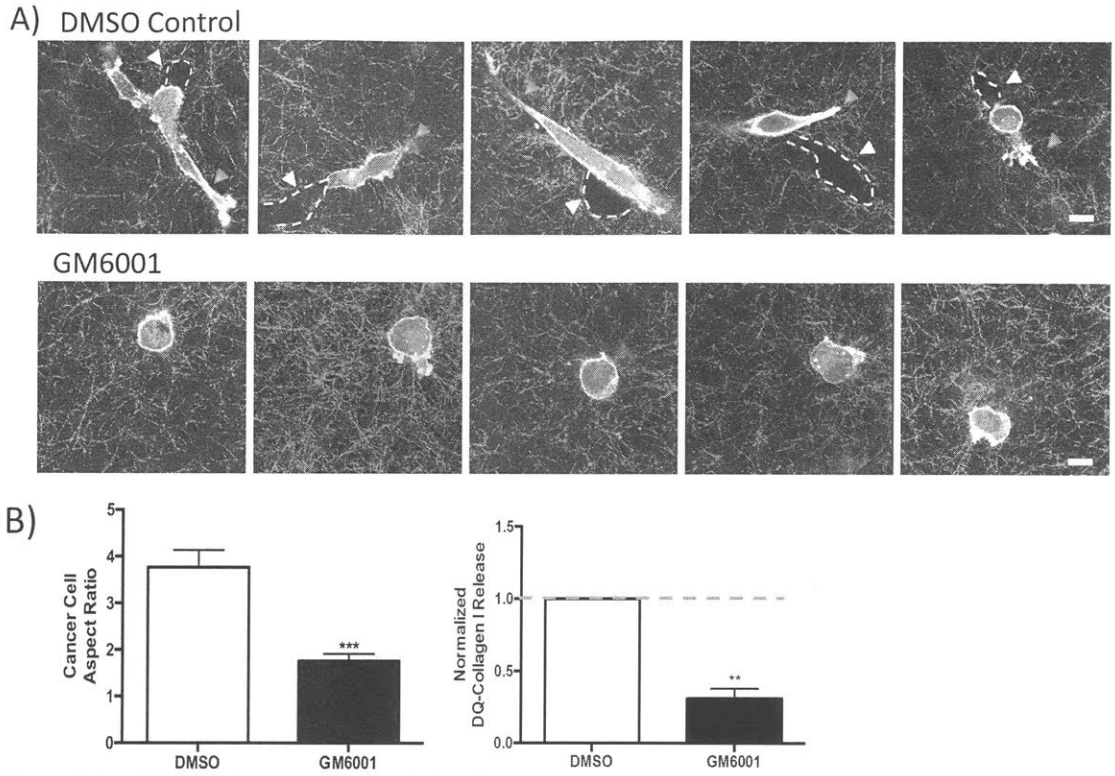

Fig. 3.7: GM6001 treatment inhibits cancer cell protrusion formation and ECM degradation. (A) Representative fluorescent confocal reflectance images showing MDA231 cancer cells (actin, green; nucleus, blue) interacting with ECM (imaged by reflectance microscopy, magenta) when cancer cells were treated with DMSO (DMSO control, top panel) or GM6001 MMP-inhibitor (GM6001, bottom panel). When cancer cells were not treated with GM6001 (top panel), they were able to form protrusion (blue arrow) in the collagen gel and degrade the gel leaving a micro-track behind (white arrow). However, when cancer cells were treated with GM6001 (bottom panel), the protrusion formation was reduced. The formation of collagen micro-track was also reduced (scale bar=15 μm). **(B)** Cancer cell aspect ratio quantification (left) and DQ-collagen I release assay quantification (right) showing that GM6001 significantly reduced cancer cell protrusion formation (left), as well as cancer cells' ability to degrade collagen I ECM (right). (B) Cancer cell aspect ratio data: bars represent mean +/- SEM of data from 40-100 cells from at least 3 independent experiments. (***: $p<0.001$). DQ-Collagen I release data: bars represent mean +/- SEM of data (fold change relative to DMSO control) from at least 3 independent experiments (ns: not significant; **: $p<0.01$).

Based on these findings, we examined the role of macrophages in regulating MMP1 and MT1-MMP expression by cancer cells. We chose to study these two MMPs since these proteases are responsible for the breakdown of collagen I matrix. Moreover, MT1-MMP and MMP1 have been shown to be present in the tumor microenvironment, and they have been implicated in tumor metastasis (19–23). To study how macrophages influence MMP expressions in cancer cells, we co-cultured cancer cells with macrophages in a transwell system, and assessed the cancer cell expression of MMP1 and MT1-MMP via western blotting. We found that co-culture of MDA231 cancer cells with Raw macrophages, as well as BMDM, significantly enhanced cancer cell expression of

MMP1 and MT1-MMP (Fig. 3.8). This result was reproduced in PC3 prostate cancer cells co-cultured with macrophages (Fig. 3.8D).

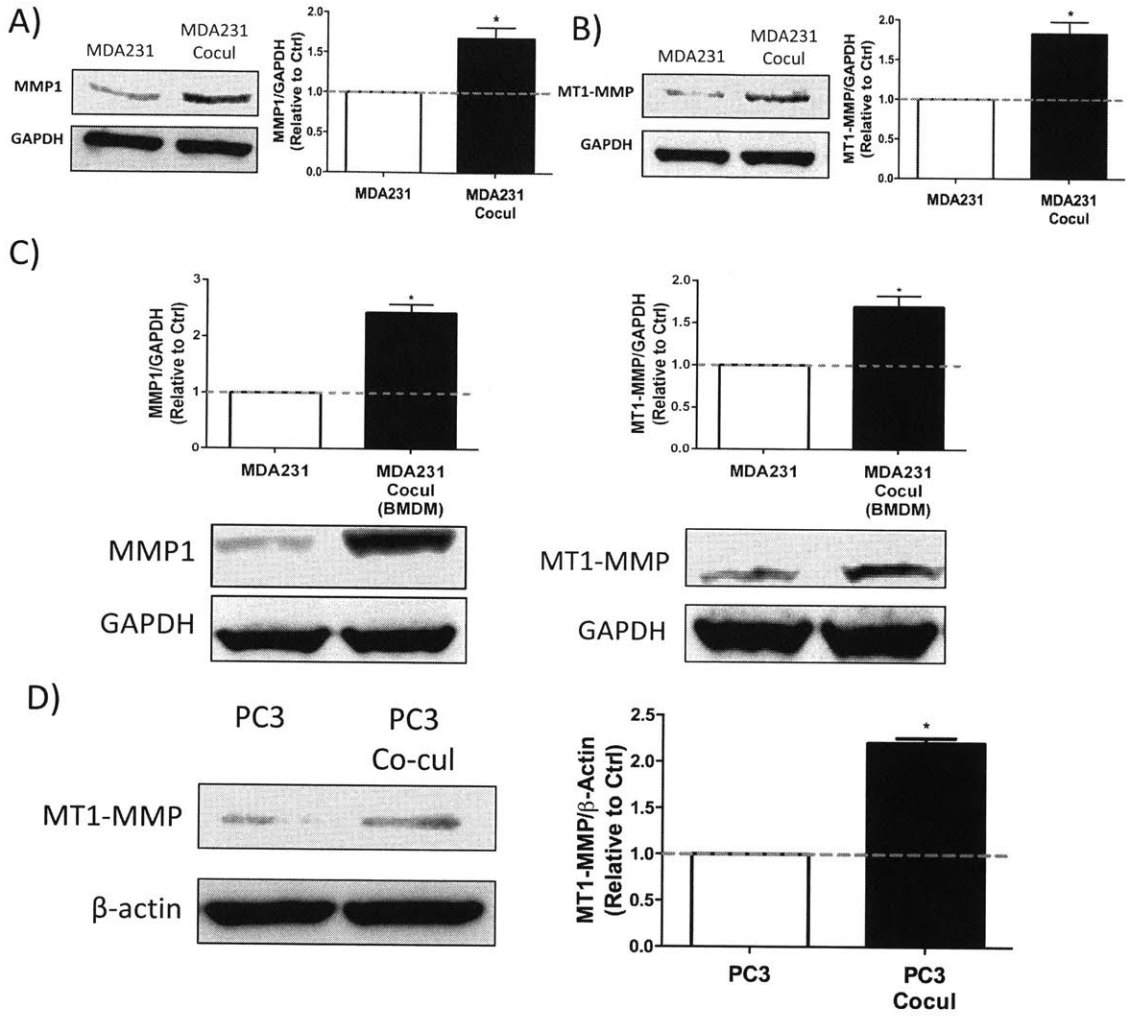

Fig. 3.8: Macrophages enhance cancer cell MMP expression. **(A and B)** Representative western blot images (left) and quantification (right) showing that co-culture of Raw macrophages with MDA231 cells (MDA231 Cocul) in 3D collagen I gels significantly enhanced the expression of MMP1 (A) and MT1-MMP protein (B) in MDA231 relative to monoculture control (MDA231, Ctrl=Control). **(C)** Representative western blot images (bottom) and quantification (top) showing that co-culture of MDA231 cells with BMDM (MDA231 Cocul (BMDM)) resulted in enhanced MMP1 (left) and MT1-MMP (right) expressions in MDA231 cells compared to the monoculture control (MDA231, Ctrl=control). **(D)** Representative western blot images (left) and quantification (right) showing that co-culture of PC3 prostate cancer cells with Raw 264.7 macrophages (PC3 Cocul) increased PC3 expression of MT1-MMP when compared to PC3 monoculture control (PC3). Bars represent mean +/- SEM of data (fold change relative to monoculture control; Ctrl=Control) from at least 3 independent experiments (ns: not significant; *: $p<0.05$).

Next, we tested whether it is necessary for macrophages to be in direct physical contact with cancer cells to promote migration. Instead of culturing Raw macrophages together with MDA231 cancer cells in the ECM, we cultured macrophages in the micro-channels flanking the ECM (Fig. 3.9). The macrophages seeded in the micro-channels were not in physical contact with the ECM or the cancer cells, but they were able to communicate with the cancer cells via the secretion of paracrine factors. Interestingly, we found that macrophages cultured in the micro-channel increased cancer cell migration total speed and directedness to the same degree as macrophages cultured in the collagen ECM (Fig. 3.9), suggesting that direct contact between macrophages and cancer cells is not necessary to enhance cancer cell migration. We also found that the conditioned media from Raw macrophages and BMDM significantly up-regulated the expression of MMP1 and MT1-MMP (Fig. 3.10 A-E) in cancer cells. These results indicate that the effects of macrophages on cancer cell migration dynamics and MMP expressions are mediated primarily through paracrine factors secreted by macrophages.

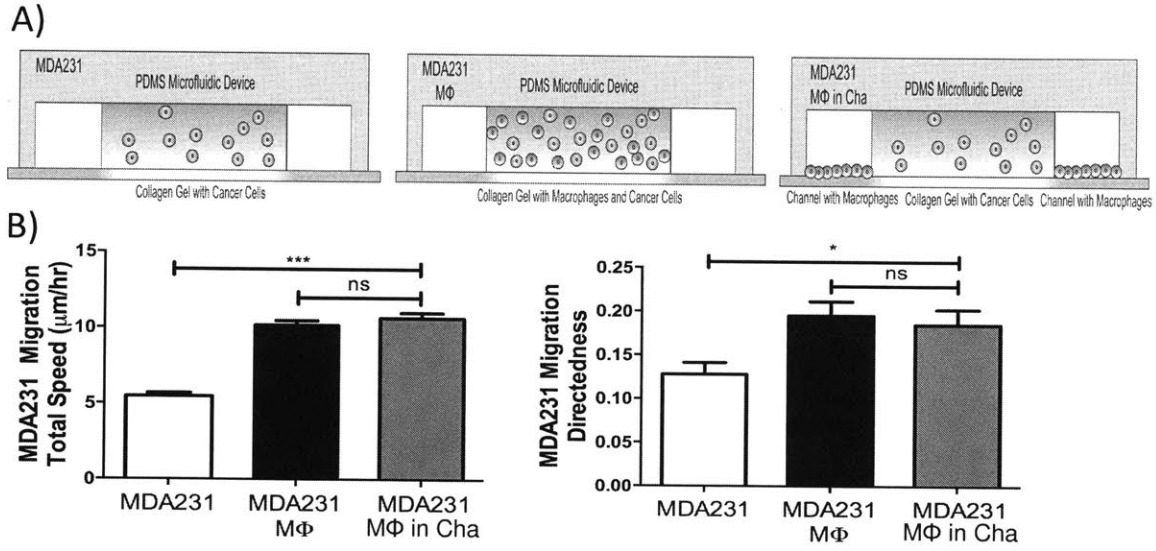

Fig. 3.9: The ability of macrophages to enhance cancer cell migration dynamics is primarily attributed to the paracrine factors secreted by macrophages. **(A)** Schematics showing the experimental conditions designed to test the effects of macrophage-released paracrine factors on cancer cell migration dynamics. (Left) Control condition with MDA-MB-231 cancer cell cultured alone (MDA231). (Middle) Treatment condition with MDA-MB-231 cancer cell cultured with Raw 264.7 macrophages inside the collagen I gel (MDA231 MΦ). (Right) Treatment condition with MDA-MB-231 cancer cell cultured in the collagen I gel and Raw 264.7 macrophages cultured in the micro-channels (MDA231 MΦ in Cha). In the "MDA231 MΦ in Cha" condition, macrophages were not in direct contact with cancer cells and collagen I gel, so the effects of macrophages on cancer cells in this condition should be attributed mostly to the paracrine factors secreted. **(B)** Quantification of migration dynamics with experimental conditions presented in (A). Culturing Raw 264.7 macrophages in micro-channel (MDA231 MΦ in Cha) significantly increased cancer cell migration total speed (left) and directedness (right) when compared to cancer cell monoculture (MDA231), to a level that is similar to the condition in which macrophages were cultured in the gel (MDA231 MΦ). Bars represent mean +/- SEM of data from 40-100 cells from at least 3 independent experiments. (ns: not significant; *: $p<0.05$; ***: $p<0.001$).

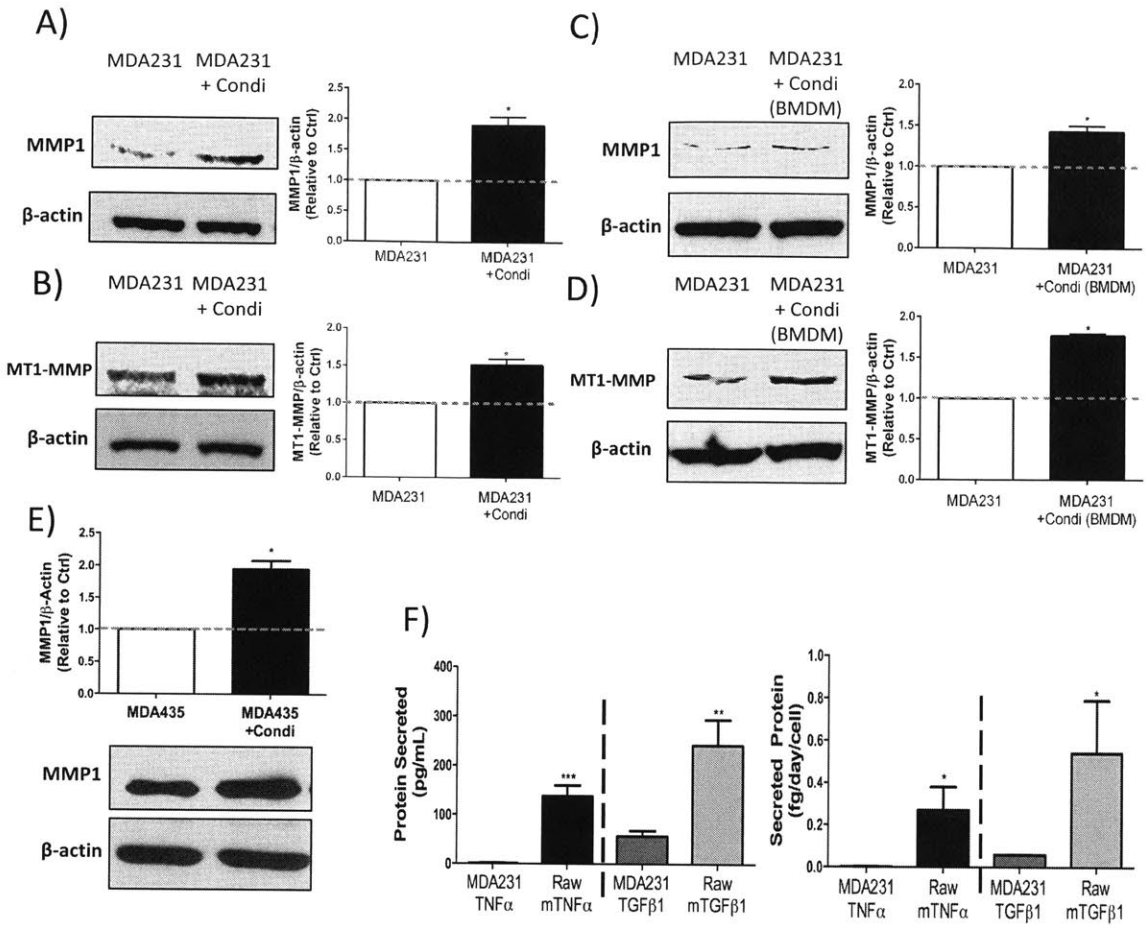

Fig. 3.10: The abilities of macrophages to enhance cancer cell expression of MMPs are primarily due to the paracrine factors secreted by macrophages. **(A)** Western blot quantification (right) and representative images (left) showing that the treatment of MDA-MB-231 cultured in 3D collagen I ECM with conditioned media from Raw 264.7 macrophages (MDA231+Condi) significantly enhanced MMP1 protein expression by MDA231 cells relative to no-treatment control (MDA231, Ctrl=control). **(B)** Western blot quantification (right) and representative images (left) showing that the treatment of MDA231 cultured in 3D collagen I ECM with conditioned media from Raw 264.7 macrophages (MDA231+Condi) significantly enhanced MT1-MMP protein expression by MDA231 cells relative to no-treatment control (MDA231, Ctrl). **(C-D)** Western blot quantification (right) and representative images (left) showing that the treatment of MDA231 cells with conditioned media from BMDM (MDA231+Condi(BMDM)) significantly up-regulated cancer cell expression of MMP1 (C) and MT1-MMP (D) proteins relative to no-treatment control (MDA231, Ctrl=Control). **(E)** Western blot quantification (top) and representative images (bottom) showing that the treatment of MDA-MB-435S cancer cells with conditioned media from Raw 264.7 macrophages (MDA435+Condi) significantly up-regulated cancer cell expression of MMP1 protein relative to no-treatment control (MDA435, Ctrl=Control). **(F)** ELISA quantifications (total amount of protein secreted (left) or amount secreted per cell per day (right)) demonstrating that Raw 264.7 macrophages secrete TNFα and TGFβ1, and the secretions of these two factors are much larger than cancer cell secretions of TNFα and TGFβ1. (A-E) Bars represent mean +/- SEM of data (fold change relative to no-treatment control, Ctrl=control) from at least 3 independent experiments. (F) Bars represent mean +/- SEM of data from at least 3 independent experiments (ns: not significant; *: $p<0.05$; **: $p<0.01$, ***: $p<0.001$).

3.6: Macrophage-released TNFα and TGFβ1 are responsible for the increases in cancer cell migration total speed and directedness.

We next performed experiments to identify the paracrine factors released by macrophages that were responsible for the increases in cancer cell migration dynamics. We hypothesized that TNFα and TGFβ1 secreted by macrophages are involved in promoting cancer cell migration, since these two factors are major secretory products of macrophages in the tumor microenvironment (24–27), and they have been implicated in tumor metastasis (28, 29). Indeed, primary macrophages such as MDMΦ and BMDM have been shown to secrete TNFα and TGFβ1 (30–33). We first verified, using ELISA, that Raw macrophages used in our study also secreted TNFα and TGFβ1 (Fig. 3.10F). To test our hypothesis further, we treated cancer cell-macrophage co-culture with neutralizing antibodies against TNFα and/or TGFβ1, and measured cancer cell migration total speed and directedness as before. The antibodies used in this study were designed to act against mouse TNFα and TGFβ1. This allowed us to specifically inhibit TNFα and TGFβ1 secreted by Raw 264.7 mouse macrophages. Antibody blocking results showed that neutralizing TNFα in co-culture slightly decreased macrophage-enhanced cancer cell migration total speed, while blocking TGFβ1 almost completely abrogated the effects of macrophages on total speed (Fig. 3.11A-B). Co-blocking both TNFα **and** TGFβ1 did not further reduce cancer cell migration total speed when compared to the blocking of only TGFβ1 (Fig. 3.11C). These results suggest that TGFβ1 is primarily responsible for the ability of macrophages to enhance cancer cell migration total speed.

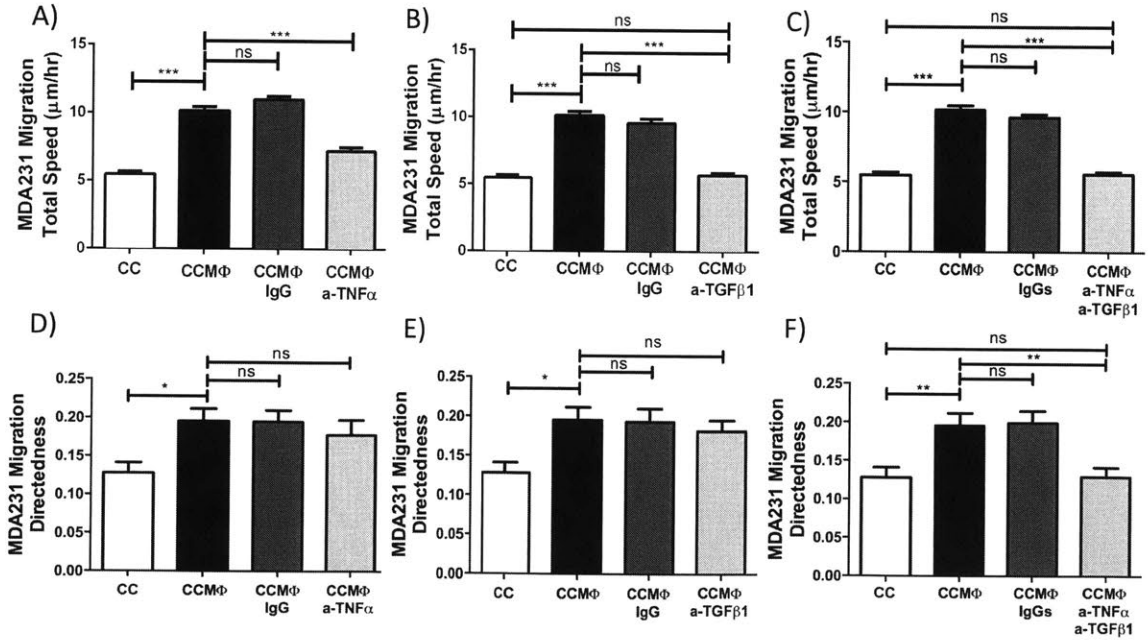

Fig. 3.11: Macrophage-released TNFα and TGFβ1 are responsible for the increase in cancer cell migration total speed and directedness. MDA231 cancer cells (CC) co-cultured with Raw cells (MΦ) were treated with neutralizing antibodies against TNFα (a-TNFα) and/or TGFβ1 (a-

TGFβ1). **(A, B, and C)** Neutralizing TNFα released by macrophages (CCMΦ a-TNFα) led to a decrease in MDA231 migration total speed compared to no-treatment control (CCMΦ) (A). However, inhibiting macrophage-released TGFβ1 (CCMΦ a-TGFβ1) led to an almost complete inhibition of macrophage's effect on MDA231 migration total speed (B), similar to the simultaneous inhibition of both TNFα and TGFβ1 (C). **(D, E, and F)** Neutralizing macrophage-released TNFα (CCMΦ a-TNFα) or TGFβ1 (CCMΦ a-TGFβ1) alone did not significantly reduce MDA231 migration directedness (D and E). However, simultaneous inhibition of both TNFα and TGFβ1 led to an almost complete abolishment of macrophage-enhanced MDA231 migration directedness (F). Bars represent mean +/- SEM of data from 40-100 cells from at least 3 independent experiments. (ns: not significant; *: $p<0.05$; **: $p<0.01$; ***: $p<0.001$).

Surprisingly, when we assessed the effects of antibody blocking on cancer cell migration directedness, we found that inhibiting either TNFα **or** TGFβ1 in co-culture did not lead to significant decreases in cancer cell migration directedness (Fig. 3.11D-E). In contrast, blocking TNFα **and** TGFβ1 simultaneously almost completely abolished the ability of macrophages to promote migration directedness (Fig. 3.11F), suggesting that both TNFα **and** TGFβ1 are important to macrophage-enhanced migration directedness. Interestingly, this result is in contrast to the antibody blocking results for total speed, which seems to suggest that macrophage-enhanced cancer cell migration total speed and directedness are controlled by two different pathways. Finally, to verify if blocking antibody treatments were specific to macrophage-secreted TNFα and TGFβ1, we treated cancer cell monocultures with anti-mouse neutralizing antibodies that we used in co-culture experiments. We found this to have no significant effect on MDA231 cell migration total speed and directedness (Fig. 3.12), indicating that the antibody inhibition was macrophage-specific.

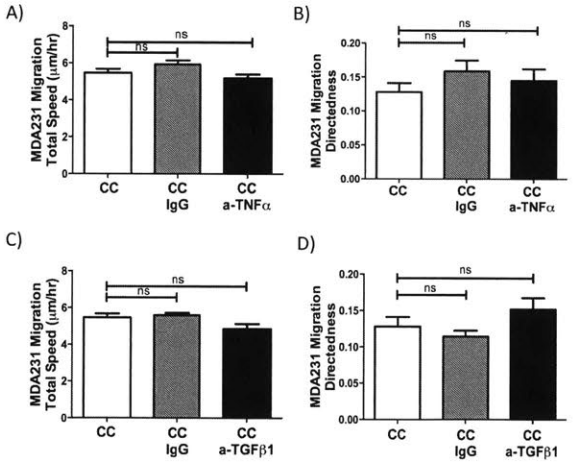

Figure 3.12: Neutralizing antibody blocking is specific to factors released by macrophages. **(A and B)** Treatment of MDA-MB-231 cancer cell monoculture with neutralizing antibody against mouse TNFα (CC a-TNFα) did not affect cancer cell migration total speed (A) or directedness (B) when compared to no-treatment control (CC) and IgG isotype-treatment control (CC IgG; IgG: Goat IgG). **(C and D)** Treatment of MDA-MB-231 cancer cell monoculture with neutralizing antibody against mouse TGFβ1 (CC a-TGFβ1) did not significantly affect cancer cell migration total speed (C) and directedness (D) when compared to no-treatment control (CC) and IgG isotype-treatment control (CC IgG; IgG: Rabbit IgG). Bars represent mean +/- SEM of data from 60-100 cells from at least 3 independent experiments (ns: not significant).

We next demonstrated that co-blocking of both TNFα and TGFβ1 in co-culture resulted in almost complete inhibition of macrophage-induced MMP1 and MT1-MMP protein expression in cancer cells (Fig. 3.13A and 3.14). These results further support our previous conclusion that macrophage-enhanced cancer cell migration total speed and directedness in 3D ECM are controlled by MMPs. Finally, as expected, since both migration total speed and directedness contribute to cancer cell invasion rate (Fig. 3.3), blocking of TNFα **or** TGFβ1 cannot completely abrogate macrophage-enhanced cancer cell invasion rate. In contrast, when both macrophage TNFα and TGFβ1 were inhibited, cancer cell invasion rate in co-culture was reduced to the level of the cancer cell monoculture control (Fig. 3.13B).

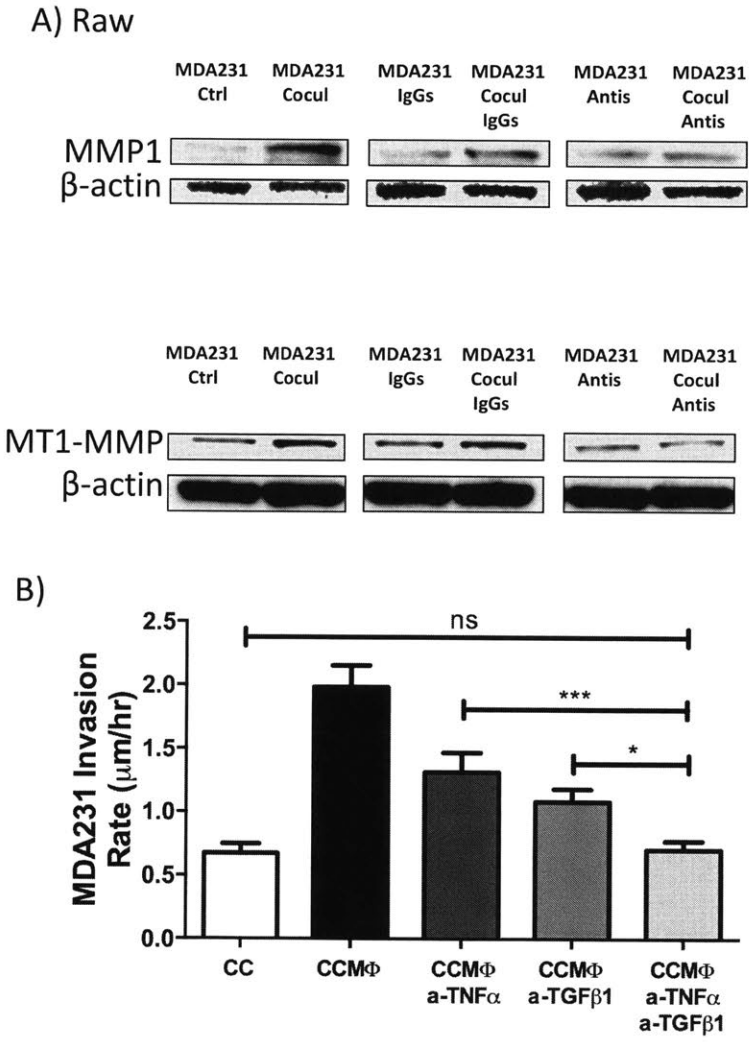

Fig. 3.13: Blocking TNFα and TGFβ1 secreted by Raw 264.7 macrophages significantly reduced macrophage-induced MMP expression and macrophage-enhanced cancer cell invasion rate. **(A)** Representative western blot images showing that co-blocking of TNFα and TGFβ1 secreted by Raw 264.7 macrophages using neutralizing antibodies against these two factors (MDA231 Cocul Antis) significantly reduced macrophage-induced MMP1 (top) and MT1-MMP expression (bottom) in MDA231 cells when compared to no-treatment (MDA231 Cocul) and IgG-treatment controls (MDA231 Cocul IgGs). **(B)** MDA-MB-231 cancer cell (CC)

invasion rate quantification showing that co-blocking of TNFα and TGFβ1 (CCMΦ a-TNFα a-TGFβ1, bar 5) secreted by Raw 264.7 macrophages using neutralizing antibodies reduced MDA-MB-231 cancer cell invasion rate to the level that is similar to cancer cell monoculture (CC, bar 1). In contrast, blocking of TNFα (CCMΦ a-TNFα, bar 3) or TGFβ1 (CCMΦ a-TGFβ, bar 4) alone cannot completely abrogate the increase in cancer cell invasion rate caused by macrophages. (B) Bars represent mean +/- SEM of data from 60-100 cells from at least 3 independent experiments (ns: not significant; *: $p<0.05$; ***: $p<0.001$).

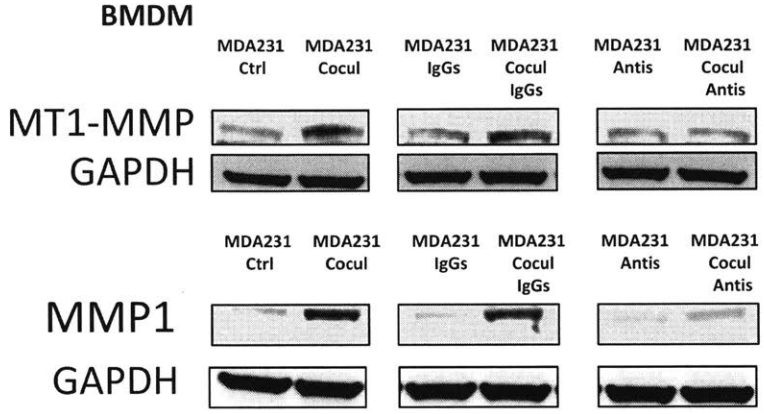

Fig. 3.14: Blocking TNFα and TGFβ1 secreted by bone marrow-derived macrophages significantly reduced macrophage-induced MMP expression. Representative western blot images showing that co-blocking of TNFα and TGFβ1 secreted by bone marrow-derived macrophages (BMDMs) using neutralizing antibodies against these two factors (MDA231 Cocul Antis) significantly reduced macrophage-induced MMP1 (bottom) and MT1-MMP expression (top) in MDA231 cells when compared to no-treatment (MDA231 Cocul) and IgG-treatment controls (MDA231 Cocul IgGs).

3.7: Macrophage-released TGFβ1 enhances cancer cell migration total speed via MT1-MMP, while macrophage-released TNFα and TGFβ1 synergistically increase cancer cell migration directedness via MMP1

We then proceeded to examine the detailed mechanisms by which macrophage-released TNFα and TGFβ1 affect cancer cell migration dynamics. We also sought to elucidate the seemingly distinct pathways that are involved in promoting migration total speed and directedness. Since it is difficult to perform a detailed and well-controlled study on molecular mechanism with blocking antibodies alone, we elected to treat cancer cell monocultures with TNFα and/or TGFβ1 and assess the resulting cell migration dynamics and MMP expressions. We found that the treatment of MDA231 cancer cell with TNFα slightly increased cancer cell migration total speed, while TGFβ1 treatment significantly enhanced total speed. No additional increase in migration total speed was observed for TNFα and TGFβ1 co-treatment over the TGFβ1 mono-treatment condition (Fig. 3.15A). These results parallel the blocking antibody experiments and further support our prior conclusion that macrophage-released TGFβ1 is the main contributor to the increase in cancer cell migration total speed.

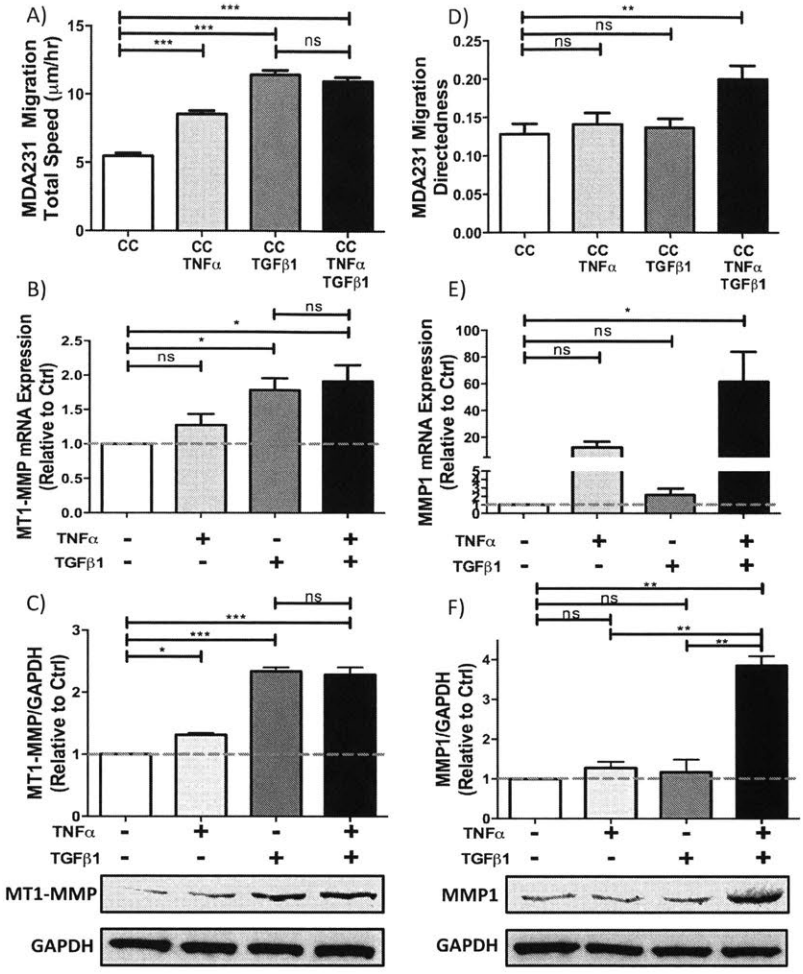

Fig. 3.15: TGFβ1 increases cancer cell migration total speed via the induction of MT1-MMP expression, while TNFα and TGFβ1 synergistically increase cancer cell migration directedness via the induction of MMP1 expression. MDA231 monoculture (CC) was treated with TNFα and/or TGFβ1, and the resulting cell migration dynamics and MMP expressions were analyzed. **(A-C)** Treatment of MDA231 with TGFβ1 (CC TGFβ1) led to larger increases in MDA231 migration total speed (A), MT1-MMP mRNA (B) and protein (C) expressions than TNFα mono-treatment (CC TNFα). However, co-treatment of both TNFα and TGFβ1 led to no further increase in migration total speed, MT1-MMP mRNA and protein expressions compared to TGFβ1 mono-treatment. Data in (A), (B), and (C) follow a similar trend. **(D-F)** TNFα and TGFβ1 synergistically increased MDA231 migration directedness (D), MMP1 mRNA expression (E), and MMP1 protein production (F) when compared to mono-treatment conditions. Data in (D), (E), and (F) follow a similar trend. Data in (C) and (F) were obtained from cells cultured in 3D collagen I ECM. (A, D) Bars represent mean +/- SEM of data from 40-100 cells from at least 3 independent experiments. (ns: not significant; *: $p<0.05$; ***: $p<0.001$). (B, C, E, F) Bars represent mean +/- SEM of data (fold change relative to no-treatment control) from at least 3 independent experiments (ns: not significant; *: $p<0.05$; **: $p<0.01$; ***: $p<0.001$).

In contrast to its effects on total speed, TNFα or TGFβ1 mono-treatment did not significantly enhance cancer cell migration directedness. When the cancer cells were treated with both TNFα and TGFβ1, however, there was a synergistic increase in cancer cell migration directedness that cannot be explained by the additive effects of TNFα and TGFβ1 mono-treatment (Fig. 3.15D). Combined, these results provide further evidence that macrophage-induced cancer cell 3D migration total speed and directedness are controlled by two distinct mechanisms. Specifically, cancer cell migration total speed is controlled primarily by macrophage-released TGFβ1, while the directedness is controlled by the combined effects of macrophage-released TNFα and TGFβ1. Finally, we found that co-treatment of cancer cell monoculture with TNFα and TGFβ1 led to levels of migration total speed and directedness (Fig. 3.16) comparable to those in co-culture, indicating that TNFα and TGFβ1 from macrophages are, indeed, the main factors responsible for the enhancement in cancer cell migration.

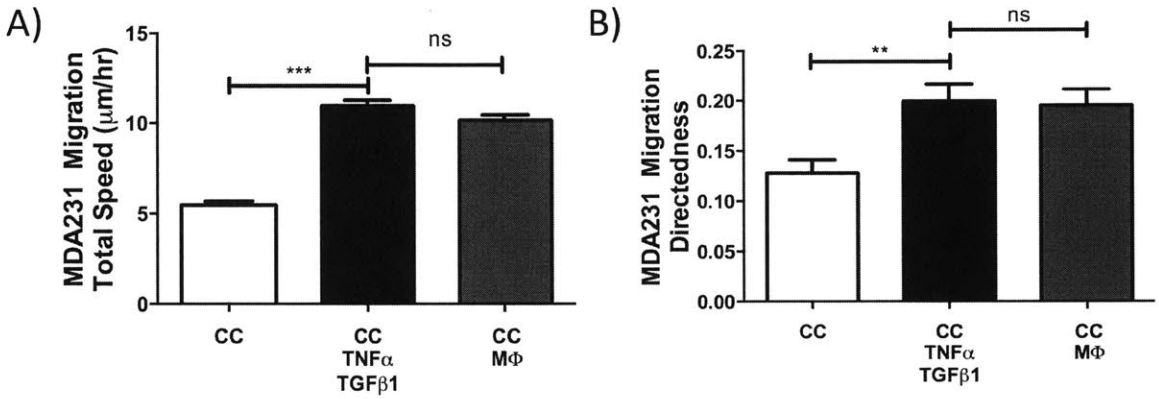

Fig. 3.16: TNFα and TGFβ1 secreted by macrophages mostly accounts for macrophage-enhanced cancer cell migration total speed and directedness. (A and B) Treatment of MDA231 cancer cells (CC) with TNFα and TGFβ1 produced similar levels of cancer cell migration total speed (A) and directedness (B) compared to that of cancer cell-macrophage co-culture (CCMΦ). Bars represent mean +/- SEM of data from 60-100 cells from at least 3 independent experiments (ns: not significant; **: $p<0.01$; ***: $p<0.001$).

For further verification that cancer cell migration total speed and directedness are controlled through two distinct pathways, we varied the concentration of TNFα and TGFβ1 in the co-treatment condition. Specifically, we treated MDA231 cancer cells with 5 ng/mL TNFα + 0.5 ng/mL TGFβ1, or 0.5 ng/mL TNFα + 5 ng/mL TGFβ1, or 5 ng/mL TNFα + 5 ng/mL TGFβ1. Interestingly, treating cancer cells with a low concentration of TGFβ1 (0.5 ng/mL), even in the co-treatment conditions, resulted in slight or no increase in the migration total speed (Fig. 3.17A). These results further illustrate that cancer cell migration total speed is mainly controlled by TGFβ1. In comparison, treating cancer cells with various concentrations of TNFα or TGFβ1 in the co-treatment regimen resulted in similar levels of increase in cancer cell migration directedness over the no-treatment control. Moreover, addition of even a minute amount (0.5 ng/mL) of TGFβ1 to TNFα mono-treatment resulted in sharp increases in cancer cell migration directedness. A similar response was observed when a minute amount of TNFα (0.5 ng/mL) was added to TGFβ1 mono-treatment (Fig. 3.17B). These results further verify that TNFα and TGFβ1 synergistically enhance cancer cell migration directedness.

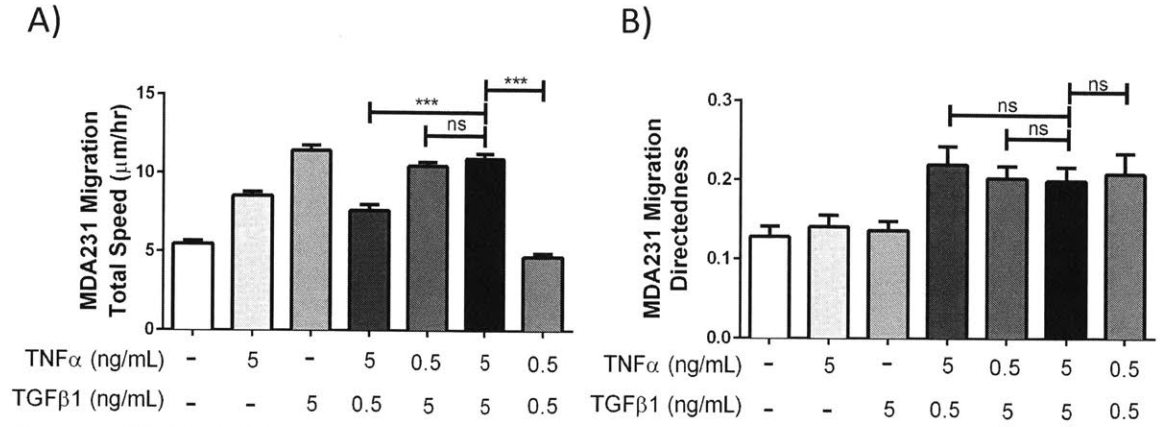

Figure 3.17: TGFβ1 has a larger effect on cancer cell migration total speed than TNFα. TNFα and TGFβ1 synergistically increase cancer cell migration directedness. MDA-MB-231 cancer cells were treated with 5 ng/mL of TNFα and 5 ng/mL of TGFβ1 or 5 ng/mL of TNFα and 0.5 ng/mL of TGFβ1 or 0.5 ng/mL of TNFα and 5 ng/mL of TGFβ1 or 0.5 ng/mL of TNFα and 0.5 ng/mL of TGFβ1. Cancer cell migration total speed and directedness under these co-treatment conditions were compared to that of no-treatment control as well as mono-treatment conditions. **(A)** Co-treatment of different concentrations of TNFα and TGFβ1 led to different levels of increases in cancer cell migration total speed over the no-treatment control, with conditions containing 5 ng/mL of TGFβ1 producing the largest increase in cancer cell migration speed (Bar 5 and Bar 6). **(B)** Co-treatment of different concentrations of TNFα and TGFβ1 led to similar levels of increases in cancer cell migration directedness relative to the no-treatment control (Bar 4, 5, 6, 7 vs. Bar 1). This is in contrast to mono-treatment conditions (Bar 2 and 3), where no noticeable increase in cancer cell migration directedness over the no-treatment control was observed. Bars represent mean +/- SEM of data from 40-100 cells from at least 3 independent experiments (ns: not significant; ***: $p<0.001$).

Since cancer cell migration in 3D ECM depends on the cell's ability to express MMPs, it seemed that the effects of TNFα and TGFβ1 on cancer cell migration dynamics might also be mediated through MMPs. To test for this hypothesis, we treated MDA231 monoculture with TNFα and/or TGFβ1 and evaluated the resulting MMP1 and MT1-MMP mRNA and protein expression. We found that the treatment of cancer cells with TNFα resulted in a slight increase in MT1-MMP mRNA and protein expression. In comparison, the treatment of cells with TGFβ1 alone markedly enhanced MT1-MMP mRNA and protein expression, while co-treatment of both TNFα and TGFβ1 led to no further increase in MT1-MMP expressions (Fig. 3.15B-C). We noted that these trends in the increases in MT1-MMP mRNA and protein expressions match the trend in the increases in cancer cell migration total speed (Fig. 3.15A). This observation points to the possibility that TGFβ1-induced increase in cell migration total speed is mediated mainly via MT1-MMP. Furthermore, we observed that TNFα and TGFβ1 synergistically enhanced cancer cell expression of MMP1 mRNA and protein (Fig. 3.15E-F). These findings are similar to the observation that TNFα and TGFβ1 synergistically promote cancer cell migration directedness (Fig. 3.15D), suggesting that TNFα/TGFβ1-induced cancer cell migration directedness is mediated mainly by MMP1 expression. Indeed,

Pearson correlation analysis revealed that MT1-MMP expression levels resulting from TNFα and/or TGFβ1 treatments strongly correlate with cancer cell migration total speed, but not directedness Similarly, MMP1 expression levels in cancer cells strongly correlate with migration directedness, but not total speed (Fig. 3.18). These results led us to hypothesize that macrophage-induced cancer cell migration total speed is controlled by MT1-MMP expression in cancer cells, while the directedness is controlled by MMP1 expression.

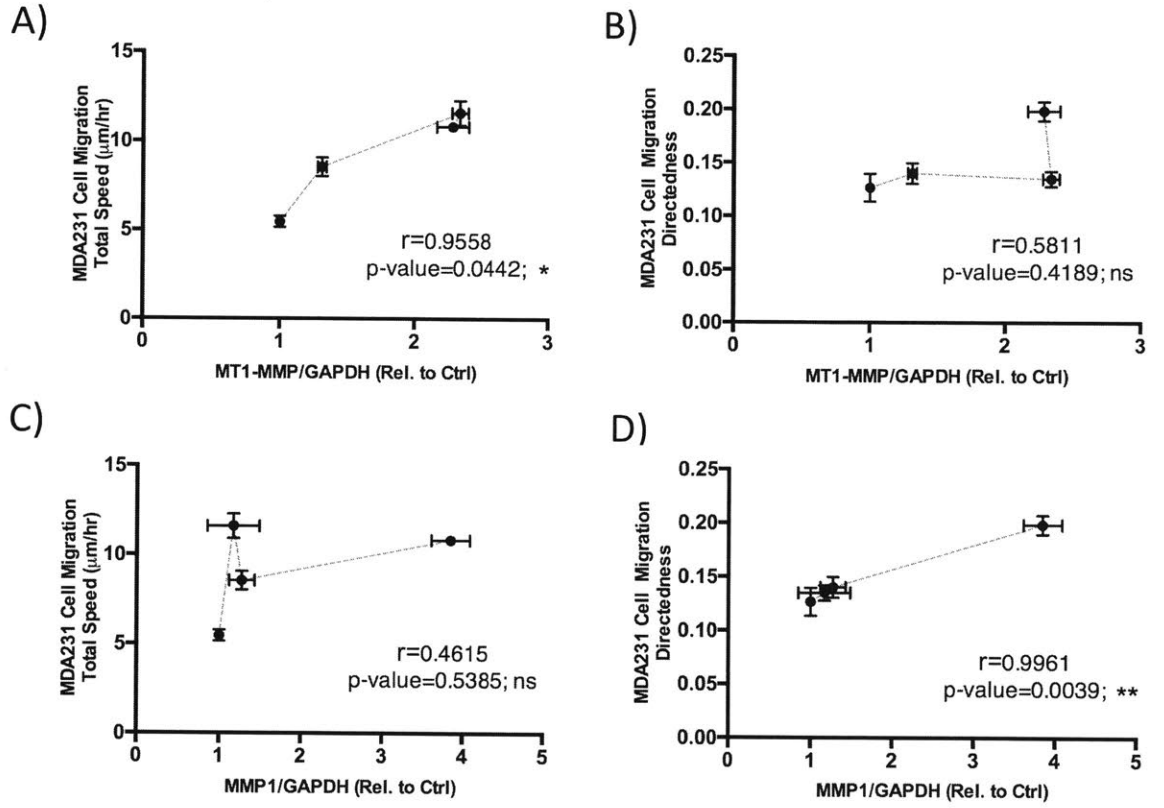

Fig. 3.18: Cancer cell migration total speed is correlated with cancer cell expression of MT1-MMP, while cancer cell migration directedness is correlated with cancer cell expression of MMP1. MDA-MB-231 (MDA231) cancer cells were treated with TNFα and/or TGFβ1, and the cell migration total speed and directedness resulting from the treatments were plotted against the expression levels of MMP1 and MT1-MMP protein (fold change relative to control; relative=Rel., control=Ctrl). **(A and B)** Pearson correlation analysis revealed that the expression of MT1-MMP in MDA-MB-231 cancer cell correlated with cancer cell migration total speed (A, p-value=0.0442) but not directedness (B, p-value=0.4189). **(C and D)** Pearson correlation analysis revealed that the expression of MMP1 in MDA-MB-231 cancer cell correlated with cancer cell migration directedness (D, p-value=0.0039) but not total speed (C, p-value=0.5385). The R-value and p-value for each Pearson correlation analysis are displayed next to the graph, with $p<0.05$ deemed statistically significant correlations.

To test whether or not macrophage-induced cancer cell migration total speed and directedness are controlled by two different MMPs, we treated cancer cell-macrophage co-culture with blocking antibodies against MT1-MMP and MMP1. We found that treating the co-culture with anti-MT1-MMP antibody resulted in a significant decrease in cancer cell migration total speed with little effect on directedness (Fig. 3.19A-B). In contrast, we observed that blocking MMP1 in co-culture with anti-MMP1 antibody had almost no effect on macrophage-induced increase in cancer cell migration total speed, while the increase in cancer cell migration directedness was significantly reduced (Fig. 3.19C-D). Furthermore, we treated cancer cell monoculture with exogenously supplied recombinant MMP1 and observed an enhancement in cancer cell migration directedness but no significant change in migration total speed (Fig. 3.19E-F). These findings, coupled with previous observations that macrophage-released TNFα and TGFβ1 up-regulated cancer cell expression of MMPs (Fig 3.13 and 14), strongly support the conclusion that macrophage-induced MMP1 expression is responsible for the increase in cancer cell migration directedness, while the induction of MT1-MMP expression is responsible for the increase in total speed. Taken together, these results demonstrate that macrophages influence cancer cell migration in 3D ECM via two different mechanisms: 1) macrophage-released TGFβ1 increases cancer cell migration total speed (speed) via the up-regulation of MT1-MMP expression, and 2) macrophage-released TNFα and TGFβ1 synergistically enhance cancer cell migration directedness (persistence) through the induction of MMP1 expression. Hence, these results strongly suggest that both of these two pathways need to be inhibited in order to effectively reduce metastasis. Indeed, using a 4T1 orthotopic breast tumor model in BALB/c mice, we found that inhibiting both TNFα and TGFβ1 in these mice resulted in a more significant reduction in lung metastasis formation compared to inhibiting TNFα or TGFβ1 alone (Fig. 3.20).

Finally, we found a similar synergistic response in MMP1 secretion due to TNFα and TGFβ1 co-treatment (Fig. 3.21), which mirrors the results of cancer cell migration directedness (Fig. 3.15D). The synergistic induction in MMP1 protein production was also observed in MDA435 and PC3 cells (Fig. 3.22).

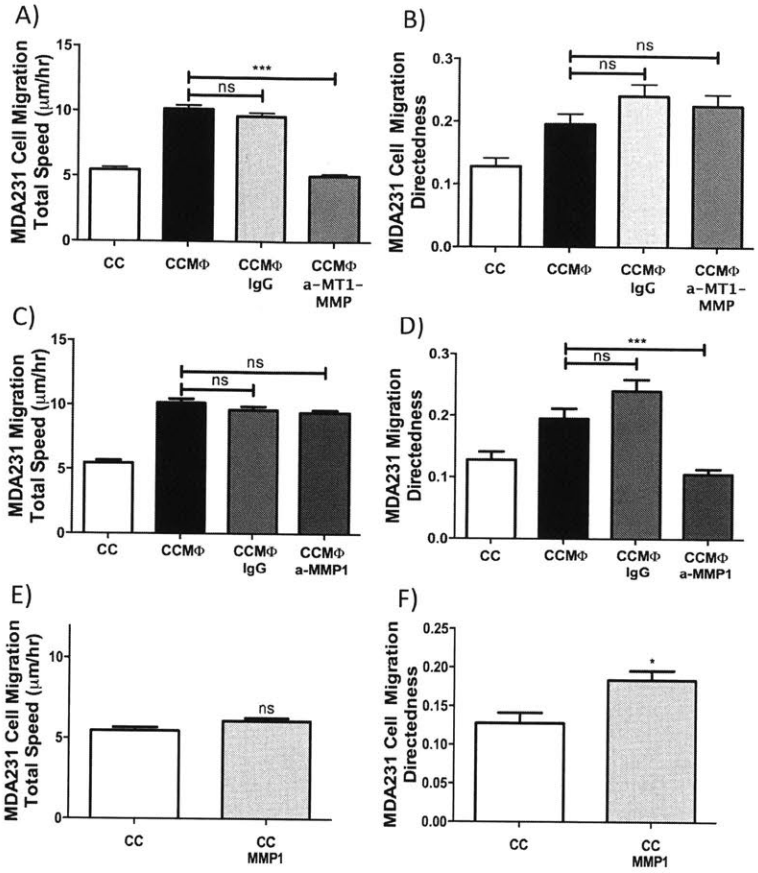

Fig. 3.19: Macrophage-induced cancer cell migration total speed is mediated via MT1-MMP, while directedness is mediated by MMP1. MDA231 cancer cells (CC)-Raw macrophages (MΦ) co-culture was treated with blocking antibodies against MT1-MMP or MMP1. **(A and B)** Treatment of co-culture with anti-MT1-MMP antibody (CCMΦ a-MT1-MMP) decreased MDA231 migration total speed (A) but not directedness (B). **(C and D)** Treatment of co-culture with anti-MMP1 antibody (CCMΦ a-MMP1) reduced MDA231 migration directedness (D) while having a minimal effect on total speed (C). **(E and F)** Treatment of MDA231 cancer cell monoculture with recombinant MMP1 (CC MMP1) enhanced MDA231 migration directedness (F), while having a minimal effect on total speed (E). Bars represent mean +/- SEM of data from 40-100 cells from at least 3 independent experiments (ns: not significant; *: $p<0.05$; ***: $p<0.001$).

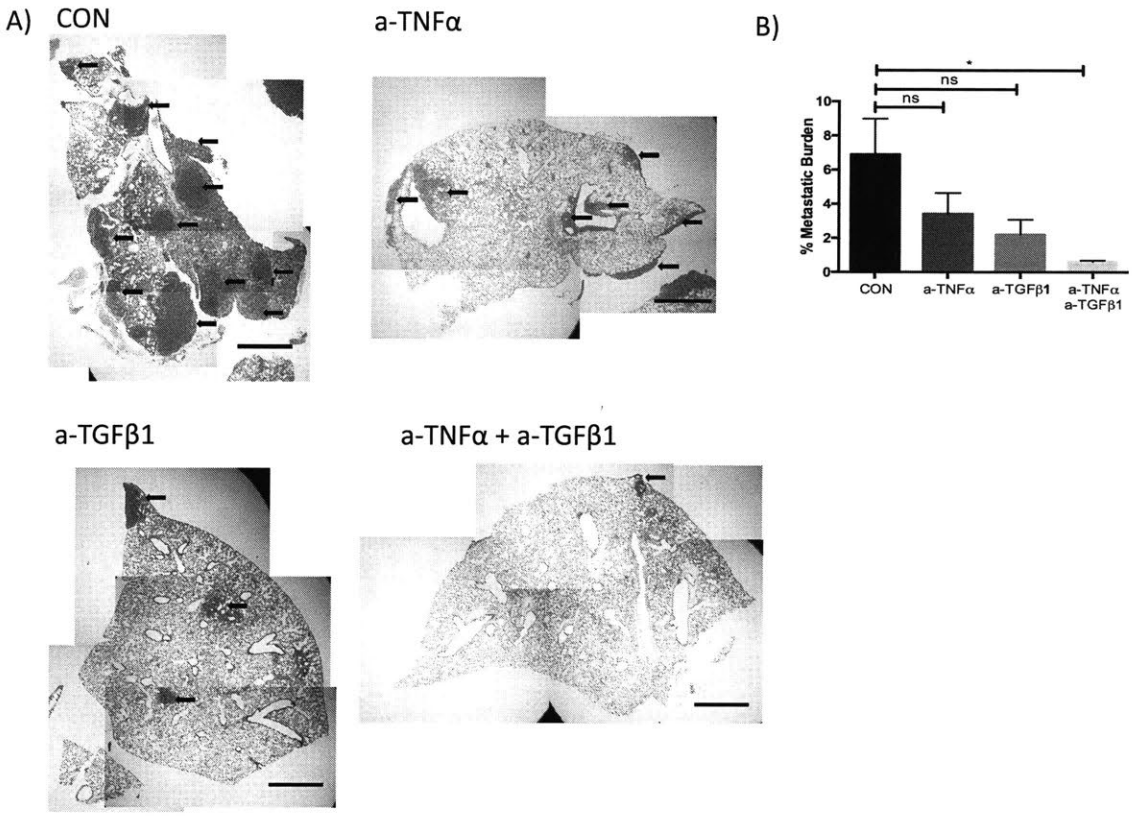

Fig. 3.20: Inhibiting both TNFα and TGFβ1 in a mice model of breast tumor effectively reduces lung metastasis. 4T1-tumor bearing mice were treated with anti-TNFα and/or anti-TGFβ1 antibodies, and the formation of metastatic lesion in the lung of the animal was compared. **(A)** Representative H&E-stained lung sections from control (CON) mice, mice treated with anti-TNFα antibody (anti-TNFα), anti-TGFβ1 antibody (anti-TGFβ1), and both antibodies. Black arrows point to metastatic lesions. Treatment of mice with both antibodies greatly reduced the occurrence of the metastatic lesions in lungs. **(B)** Quantification of the percent of lungs (by area) with metastatic lesion (% metastatic burden) showing that co-treatment of both antibodies led to the most pronounced reduction in metastatic formation in lung. Bars represents mean +/- SEM of data from 5 mice each group (ns=not significant, *: $p<0.05$).

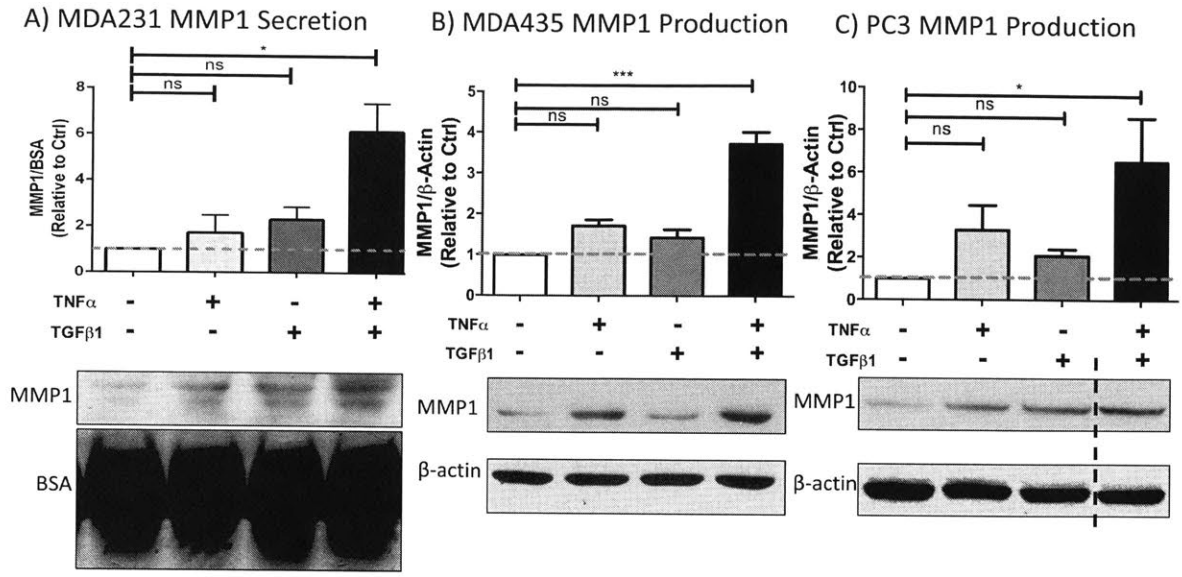

Fig. 3.21: TNFα and TGFβ1 co-treatment synergistically up-regulate cancer cell MMP1 protein production and secretion. (A) TNFα and TGFβ1 co-treatment synergistically increased the secretion of MMP1 by MDA-MB-231 cancer cells. Conditioned media from MDA-MB-231 cancer cells under various treatment conditions (as indicated) were collected. Western blot analysis was performed to measure the relative levels of MMP1 in the conditioned media. Representative western blot images (bottom) and quantification (top) are shown (Top band=glycosylated active MMP1, 47 kDa; bottom band=unglycosylated active MMP1, 42 kDa). **(B)** TNFα and TGFβ1 co-treatment synergistically enhanced MDA435 cancer cell production of MMP1 protein compared to no-treatment control. Western blot quantification (top) and representative western blot image (bottom) are shown. **(C)** TNFα and TGFβ1 co-treatment synergistically enhanced MMP1 protein production in PC3 compared to no-treatment control. Western blot quantification (top) and representative western blot images (bottom) are shown. Bars represent mean +/- SEM of data (fold change relative to no-treatment control) from at least 3 independent experiments (ns: not significant; *: $p<0.05$; *** $p<0.001$).

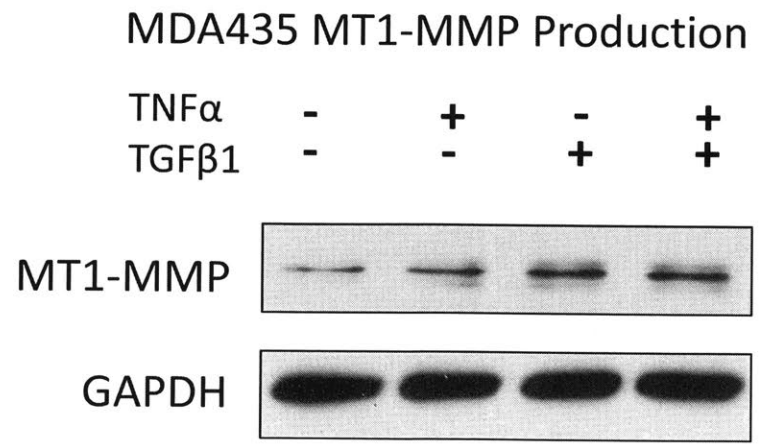

Fig. 3.22 TGFβ1 is mainly responsible for the increase in MT1-MMP protein production. Representative western blot images showing that TGFβ1 is mainly responsible for the increase in MT1-MMP expression in MDA435 cancer cells.

3.8: TNFα and TGFβ1 synergistically increase nuclear localization of NF-κB

To further understand the synergistic effects of TNFα and TGFβ1 on the expression of MMP1 in cancer cells, we tested whether TNFα and/or TGFβ1 could alter the expression or nuclear localization of NF-κB, a transcription factor for MMP1 (34). We first treated MDA231 cancer cells with TNFα and/or TGFβ1 for 48 hrs, and found that these two factors did not change the protein production of NF-κB by cancer cells (Fig. 3.23A). We then tested whether the treatment of these two factors could alter the nuclear localization of NF-κB. Indeed, co-treatment of TNFα and TGFβ1 synergistically enhanced NF-κB expression inside the nucleus of the cancer cells (Fig. 3.23B-C). These results support the conclusion that TNFα and TGFβ1 act together to enhance the expression of MMP1 via the synergistic induction of NF-κB nuclear translocation. Similar results were also observed in MDA435 cells (Fig. 3.24).

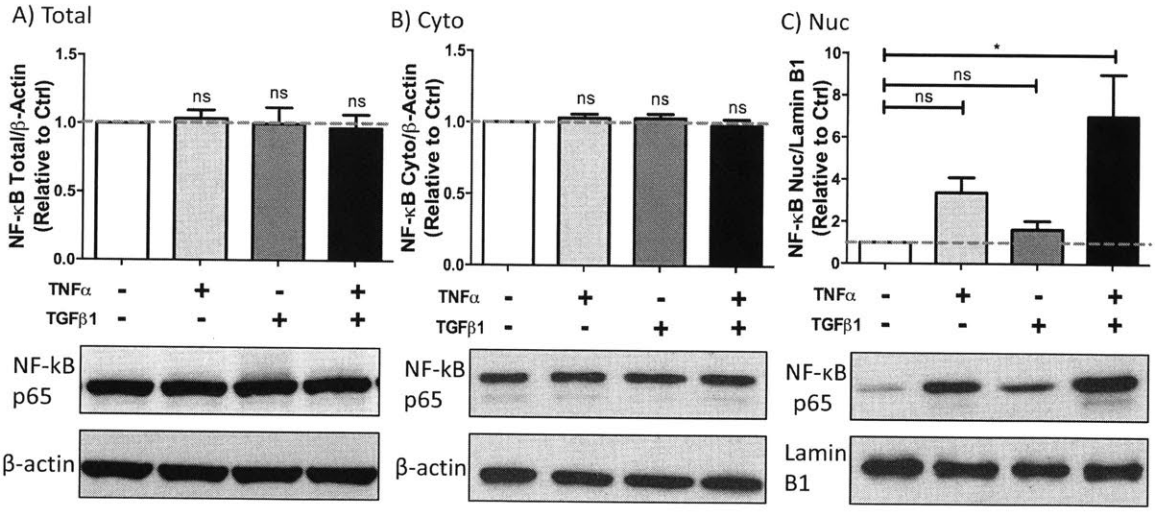

Figure 3.23: TNFα and TGFβ1 synergistically increase NF-κB nuclear localization. (A) Western blot quantification (top) and representative images (bottom) showing 48-hr TNFα and/or TGFβ1 treatments of MDA231 cells did not alter the production of NF-κB (NF-κB total). **(B and C)** Western blot quantifications (top) and representative images (bottom) showing 2-hr TNFα and TGFβ1 co-treatment of MDA231 synergistically increased the level of NF-κB in the nuclear fraction of MDA231 (NF-κB Nuc, C), but not in the cytoplasmic fraction of the cells (NF-κB Cyto, B). Bars represent mean +/- SEM of data (fold change relative to no-treatment control, Ctrl=control) from at least 3 independent experiments (ns: not significant; *: $p<0.05$).

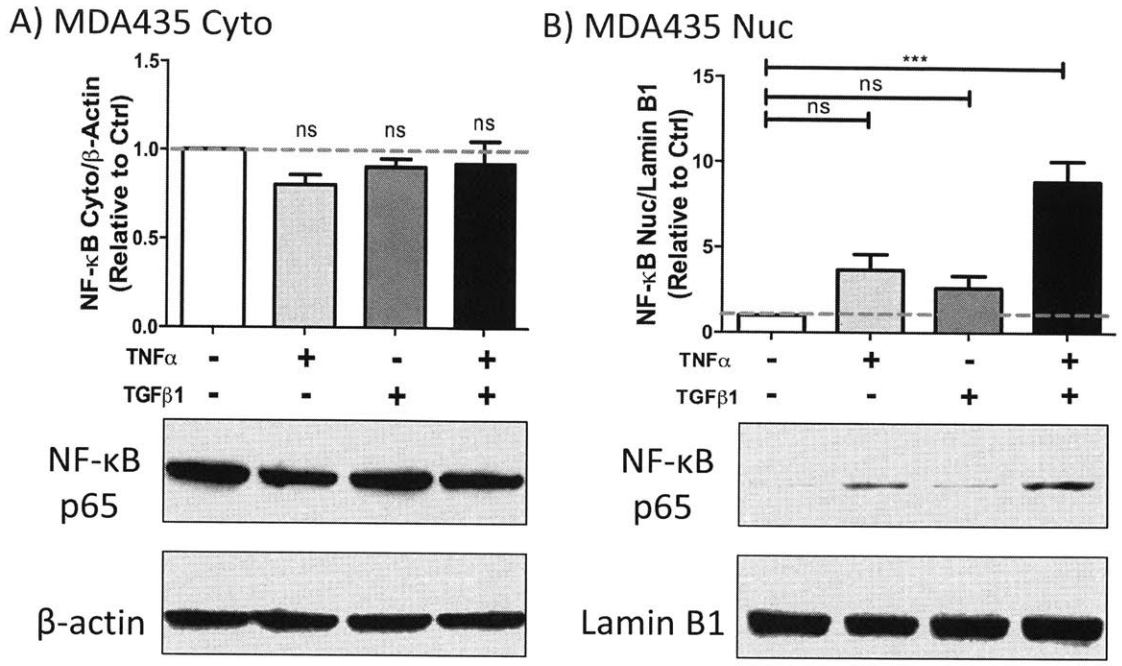

Figure 3.24: TNFα and TGFβ1 co-treatment synergistically enhance NF-κB nuclear localization in MDA-MB-435S cells. **(A)** Western blot quantification (top) and representative western blot images (bottom) showing no changes in the levels of NF-κB in the cytoplasmic fraction of MDA-MB-435S (MDA435) under various treatment conditions as indicated. (B) Western blot quantification (top) and representative western blot images (bottom) showing TNFα and TGFβ1 co-treatment synergistically increased the level of NF-κB in the nuclear fraction of MDA435 compared to no-treatment control. Bars represent mean +/- SEM of data (fold change relative to no-treatment control, Ctrl=control) from at least 3 independent experiments (ns: not significant; ***: $p<0.001$).

3.9: Discussion

Macrophages in the tumor microenvironment are key promoters of cancer cell metastasis (35), suggesting that the control of these cells and their released factors can be a viable strategy in treating metastasis. Yet, it is still unclear how macrophages affect different aspects of cancer cell migration, such as speed and persistence, especially in 3D ECM that closely mimics the *in vivo* tumor microenvironment. To address this gap in knowledge, we utilized a microfluidic 3D cell migration assay that allows us to study, in high resolution, the effects of macrophages on cancer cell migration speed (total speed) and persistence (directedness) in 3D ECM.

From our study, we found that macrophages increase cancer cell migration speed and persistence in 3D collagen I ECM, suggesting that macrophages may help cancer cells to invade and gain access to intravasation sites more efficiently. In contrast to the 3D results, we discovered that on 2D tissue culture plastic, macrophages tend to increase cancer cell migration speed but decrease persistence, so that cancer cells move faster, but more randomly. This disparity, similar to results obtained from previous works, illustrates

a fundamental difference in how cancer cells migrate in 2D compared to 3D (16). We also note that the cancer cells in our 3D microfluidic system migrated at a total speed of 5-11 μm/hr, a value which closely matches the speed values obtained from *in vivo* intravital imaging experiments (36). In sum, these results demonstrate the advantages of our microfluidic assay, which allows us to perform physiologically relevant studies with precise control of experimental conditions.

In 3D, cell migration critically depends on the ability of cancer cells to degrade ECM. Indeed, MMP expression is dispensable for 2D cell migration, but not for 3D (16). In the present study, we showed that macrophages enhanced cancer cell migration in 3D ECM via the up-regulation of MMP expression in cancer cells. We further identified that macrophage-released TGFβ1 increased cancer cell migration speed, while macrophage-released TNFα and TGFβ1 synergistically enhanced cancer cell migration persistence. Previous studies have shown that EGF released by macrophages can promote cancer cell migration (11). Here, we report that macrophage-released TNFα and TGFβ1 can also promote cancer cell migration. The clinical relevance of this finding is demonstrated by the fact that the expression levels of TNFα and TGFβ1 in tumor-associated macrophages correlates with metastasis for human tumors (24, 37). Moreover, this study, to our knowledge, is the first to report that macrophage-released TNFα and TGFβ1 control different aspects of cancer cell migration (speed vs. persistence) differently. Thus, although prior studies have implicated TNFα and TGFβ1 in cancer cell invasion and metastasis (28, 29), our results now demonstrate subtle but important differences in their effects on cancer cell migration.

We also found that TGFβ1 released by macrophages promotes cancer cell migration speed through up-regulation of MT1-MMP. We suspect this is due to the fact that MT1-MMP can influence cell intrinsic migration behaviors as well as cell extrinsic matrix properties, both of which are known determinants of cell migration speed in 3D matrix (16, 38). Two examples of cell intrinsic behaviors that control cell migration speed are the activities of kinases and the expression of integrin. It has been shown that intermediate levels of integrin α2β1 contribute to an optimum cell migration speed (39, 40); and inhibiting integrin could lead to a decrease in cell migration speed, but not persistence (14). Similarly, inhibiting Akt/PI3K activities in cells has been reported to result in a decrease in migration speed (41). In addition to cell intrinsic properties, cell extrinsic matrix properties, such as the pore size of the matrix that can be modified by MMPs, also affect cell migration speed in 3D (38). Unlike MMP1, which primarily degrades collagen I matrix to alter the cell extrinsic properties, MT1-MMP modifies both cell intrinsic and cell extrinsic properties. Besides degrading collagen I matrix, MT1-MMP can process integrin (42), mediate Akt phosphorylation (43), and promote syndecan shedding (44), all of which are parts of cell intrinsic pathways of migration. Hence, since both intrinsic and extrinsic properties control cell migration speed, it stands to reason that MT1-MMP should be the major determinant of migration speed over MMP1.

We further demonstrated that macrophage-enhanced cancer cell migration persistence, in contrast to total speed, was mediated primarily by the expression of

MMP1, but not MT1-MMP. This result may be explained by the fact that MMP1 is more efficient in degrading collagen I matrix and altering extrinsic matrix properties (pore size) than MT1-MMP (45). Although cell intrinsic properties (such as Rac activities (46)) control migration persistence in 2D, it has been reported that cell extrinsic matrix properties seem to dominate over intrinsic property as the primary determinant of 3D migration persistence (16, 47). Since MMP1 is more efficient in degrading collagen I ECM and altering extrinsic matrix properties than MT1-MMP, MMP1 should therefore be a major contributor to migration persistence.

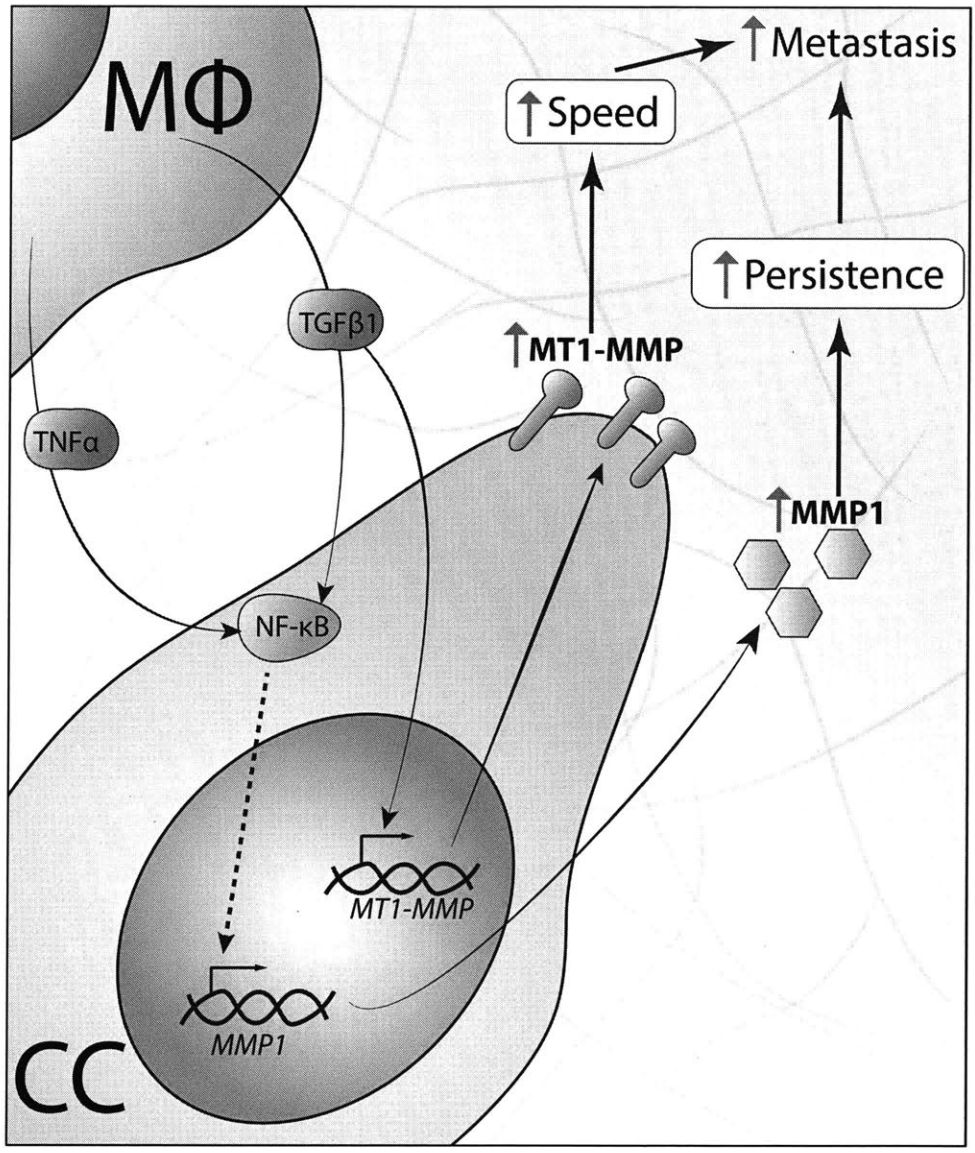

Fig. 3.25: Proposed mechanism explaining the effects of macrophages (MΦ) on cancer cell (CC) migration speed and persistence. Macrophage-released TNFα and TGFβ1 synergistically enhance NF-κB nuclear localization in cancer cells, leading to synergistic increases in cancer cell MMP1 mRNA expression, protein production, and protein secretion. This increase in MMP1 secretion by cancer cells leads to an increase in cancer cell migration persistence (directedness).

Meanwhile, macrophages increase cancer cell migration speed (total speed), mainly through TGFβ1-induced cancer cell expression of MT1-MMP.

Based on our findings, we propose a novel mechanism whereby macrophages promote cancer cell migration speed (total speed) and persistence (directedness) via two distinct mechanisms (Fig. 3.25). First, macrophage-released TNFα and TGFβ1 synergistically induce nuclear translocation of NF-κB in cancer cells, leading to synergistic increases in the expressions of MMP1, which results in a synergistic enhancement in cancer cell migration persistence. In contrast to the mechanism for the persistence, macrophages increase cancer cell migration speed, mainly through TGFβ1, by the up-regulation of cancer cell MT1-MMP expression. These findings establish that TNFα and TGFβ1 released by macrophages influence speed and persistence of cancer cell migration differently, and both of these factors need to be targeted to effectively inhibit macrophage-assisted cancer cell 3D migration and metastasis. Moreover, these findings also broaden our current view on the molecular determinants of 3D migration, suggesting that MT1-MMP primarily controls cell migration speed, whereas MMP1 mainly controls migration persistence. In conclusion, our findings provide new insights into macrophage-assisted cancer cell migration in 3D tumor microenvironment, and these could ultimately lead to novel therapeutic strategies to effectively inhibit tumor invasion and metastasis.

3.10: References

1. Lu P, Weaver VM, Werb Z (2012) The extracellular matrix: a dynamic niche in cancer progression. *J Cell Biol* 196(4):395–406.
2. Friedl P, Wolf K (2003) Tumour-cell invasion and migration: diversity and escape mechanisms. *Nat Rev Cancer* 3(5):362–74.
3. Egeblad M, Werb Z (2002) New functions for the matrix metalloproteinases in cancer progression. *Nat Rev Cancer* 2(3):161–74.
4. Kerkela E, Saarialho-Kere U (2003) Matrix metalloproteinases in tumor progression: focus on basal and squamous cell skin cancer. *Exp Dermatol* 12(2):109–125.
5. Yamaguchi H, Condeelis J (2007) Regulation of the actin cytoskeleton in cancer cell migration and invasion. *Biochim Biophys Acta* 1773(5):642–52.
6. Lewis CE, Pollard JW (2006) Distinct role of macrophages in different tumor microenvironments. *Cancer Res* 66(2):605–12.
7. Chen P, et al. (2011) Tumor-associated macrophages promote angiogenesis and melanoma growth via adrenomedullin in a paracrine and autocrine manner. *Clin Cancer Res* 17(23):7230–9.
8. Wyckoff JB, et al. (2007) Direct visualization of macrophage-assisted tumor cell intravasation in mammary tumors. *Cancer Res* 67(6):2649–56.
9. Zervantonakis IK, et al. (2012) Three-dimensional microfluidic model for tumor cell intravasation and endothelial barrier function. *Proc Natl Acad Sci* 109(34):13515–13520.
10. Patsialou A, et al. (2009) Invasion of human breast cancer cells in vivo requires both paracrine and autocrine loops involving the colony-stimulating factor-1 receptor. *Cancer Res* 69(24):9498–506.
11. Goswami S, et al. (2005) Macrophages promote the invasion of breast carcinoma cells via a colony-stimulating factor-1/epidermal growth factor paracrine loop. *Cancer Res* 65(12):5278–83.
12. Polacheck WJ, Zervantonakis IK, Kamm RD (2013) Tumor cell migration in complex microenvironments. *Cell Mol Life Sci* 70(8):1335–56.
13. Haessler U, Teo JCM, Foretay D, Renaud P, Swartz M a (2012) Migration dynamics of breast cancer cells in a tunable 3D interstitial flow chamber. *Integr Biol (Camb)* 4(4):401–9.
14. Maheshwari G, Lauffenburger D a (1998) Deconstructing (and reconstructing) cell migration. *Microsc Res Tech* 43(5):358–68.
15. Polacheck WJ, Charest JL, Kamm RD (2011) Interstitial flow influences direction of tumor cell migration through competing mechanisms. *Proc Natl Acad Sci U S A* 108(27):11115–20.
16. Kim H-D, et al. (2008) Epidermal growth factor-induced enhancement of glioblastoma cell migration in 3D arises from an intrinsic increase in speed but an extrinsic matrix- and proteolysis-dependent increase in persistence. *Mol Biol Cell* 19(10):4249–59.
17. Kauppila S, Stenbäck F, Risteli J, Jukkola A, Risteli L (1998) Aberrant type I and type III collagen gene expression in human breast cancer in vivo. *J Pathol* 186(3):262–8.

18. Provenzano PP, et al. (2008) Collagen density promotes mammary tumor initiation and progression. *BMC Med* 6:11.
19. Liu H, et al. (2012) The role of MMP-1 in breast cancer growth and metastasis to the brain in a xenograft model. *BMC Cancer* 12:583.
20. Poola I, et al. (2005) Identification of MMP-1 as a putative breast cancer predictive marker by global gene expression analysis. *Nat Med* 11(5):481–3.
21. Lu X, et al. (2009) ADAMTS1 and MMP1 proteolytically engage EGF-like ligands in an osteolytic signaling cascade for bone metastasis. *Genes Dev* 23(16):1882–94.
22. Jacob A, Prekeris R (2015) The regulation of MMP targeting to invadopodia during cancer metastasis. *Front cell Dev Biol* 3:4.
23. Ha HY, et al. (2001) Overexpression of membrane-type matrix metalloproteinase-1 gene induces mammary gland abnormalities and adenocarcinoma in transgenic mice. *Cancer Res* 61(3):984–90.
24. Miles DW, et al. (1994) Expression of tumour necrosis factor (TNF alpha) and its receptors in benign and malignant breast tissue. *Int J Cancer* 56(6):777–82.
25. Chong H, Vodovotz Y, Cox GW, Barcellos-Hoff MH (1999) Immunocytochemical localization of latent transforming growth factor-beta1 activation by stimulated macrophages. *J Cell Physiol* 178(3):275–83.
26. Mantovani A, Sozzani S, Locati M, Allavena P, A S (2002) Macrophage polarization: tumor-associated macrophages as a paradigm for polarized M2 mononuclear phagocytes. *Trends Immunol* 23(11):549–555.
27. Loercher AE, Nash MA, Kavanagh JJ, Platsoucas CD, Freedman RS (1999) Identification of an IL-10-producing HLA-DR-negative monocyte subset in the malignant ascites of patients with ovarian carcinoma that inhibits cytokine protein expression and proliferation of autologous T cells. *J Immunol* 163(11):6251–60.
28. Massagué J (2008) TGFbeta in Cancer. *Cell* 134(2):215–30.
29. Balkwill F (2006) TNF-alpha in promotion and progression of cancer. *Cancer Metastasis Rev* 25(3):409–16.
30. Cudejko C, et al. (2011) p16INK4a deficiency promotes IL-4-induced polarization and inhibits proinflammatory signaling in macrophages. *Blood* 118(9):2556–66.
31. Li D, et al. (2014) IL-33 promotes ST2-dependent lung fibrosis by the induction of alternatively activated macrophages and innate lymphoid cells in mice. *J Allergy Clin Immunol* 134(6):1422–1432.e11.
32. Daigneault M, Preston JA, Marriott HM, Whyte MKB, Dockrell DH (2010) The Identification of Markers of Macrophage Differentiation in PMA-Stimulated THP-1 Cells and Monocyte-Derived Macrophages. *PLoS One* 5(1):e8668.
33. Nacu N, et al. (2008) Macrophages produce TGFβ1 (BIGH3) following ingestion of apoptotic cells and regulate MMP14 levels and collagen turnover in fibroblasts. *J Immunol* 180(7):5036–44.
34. Vincenti MP, Coon CI, Brinckerhoff CE (1998) Nuclear factor kappaB/p50 activates an element in the distal matrix metalloproteinase 1 promoter in interleukin-1beta-stimulated synovial fibroblasts. *Arthritis Rheum* 41(11):1987–94.
35. Pollard JW (2004) Tumour-educated macrophages promote tumour progression and metastasis. *Nat Rev Cancer* 4(1):71–8.
36. Gligorijevic B, Bergman A, Condeelis J (2014) Multiparametric classification

links tumor microenvironments with tumor cell phenotype. *PLoS Biol* 12(11):e1001995.
37. Ye X, et al. (2012) Tumor-associated microglia/macrophages enhance the invasion of glioma stem-like cells via TGF-β1 signaling pathway. *J Immunol* 189(1):444–53.
38. Wolf K, et al. (2013) Physical limits of cell migration: control by ECM space and nuclear deformation and tuning by proteolysis and traction force. *J Cell Biol* 201(7):1069–84.
39. Palecek SP, Loftus JC, Ginsberg MH, Lauffenburger DA, Horwitz AF (1997) Integrin-ligand binding properties govern cell migration speed through cell-substratum adhesiveness. *Nature* 385(6616):537–40.
40. Huttenlocher A, Horwitz AR (2011) Integrins in cell migration. *Cold Spring Harb Perspect Biol* 3(9):a005074.
41. Montero J-A, Kilian B, Chan J, Bayliss PE, Heisenberg C-P (2003) Phosphoinositide 3-Kinase Is Required for Process Outgrowth and Cell Polarization of Gastrulating Mesendodermal Cells. *Curr Biol* 13(15):1279–1289.
42. Deryugina EI, Ratnikov BI, Postnova TI, Rozanov D V, Strongin AY (2002) Processing of integrin alpha(v) subunit by membrane type 1 matrix metalloproteinase stimulates migration of breast carcinoma cells on vitronectin and enhances tyrosine phosphorylation of focal adhesion kinase. *J Biol Chem* 277(12):9749–56.
43. Eisenach PA, Roghi C, Fogarasi M, Murphy G, English WR (2010) MT1-MMP regulates VEGF-A expression through a complex with VEGFR-2 and Src. *J Cell Sci* 123(Pt 23):4182–93.
44. Endo K, et al. (2003) Cleavage of syndecan-1 by membrane type matrix metalloproteinase-1 stimulates cell migration. *J Biol Chem* 278(42):40764–70.
45. Imai K (1997) Membrane Type 1Matrix Metalloproteinase Digests Interstitial Collagens and Other Extracellular Matrix Macromolecules. *J Biol Chem* 272(4):2446–2451.
46. Pankov R, et al. (2005) A Rac switch regulates random versus directionally persistent cell migration. *J Cell Biol* 170(5):793–802.
47. Wu P-H, Giri A, Sun SX, Wirtz D (2014) Three-dimensional cell migration does not follow a random walk. *Proc Natl Acad Sci U S A* 111(11):3949–54.

Chapter 4. Effects of Interstitial Flow on Macrophage Migration and Polarization

4.1: Abstract

This chapter contains contents from a manuscript entitled "**Interstitial Flow Promotes Macrophage Migration and Polarization in 3D ECM**" with authors *Ran Li, Hao Xing, Tara Lee, Hesham Azizgolshani, and Roger Kamm*. This manuscript has been submitted to the Proceedings of the National Academy of Sciences, and it is currently under review.

The growth of solid tumor is often accompanied by an increase in interstitial fluid flow from the center of the tumor to the surrounding stroma. Recent studies have shown that interstitial flow (IF) can influence the migration of cancer cells and fibroblasts. However, the effects of IF on macrophages, one of the key tumor-associate immune cell types, have not been explored. We used microfluidic and transwell assays to investigate how tumor-associated IF affects macrophage migration and protein expression. We found that IF not only promoted macrophage migration in 3D extracellular matrix, but also directed macrophages to migrate against the flow. Moreover, IF significantly enhanced macrophage expression of pro-metastatic M2 markers arginase-I (ArgI) and TGFβ through β1 integrin/Src-mediated activation of STAT3/6. Consistent with this flow-induced pro-metastatic M2 polarization, macrophages treated with IF were shown to have an enhanced ability to promote cancer cell migration. Taken together, these results suggest that IF can contribute to metastasis through its effects on macrophages. Specifically, since macrophages migrate against the flow, IF, which emanates from the center of the tumor to the surrounding stromal tissues, can act as a mechanical stimulus to recruit macrophages into the tumor. Moreover, IF can polarize these macrophages toward a pro-metastatic M2 phenotype to further promote metastasis and immunosuppression. Therefore, our study demonstrates that IF can be a critical regulator of macrophage phenotypes and immune microenvironment.

4.2: Introduction

In Chapter Three, we investigated how chemical factors secreted by macrophages in the tumor microenvironment affect subtle, yet important, features (speed vs. persistence) of cancer cell migration. However, in addition to these chemical factors, biophysical forces within the tumor microenvironment can also affect tumor progression and metastasis. As discussed in Chapter One, fluid force produced by elevated interstitial flow (IF) is a key biomechanical factor inside the tumor microenvironment. This flow of interstitial fluid through the extracellular matrix (ECM) is the result of pressure gradients and lymphatic drainage within the tissue (1). In the normal tissue, IF is estimated to be around ~0.5 μ m/s. However, in the tumor tissue, the build-up of fluid pressure in the tumor core increases IF emanating from the center of the tumor and draining into the surrounding stroma (2). This tumor-associated IF, ranging from 1-5 μm/s, is highest at

the tumor margin (1–3). Previous studies have shown that IF can influence the migration of cancer cells (4–6) (7), fibroblasts (8), endothelial cells (9, 10), and smooth muscle cells (11) via mechanotransduction pathways or flow-induced gradients of autocrine factors. Nevertheless, the effects of this crucial tumor-associated biophysical force on macrophages, a key immune cell type in the tumor microenvironment, have not been explored.

As shown in Chapter Three, macrophages play critical roles in tumor metastasis (12). Macrophages are innate immune cells that can rapidly adopt different phenotypes based on the stimuli they encounter in their environment. These functionally plastic cells can polarize toward a pro-inflammatory M1 phenotype or an immunosuppressive, pro-metastatic, and pro-wound healing M2 phenotype (13). Macrophages in the tumor microenvironment often adopt an M2 phenotype, and the number of M2 macrophages that reside in the tumor tissues correlates with metastasis and poor prognosis (14). Indeed, M2 macrophages produce various growth factors and cytokines that promote cancer cell migration, intravasation, and immune escapes (13, 15). In contrast, M1 macrophages are thought to promote tumor suppression by activating anti-tumor immunity.

The dual roles that macrophages (M1 vs. M2) play in tumor progression make them attractive targets for anti-tumor therapy. Tumor-associated macrophages tend to reside near the tumor margin (15–17). Since IF is highest there, we expect these macrophages to experience an elevated IF *in vivo*. Therefore, it is important to study how this tumor-associated physical factor affects macrophages to gain a detailed understanding of the tumor microenvironment. This in turn can aid in the design of cancer immunotherapy. Moreover, integrin and glycocalyx, both of which have been implicated in flow-induced mechanotransduction in cancer cells and smooth muscle cells, are conserved in macrophages (18, 19). Since these molecules play important roles in macrophage migration and protein production (20–23), we hypothesized that IF could influence macrophage movement and protein expression.

In this study, we investigated the effects of tumor-associated IF (~3 μm/s) on macrophages seeded inside a 3D ECM. Using the microfluidic flow assay discussed in Chapter Two, we demonstrate that IF significantly enhances macrophage migration speed and persistence. Interestingly, IF treatment leads to the accumulation of actin and formation of protrusions on the flow-facing (upstream) side of the cell, resulting in the migration of macrophages against the flow direction (upstream). Next, we used the previously discussed transwell flow assay to show that IF activates FAK and Akt, kinases involved in macrophage migration. More importantly, we provide evidence that IF up-regulates the macrophage expression of M2 markers ArgI and TGF-β via β1 integrin/Src-mediated activation of STAT3/6. Concomitantly, IF treatment enhances the ability of macrophages to promote cancer cell migration and protrusion formation. Taken together, our results reveal, for the first time, that IF induces macrophage upstream (against the flow) migration and polarization toward a pro-metastatic M2 phenotype. Since IF emanates from the center of the tumor, these results suggest that IF can enhance

metastasis by promoting not only macrophage M2 polarization but also macrophage infiltration into the tumor core.

4.3: Method

To study the effects of interstitial flow on macrophage migration and protein expression, we utilized the microfluidic and transwell flow assays discussed in Chapter Two. Briefly, for the microfluidic flow assay, macrophages were seeded in a 2.5 mg/mL collagen I ECM embedded in the microfluidic device with two large media reservoirs attached to the top of the device. The collagen I ECM containing the cells was flanked by two media channels connected to the reservoirs. A media-height difference of 1.5 mm was established between the two reservoirs to generate a hydrostatic pressure gradient across the gel region, which we estimated, based on the measured collagen gel hydraulic permeability of $7x10^{-14}$ m^2, to drive interstitial fluid flow with a mean velocity of ~3 μm/s through the collagen gel containing macrophages. We chose the velocity of 3 μm/s to match the level of IF in the tumor tissues measured *in vivo*. Time-lapse microscopy was used to track macrophage migration under the effects of IF, and macrophage migration dynamics were computed as discussed in Chapter Two.

To investigate the effects of IF on macrophage protein expression, the transwell flow assay was used. Macrophages were seeded inside a 2.5 mg/mL collagen I ECM loaded into a transwell insert. Growth media-height difference (~10 mm) was established between the inside and the outside of the insert to drive an IF of ~3 μm/s through the collagen gel containing macrophages. To maintain the media-height difference, the transwell system was connected to a pump that re-circulates media from the outside to the inside of the insert. After IF treatment, cell lysates were collected for western blot analysis. A detailed description of the experimental procedures and assays used in this study can be found in Chapter Two and Appendix B.

All statistical analyses were performed using GraphPad Prism with a P-value of <0.05 considered statistically significant. The difference between groups was evaluated by two-tailed student t-test. In all figures, ns represents not significant, * represents $p<0.05$, ** represents $p<0.01$, and *** represents $p<0.001$. For cell migration quantification, bars represent mean ± standard error of mean (SEM) of data from 40-100 cells from 3 independent experiments. For western blot quantification, bars represent mean ± SEM of data (fold increase relative to no-flow control) from at least 3 independent experiments.

4.4: Interstitial flow (IF) enhances macrophage migration in 3D ECM

Using the microfluidic flow assay, we treated macrophages in the 3D ECM with 3 μm/s IF, and we tracked the movement of macrophages to map cell migration trajectories. Two aspects of macrophage migration were quantified: speed and persistence. Speed was quantified by measuring migration total speed, which is defined as the total distance that a macrophage travelled divided by time. Persistence was quantified by measuring migration directedness, which is defined as the ratio between the

displacement and the total distance travelled (Fig. 2.5). Trajectory plots (Fig. 4.1A) and migration quantification (Fig. 4.1B) show that IF significantly increased both migration total speed and directedness of Raw 264.7 macrophages (Raw) and primary bone marrow-derived macrophages (BMDM). These results indicate that IF promotes macrophages to migrate faster and more persistently in the 3D ECM. Finally, we verified that IF treatment did not alter the viability of macrophages as assessed through live/dead assay (Fig 4.2).

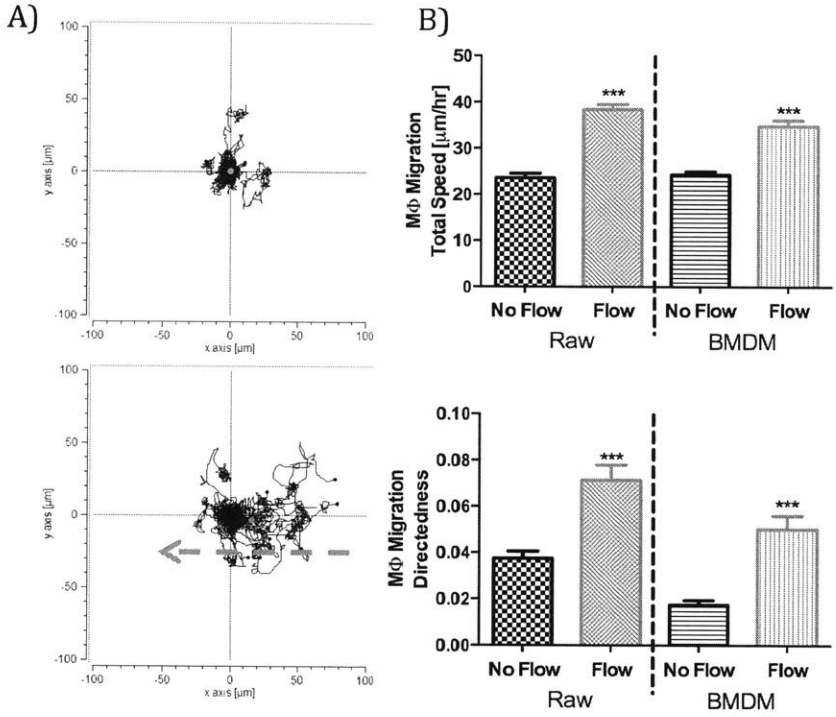

Fig. 4.1: Interstitial flow (IF) promotes macrophage migration in 3D ECM. (A) Representative migration trajectories for Raw macrophages in ECM under no-flow (top) and flow (bottom) conditions. The arrow indicates flow direction. **(B)** 3 μm/s IF increased macrophage migration total speed (top) and directedness (bottom) for both Raw macrophages and BMDM. Bars represent mean ± standard error of mean (SEM) of data from 60-100 cells (n=3, n = # of independent experiments; ***: $p<0.001$).

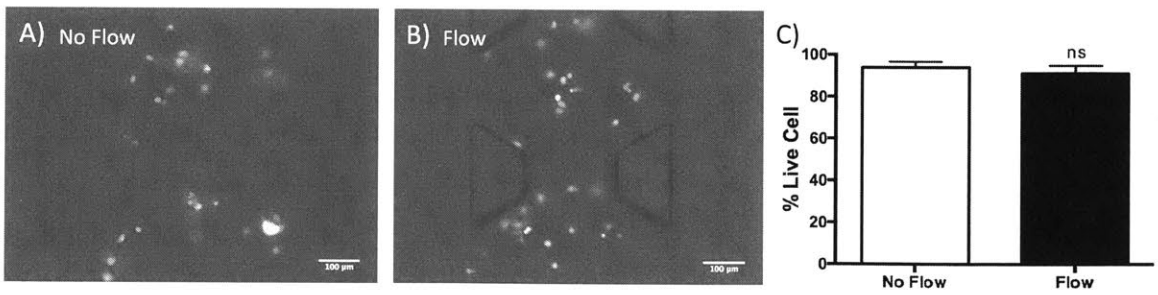

Fig. 4.2: IF did not affect macrophage viability. Raw 264.7 macrophages seeded in the microfluidic device were treated with 3 μm/s interstitial flow for 48 hrs, and the viability of the macrophages was assessed using live-dead assay. **(A and B)** Fluorescent micrographs showing the live/dead staining of macrophages treated with (B) or without interstitial flow (A) in the

microfluidic devices (Green=live cell; Red=dead cell). **(C)** Quantification of the live-dead staining shows that interstitial flow treatment did not change the % live cell count compared to no-flow control. Bars represent mean ± SEM of data (n=3, ns=not significant).

Since Akt and FAK phosphorylation can increase macrophage motility (24, 25), we conducted experiments in a transwell flow chamber to determine if IF could induce the activation (phosphorylation) of these two kinases. Using the transwell flow chamber, we treated macrophages with IF for 1 hr and collected the cell lysates for western blot analysis. We found that, compared to no-flow control, IF induced 2-3 fold increases in the phosphorylation of Akt and FAK at Ser473 and Tyr397, respectively (Fig. 4.3). These results suggest that flow-enhanced migration of macrophages may be the results of IF-induced activation of Akt and FAK.

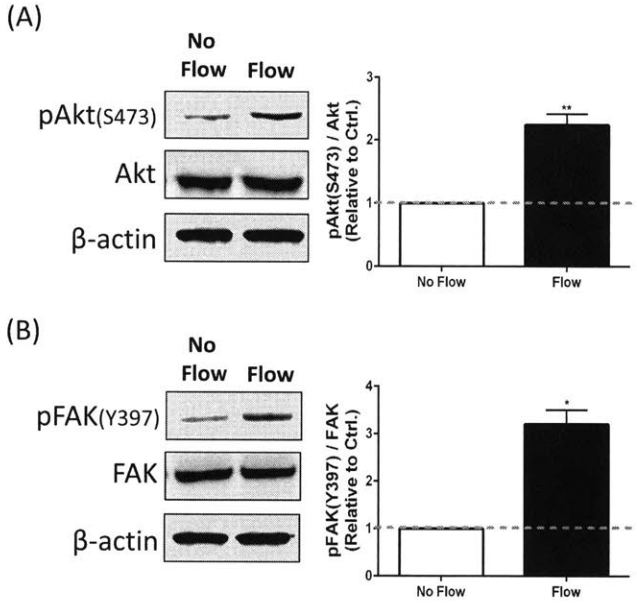

Fig. 4.3: IF activates Akt and FAK. IF activates kinases involved in cell migration. Western blot quantification (right) and representative images (left) showing that 1-hr IF (~3 μm/s) treatment up-regulated the phosphorylation of Akt at Ser473 (A) and FAK at Tyr397 (B) in Raw 264.7 macrophages. Bars represent mean ± SEM of data (fold change relative to no-flow control, Ctrl=control; n=3; *: $p<0.05$, **: $p<0.01$).

4.5: IF directs macrophage migration against flow

Upon a closer examination of cell trajectories, we noticed that IF biased macrophage migration against the flow direction (upstream). This is evident by the center of the mass of macrophage migration, which represents the population average of macrophage migration end-points. Cell trajectory plots show that IF shifted the center of mass of macrophage migration (red dot in Fig. 4.1) against the direction of the flow. This is in contrast to the no-flow control condition, which shows that the center of mass remained at origin (no directional preference in cell migration). This upstream migration

was further verified by Rose plots (Fig. 4.4 A and B), which show that ~70% of macrophages migrated upstream under IF treatment compared to roughly an equal number (~50%) migrating in both directions for no-flow control (Fig. 4.4 C).

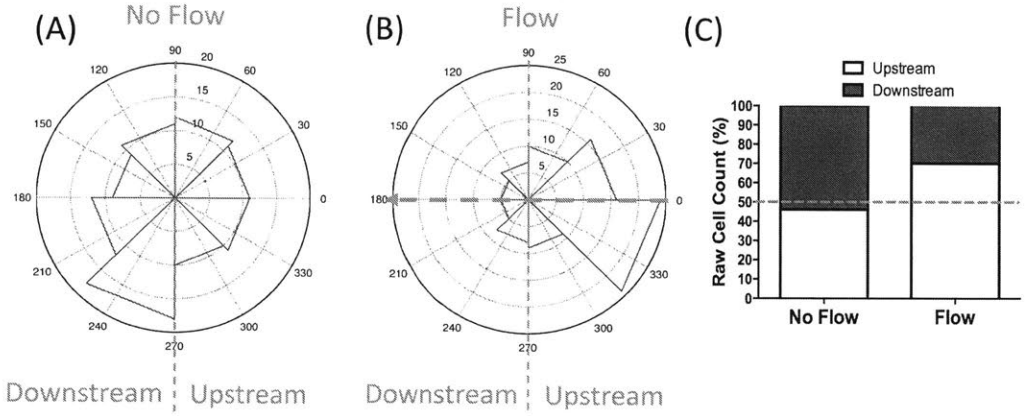

Fig. 4.4: IF directs macrophage migration upstream. (A and B) Rose plots showing the distribution of angles of net migration vectors for Raw macrophages in no-flow (A) and IF conditions (B). The red arrow represents the direction of flow. Note that more macrophages migrated upstream (against the direction of the flow). **(C)** Quantification of the percentage of the Raw macrophages that migrated upstream and downstream. More macrophages migrated upstream under flow conditions.

To further quantify this upstream migration, we calculated upstream velocity and upstream directedness of macrophage migration. Upstream velocity is calculated as the vector component of macrophage displacement against the flow direction (D_{up}) divided by time (t). Upstream directedness is defined as D_{up} divided by the total distance travelled (L), and represents how persistently the macrophages migrate against the flow (Fig. 2.5). Hence, a cell traveling upstream will have positive upstream velocity and directedness values, while a cell traveling downstream will have negative values. When treated with IF, macrophages migrated with positive mean upstream velocity and upstream directedness for both Raw cells and BMDM. By comparison, macrophages that were not treated with flow have population average values near zero, indicating no directional preference in migration (Fig. 4.5 A and B). Further analysis of the histograms of upstream migration velocity and directedness verified that IF induced more macrophages to migrate against the direction of flow. In addition, the histograms reveal that there seems to be a subpopulation of macrophages that migrated with higher upstream velocity and directedness than the rest of the cells (Fig. 4.6). This result indicates there may be heterogeneity in macrophages' responses to IF. Moreover, IF also increased the accumulation of actin and the formation of the protrusions on the upstream (flow-facing) side of the macrophages (Fig. 4.7). Collectively, these results demonstrate that IF promotes the actin accumulation and protrusion formation favoring the upstream side of the macrophages, resulting in a preferential migration against the direction of flow (upstream velocity and directedness).

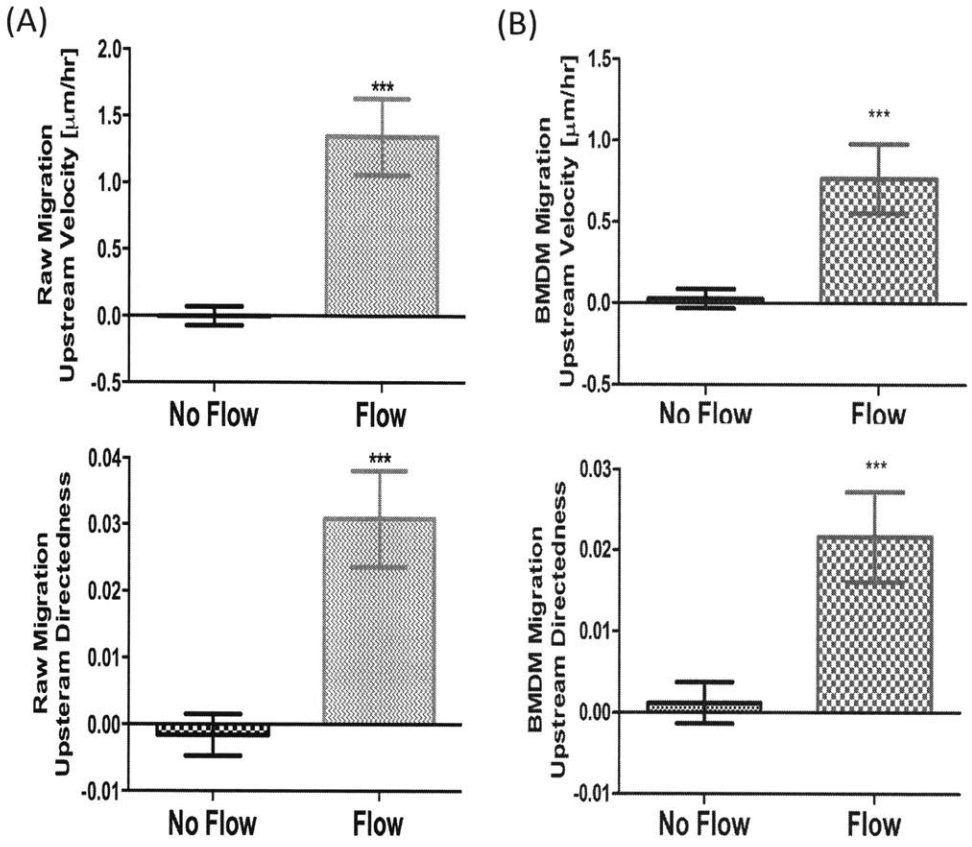

Fig. 4.5: IF (~3 μm/s) enhanced the upstream migration velocity (up) and directedness (down) for both Raw macrophages (A) and BMDM (B). Bars represent mean ± SEM of data from 60-100 cells (n=3; ***: $p<0.001$).

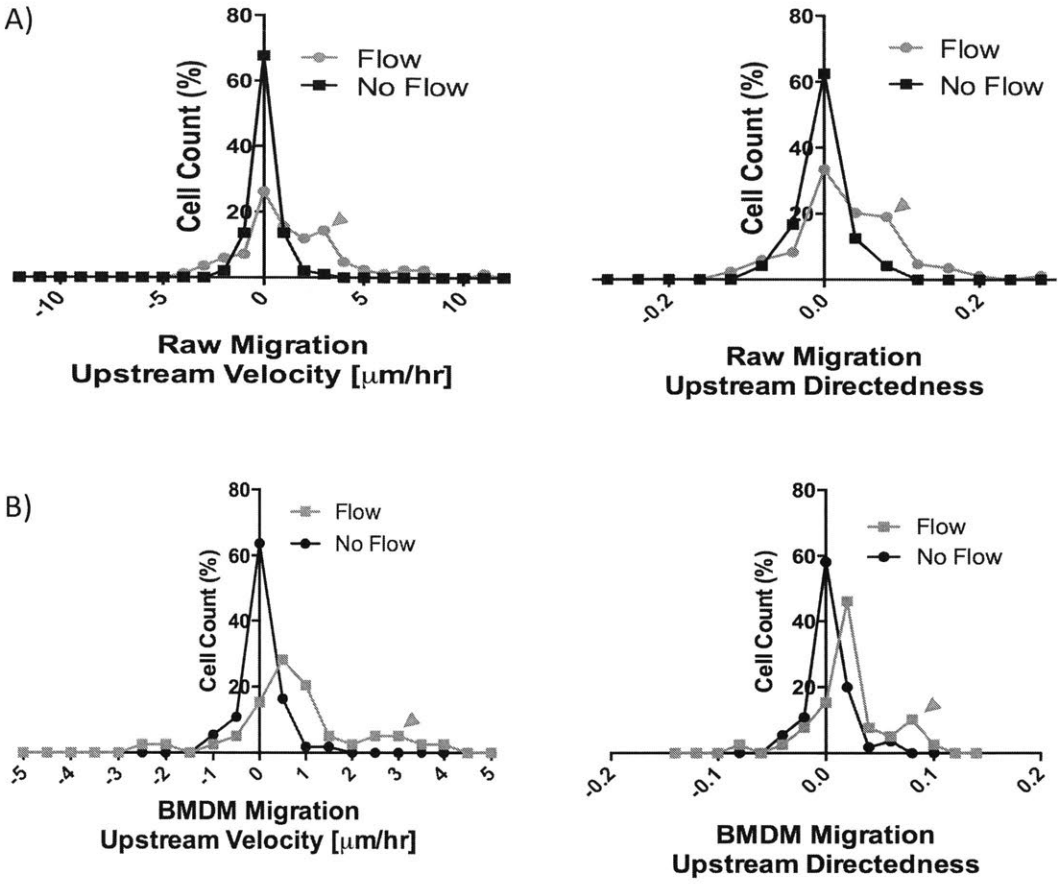

Fig. 4.6: Histograms of macrophage upstream migration velocity and directedness. The histograms show that interstitial flow enhanced the percent of cells migrating with positive upstream velocity (left) and upstream directedness (right) for both Raw 264.7 macrophages (A) and BMDMs (B). A careful observation of the histograms reveals that IF treatment resulted in a subpopulation of cells (blue arrow) that migrated with higher upstream velocity and directedness than the rest of the population. Data from 60-100 cells per condition.

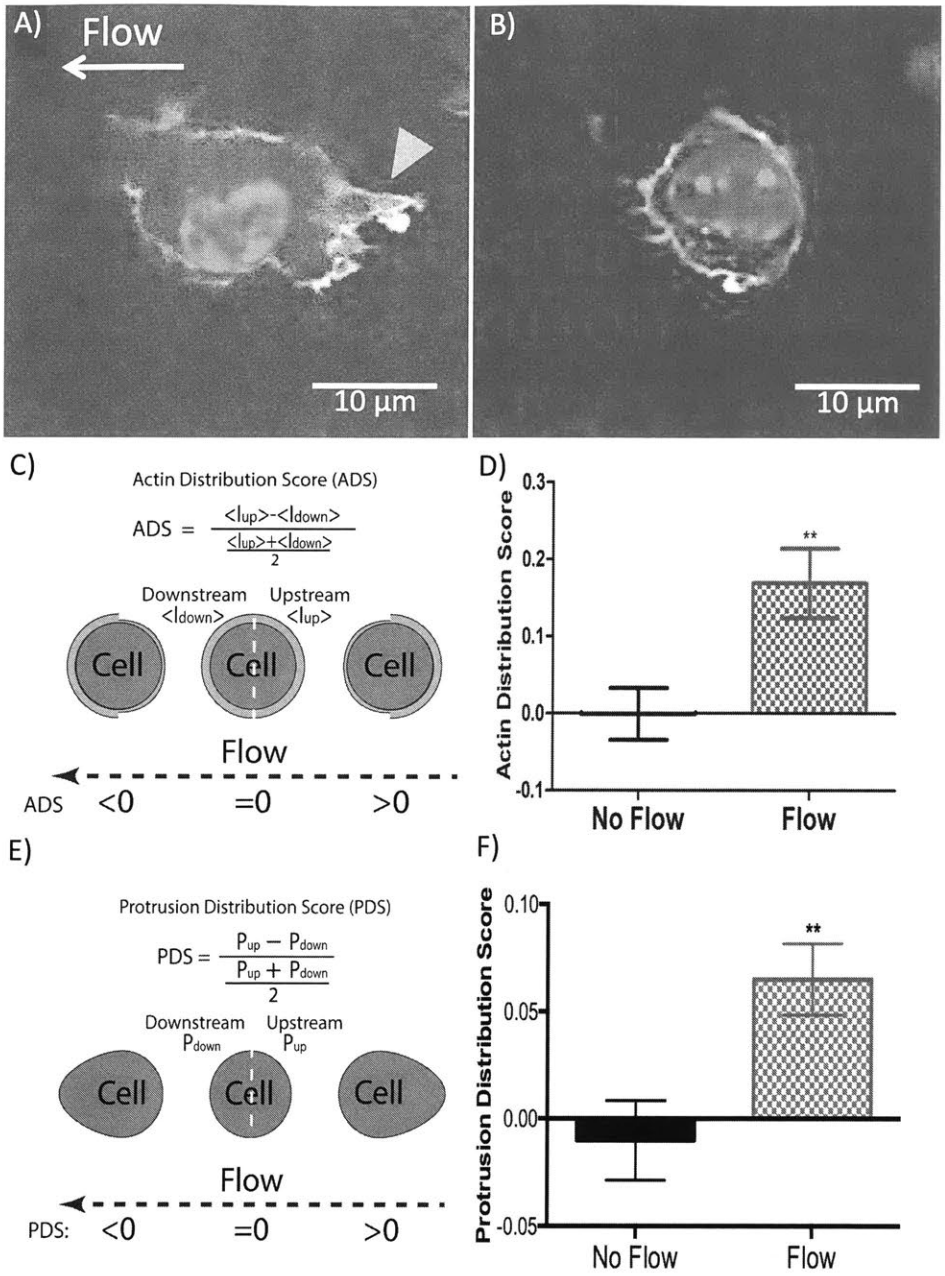

Fig. 4.7: Interstitial flow promotes the accumulation of actin and protrusion formation against the direction of flow. (A and B) Representative confocal fluorescent microscopy images (green=actin, blue=nucleus) showing actin localized to the periphery of the Raw macrophages when cells were cultured in 3D ECM. IF (~3 μm/s) treatment led to the accumulation of actin (green) and formation of protrusion (blue arrow) at the upstream (flow-facing) side of the macrophages (white arrow represents flow direction) (A). This is in contrast to no-flow control condition (B). **(C)** Actin distribution in macrophages was quantified with actin distribution score (ADS), which is defined as the difference between the average fluorescent intensities of actin on the upstream ($<I_{up}>$) and downstream side of the cell ($<I_{down}>$) divided by the average fluorescent intensity of the entire cell. Positive ADS indicates actin is accumulated on the upstream side, while a negative ADS indicates actin is accumulated on the downstream side. Zero ADS indicates no spatial preference. **(D)** Interstitial flow treatment resulted in a positive population average

ADS, indicating that actin accumulated to the upstream side in most macrophages treated with IF. This is in contrast to macrophages that were not treated with flow, which showed a population average ADS of zero. **(E)** The spatial distribution of macrophage protrusion was quantified by protrusion distribution score (PDS), which is defined as the difference between the perimeters of upstream side (P_{up}) and downstream side (P_{down}) of the cells divided by the average. Positive PDS means protrusion preferentially formed on the upstream side, while negative PDS means protrusion formed on the downstream side. Zero PDS indicates no spatial preference. **(F)** IF treatment resulted in a positive population average PDS, meaning IF drives the formation of protrusion against the flow direction. Bars represent mean ± SEM of data from 40-80 cells (n=3; **: $p<0.01$).

4.6: IF promotes macrophage M2 polarization via the activation of STAT3/6

M2 macrophages inside the tumor tissues can promote metastasis by enhancing tumor angiogenesis and migration (13). Since elevated IF has been shown to correlate with metastasis (2), we hypothesized that IF could promote macrophage M2 polarization. To test this hypothesis, we treated macrophages with IF for 48 hrs in absence of any externally applied chemical stimulus, and assessed the effects of IF on macrophage expression of M2 and M1 markers. We found that IF up-regulated the protein expressions of M2 markers arginase-I (ArgI) and TGFβ by ~12 folds and 6 folds, respectively. Concomitantly, IF slightly reduced the expression of the M1 marker iNOS compared to the no-flow control (Fig. 4.8). Hence, we conclude that IF can polarize macrophages toward an M2 phenotype.

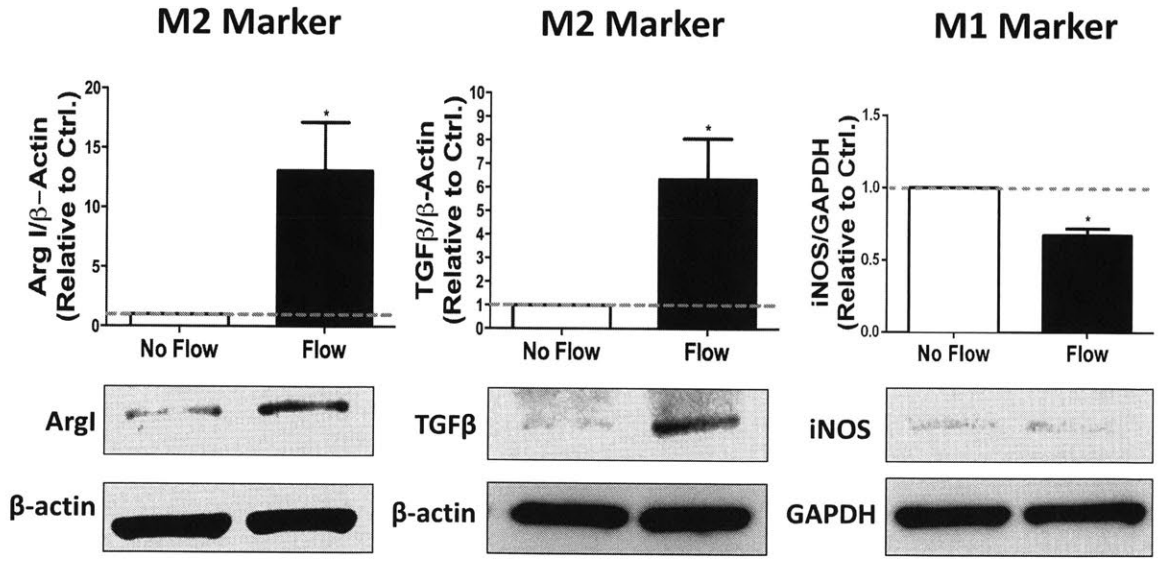

Fig. 4.8: IF induces macrophage M2 polarization. Western blot quantification (top) and representative images (bottom) showing 48-hrs IF (~3 μm/s) treatment up-regulated protein expression of M2 markers ArgI and TGFβ (left and center), and slightly down-regulated protein expression of M1 marker iNOS (right) in Raw macrophages. Bars represent mean ± SEM of data (fold change relative to no-flow control, Ctrl=control; n=3; *: $p<0.05$; **: $p<0.01$).

STAT3 and STAT6 are known transcription factors, when activated (phosphorylated), leading to the production of M2 markers in macrophages (26, 27). To further probe the mechanisms of flow-induced M2 polarization, we tested the effects of IF on the activation of STAT3/6 pathways in macrophages. We found that 15-60 min IF treatment enhanced the phosphorylation of STAT6 at Tyr641, as well as STAT3 at both Tyr705 and Ser727 (Fig. 4.9). In contrast, IF treatment did not activate STAT1, a transcription factor for M1 polarization (Fig. 4.10) (27). Collectively, these results illustrate that IF induces the M2 polarization of macrophages via the selective activation of M2-associated STAT3/6 pathway. Indeed, when we inhibited the phosphorylation of STAT3/6 with ruxolitinib, flow-induced expression of ArgI and TGFβ was reduced (Fig. 4.11).

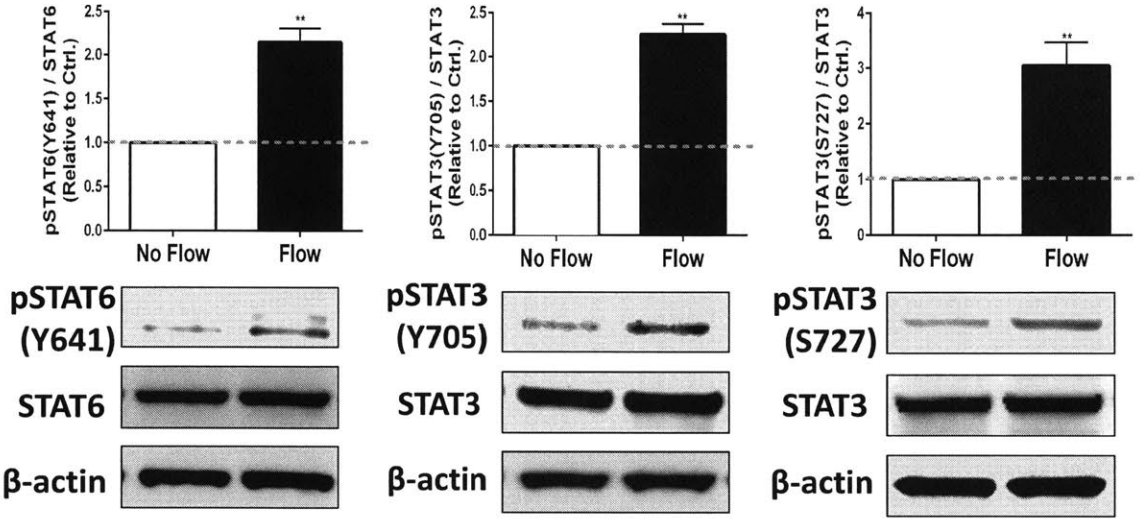

Fig. 4.9: IF induces activation of STAT3 and 6 in macrophages: Western blot quantification (top) and representative images (bottom) showing that 15-min IF (3 μm/s) treatment increased the phosphorylation of STAT6 at Tyr641 (left) and STAT3 at Tyr705 (center). In addition, 60-min IF treatment resulted in an increase in the phosphorylation of STAT3 at Ser727 (right). Bars represent mean ± SEM of data (fold change relative to no-flow control, Ctrl=control; n=3; *: $p<0.05$; **: $p<0.01$).

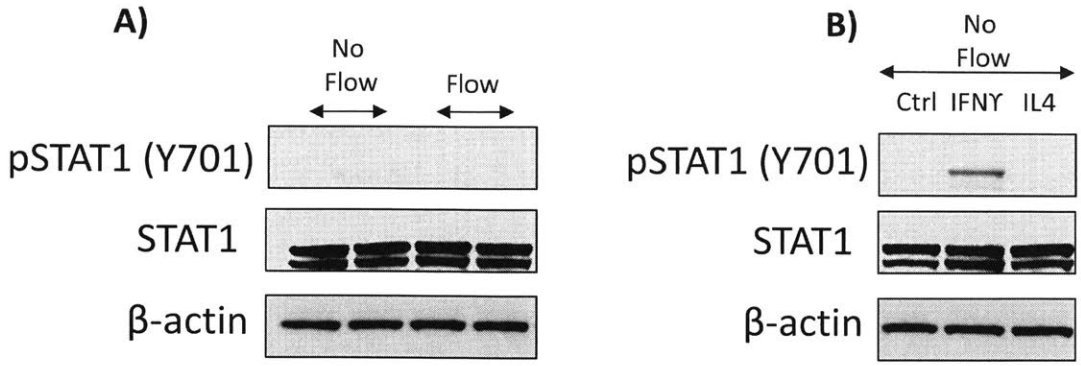

Fig. 4.10: Interstitial flow did not promote the activation of STAT1. (A) Representative western blot images showing that IF did not promote the phosphorylation of STAT1, a transcription factor for M1 polarization, in Raw macrophages compared to no flow control. In fact, no STAT1 phosphorylation was observed for both no-flow and flow conditions. **(B)** Untreated macrophages (Ctrl) and macrophages treated with 20 ng/mL mouse IL-4 were used as negative controls for STAT1 activation. Meanwhile, macrophages that were treated with 20 ng/mL mouse IFNγ were used as a positive control for STAT1 phosphorylation.

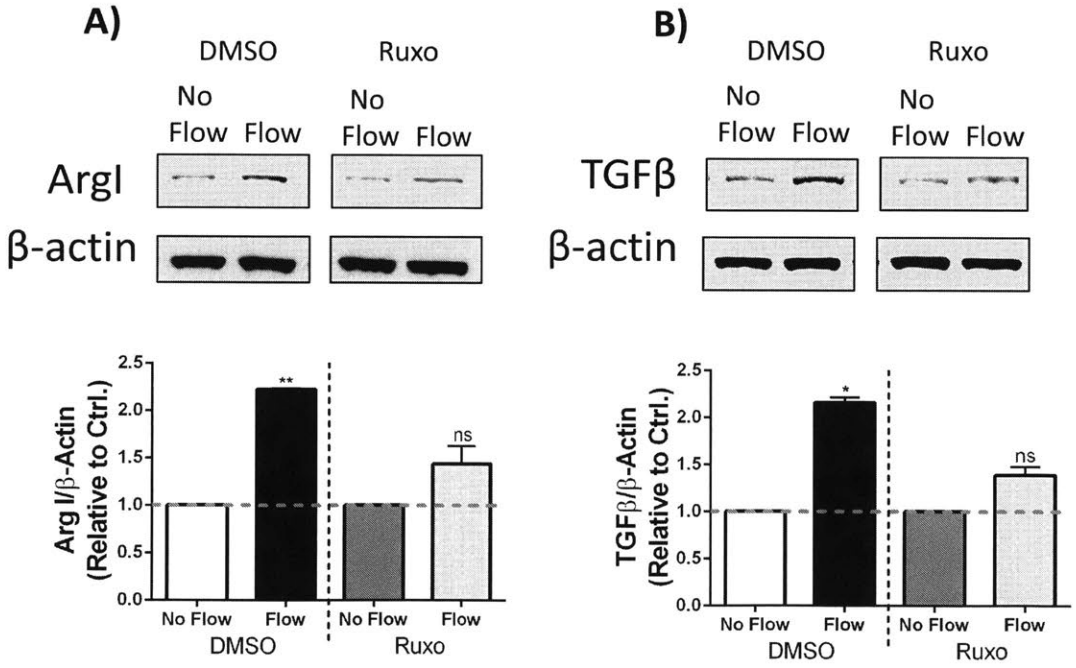

Fig. 4.11: STAT3 and 6 activations are crucial for flow-induced M2 polarization. Raw 264.7 macrophages were treated with ruxolitinib, an inhibitor of STAT3/6 activation, and subjected to IF treatment for 48 hrs. **(A)** Representative western blot images (up) and quantification (down) showing that ruxolitinib (Ruxo) treatment diminished flow-induced ArgI expression compared to DMSO controls. **(B)** Representative western blot images (up) and quantification (down) showing that ruxolitinib (Ruxo) treatment diminished flow-induced TGFβ expression compared to DMSO

controls. Bars represent mean ± SEM of data (fold change relative to no-flow control) from at least 3 independent experiments (*: $p<0.05$; **: $p<0.01$; ns=not significant).

We next considered which molecules are responsible for flow-induced STAT3/6 activation and subsequent M2 polarization. We suspected that integrin could be involved in this process, since it is a known flow-sensor, and crosstalk between STAT and integrin-Src pathways has been observed (28, 29). To test this hypothesis, we treated macrophages with Src inhibitor PP2 or anti-β1 integrin blocking antibody, and subjected these macrophages to IF. We found that inhibiting Src and β1 integrin greatly decreased flow-induced STAT3 and 6 phosphorylation (Fig. 4.12). These results reveal that β1 integrin and Src play an important role in IF-induced STAT3/6 activation. Finally, we also found that inhibiting β1 integrin led to a reduction in flow-induced phosphorylation of Akt and FAK (Fig. 4.13), indicating that β1 integrin is involved in the activation of these two kinases in macrophages treated with IF.

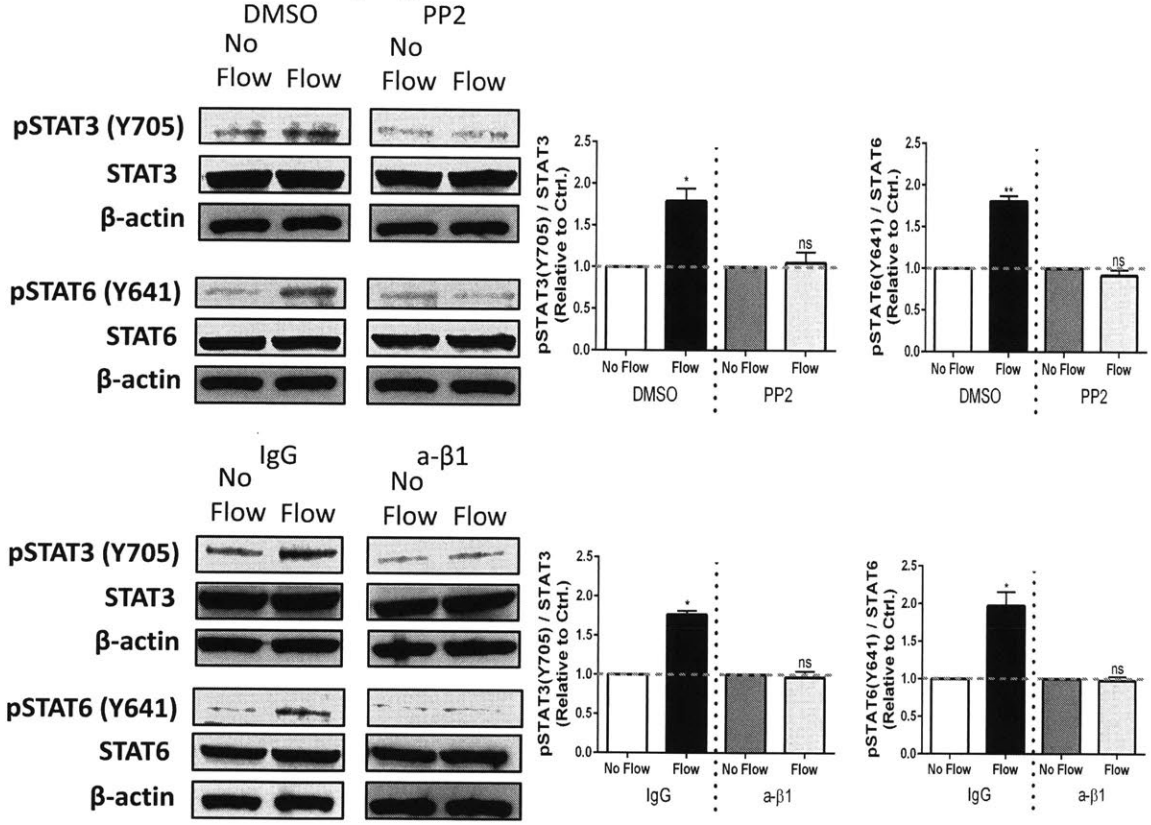

Fig. 4.12: Src and β1 integrin play crucial roles in flow-induced STAT3/6 activation. (A) Representative western blot images (left) and quantification (right) showing that the treatment of Raw macrophages with Src inhibitor PP2 abolished flow-induced STAT3 Tyr705 and STAT6 Tyr641 phosphorylation compared to DMSO control. No statistically significant difference in phosphorylation was observed between flow and no-flow conditions for cells treated with PP2. **(B)** Representative western blot images (left) and quantification (right) showing that anti-β1 integrin neutralizing antibody decreased the flow-induced STAT3 Tyr705 and STAT6 Tyr641 phosphorylation compared to IgG isotype control. Bars represent mean ± SEM of data (fold change relative to no-flow control; n=3; *: $p<0.1$; **: $p<0.01$; ns=not significant).

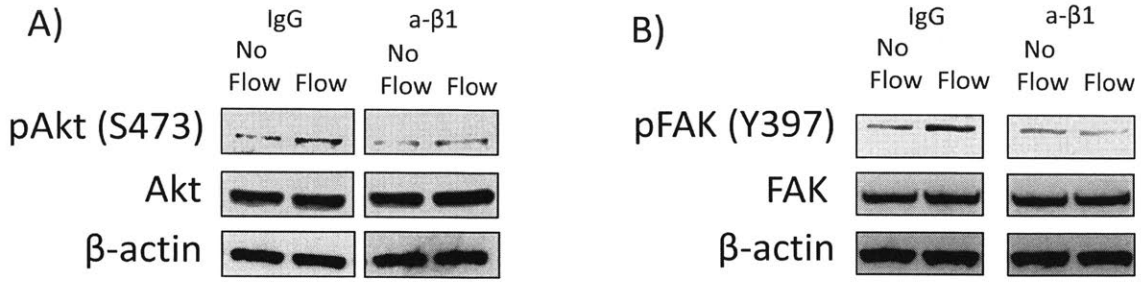

Fig. 4.13: β1 integrin plays a key role in IF-induced Akt and FAK activation. Raw 264.7 macrophages were treated with anti-β1 integrin blocking antibody and subsequently subjected to IF treatment for 15 mins. Representative western blot images showing that inhibiting β1 integrin resulted in reductions in flow-enhanced phosphorylation of Akt at Ser473 (A) and FAK at Tyr397 (B) compared to IgG isotype control.

Finally, we wonder whether there is any connection between flow-enhanced macrophage migration (Fig. 4.1) and M2 polarization (Fig. 4.8). To test this hypothesis, we first treated Raw 264.7 macrophages with lipopolysaccharide (LPS) or IL4 to chemically polarize these cells to M1 or M2 phenotype, respectively. We then measured the total speed and directedness of these polarized macrophages migrating within the 2.5 mg/mL collagen I ECM. In these experiments, M1 and M2 macrophages were not treated with interstitial flow. We found that similar to macrophages treated with IF, M2 macrophages had higher migration total speed and directedness compared to control (no flow) and M1 macrophages. More importantly, the migration total speed and directedness of M2 macrophages are similar to that of macrophages treated with IF (Fig. 4.14A and B). However, in contrast, no directional migration of M1 and M2 macrophages was observed, since the upstream velocity and directedness of these two types of macrophages were close to zero (Fig. 4.14C). These results seem to suggest that the flow-enhanced macrophage motility, but not directional migration, may be the phenotypic consequence of flow-induced M2 polarization.

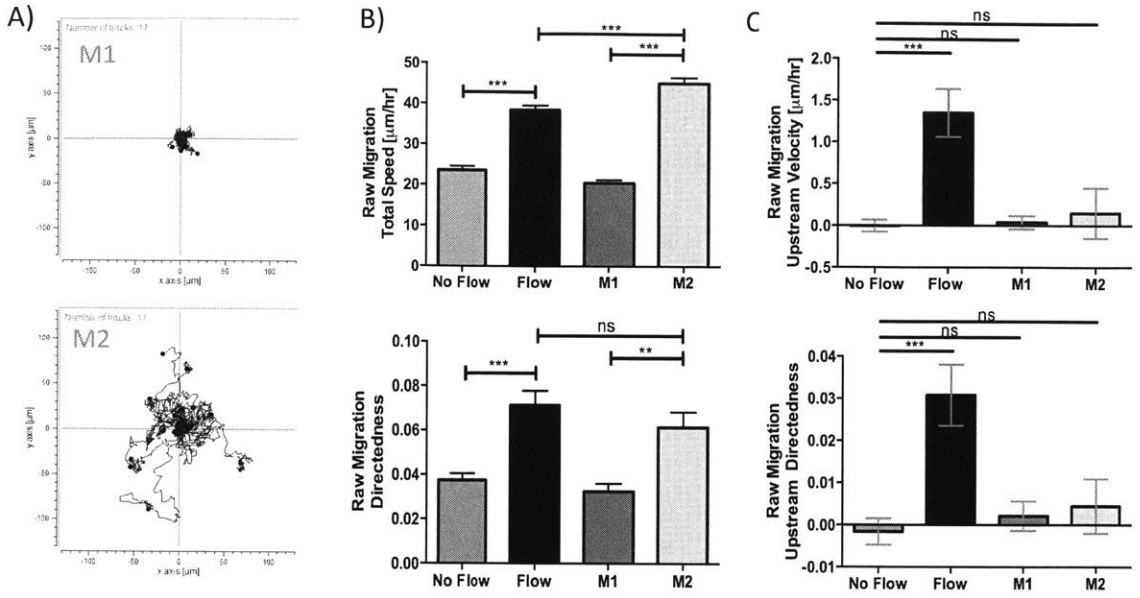

Fig. 4.14: Interstitial flow promotes M2 migration characteristic. Un-polarized Raw 264.7 macrophages were treated with interstitial flow (~3 μm/s) and the resulting migration characteristics (speed, directedness, upstream velocity, and upstream directedness) were compared to that of macrophages that were not treated with flow, macrophages that were chemically polarized to M1 phenotype with LPS (M1), and macrophages that were chemically polarized to M2 phenotype with mouse IL4 (M2). It should be noted that M1 and M2 macrophages were not treated with flow. **(A)** Representative migration trajectory plots of M1 (up) and M2 (down) macrophages showing M2 macrophages were more motile than M1 macrophages. **(B)** Macrophages treated with interstitial flow have similar migration total speed (up) and directedness (down) compared to M2 macrophages, but not M1 macrophages. **(C)** Macrophages treated with interstitial flow showed elevated upstream migration velocity (up) and directedness (down) compared to no-flow control, M1 macrophages, and M2 macrophages. Bars represent mean +/- SEM of data from 60-100 cells from at least 3 independent experiments (**: $p<0.01$; ***: $p<0.001$; ns=not significant).

4.7: IF promotes pro-metastatic phenotype of macrophages

Knowing that IF polarizes macrophages toward an M2 phenotype, we next examined whether IF-treated macrophages are also functionally pro-metastatic. We pre-treated macrophages (MΦ) seeded inside the 3D collagen I ECM with ~3 μm/s IF for 48 hrs, and then co-cultured these macrophages with cancer cells using a transwell system for an additional 24 hrs (treatment group). We first compared the ability of flow-conditioned macrophages to alter cancer cell morphology with that of macrophages that were not treated with flow (control group) (Fig. 4.15A). We found that co-culture of MDA-MB-435S (MDA435) melanoma cells with IF-pretreated macrophages resulted in the elongation of cancer cells (suggesting a migratory phenotype) compared to the control group (Fig. 4.16A). Indeed, quantification of cancer cell morphology showed that MDA435 cells, MDA-MB-231 (MDA231) breast cancer cells, and Du145 prostate cancer cells co-cultured with macrophages that were pretreated with IF have higher aspect ratio

(Fig. 4.16B) and lower circularity (Fig. 4.16C) than cells co-cultured with macrophages that did not receive IF pre-treatment.

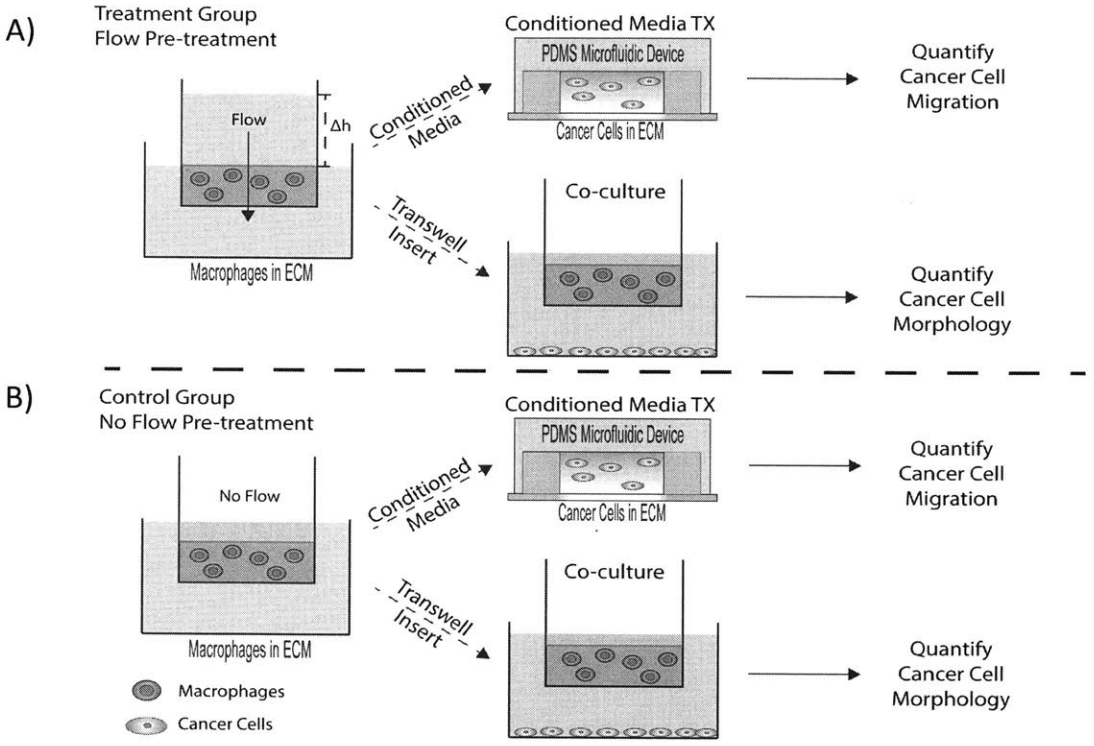

Fig. 4.15: Schematics of experiments designed to test the effects of IF on macrophages' abilities to promote cancer cell migration and protrusion formation. Macrophages were first seeded in a collagen I ECM contained within the transwell flow chamber. Half of the macrophages were subsequently pre-treated with IF for 48 hrs in the chamber (A), while the other half were not subjected to IF (control macrophages, B). After the flow treatment, conditioned media from the transwells were collected. MDA-MB-231 GFP breast cancer cells that were pre-seeded in a collagen I ECM in the microfluidic device were treated with these conditioned media. The migration of cancer cells was tracked to quantify their movement. In a separate experiment, the transwell inserts containing macrophages were removed from the flow chamber after IF treatment and then placed into a six-well plate pre-seeded with MDA-MB-231 GFP breast cancer cells (MDA231), MDA-MB-435S melanoma cells (MDA435), or Du145 prostate cancer cells (Du145). The macrophages were co-cultured with cancer cells for an additional 24 hrs in absence of flow to assess the effects of macrophages on cancer cell morphology.

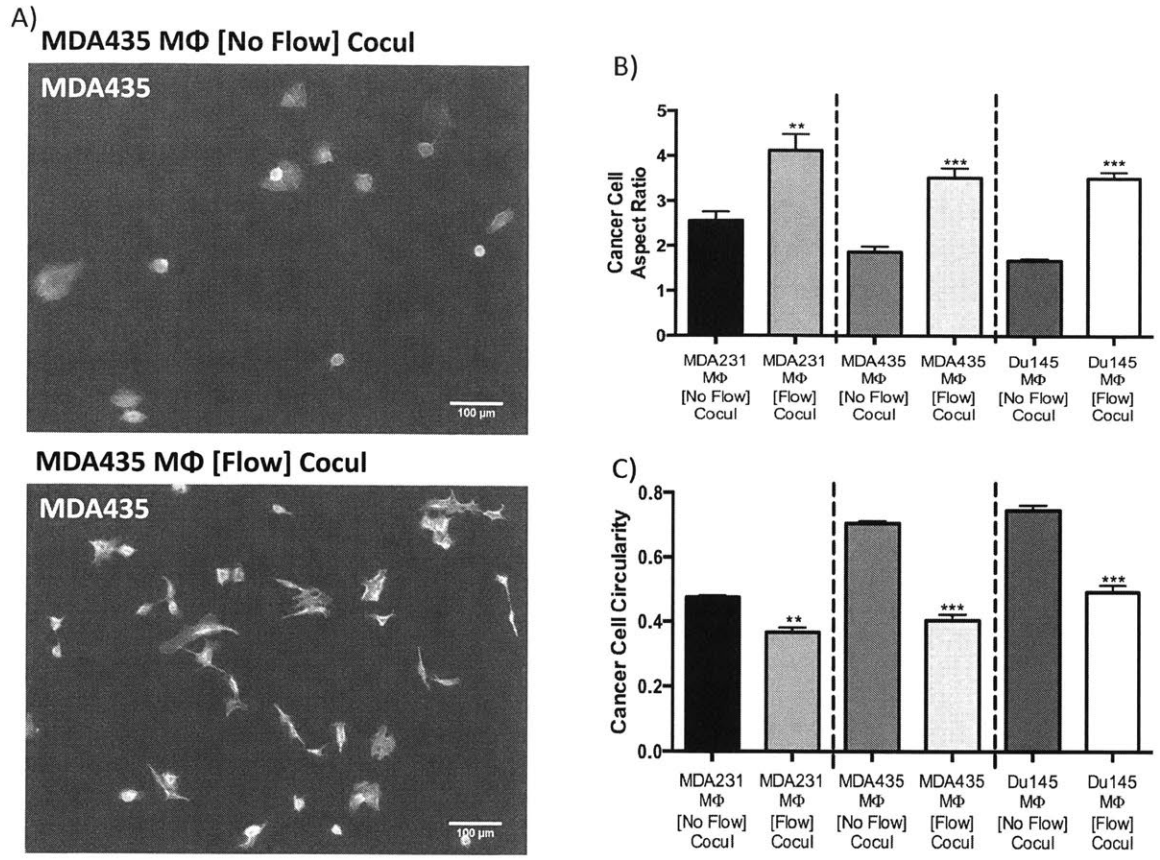

Fig. 4.16: IF enhances the ability of macrophages to promote cancer cell protrusion formation. Raw macrophages were pre-treated with IF (3 μm/s for 48 hrs) and subsequently co-cultured with cancer cells to assess their effects on cancer cell morphology and migration. **(A)** Representative fluorescent micrographs (green=actin, blue=DAPI) showing that MDA435 cancer cells co-cultured with Raw macrophages pre-treated with IF (MDA435 MΦ [Flow] Cocul, bottom) were more protrusive than cancer cells co-cultured with macrophages that were not pre-treated with flow (MDA435 MΦ [No Flow] Cocul, top). **(B)** Quantification of cancer cell morphology showing that cancer cells (MDA231, MDA435, and Du145) co-cultured with macrophages pre-treated with IF have higher aspect ratio than ones co-cultured with control macrophages that were not treated with flow. **(C)** Cancer cells (MDA231, MDA435, and Du145) co-cultured with macrophages pre-treated with IF have lower circularity than those co-cultured with control macrophages. Bars represent mean ± SEM of data from 35-70 cells (n=3; **: $p<0.01$, ***: $p<0.001$).

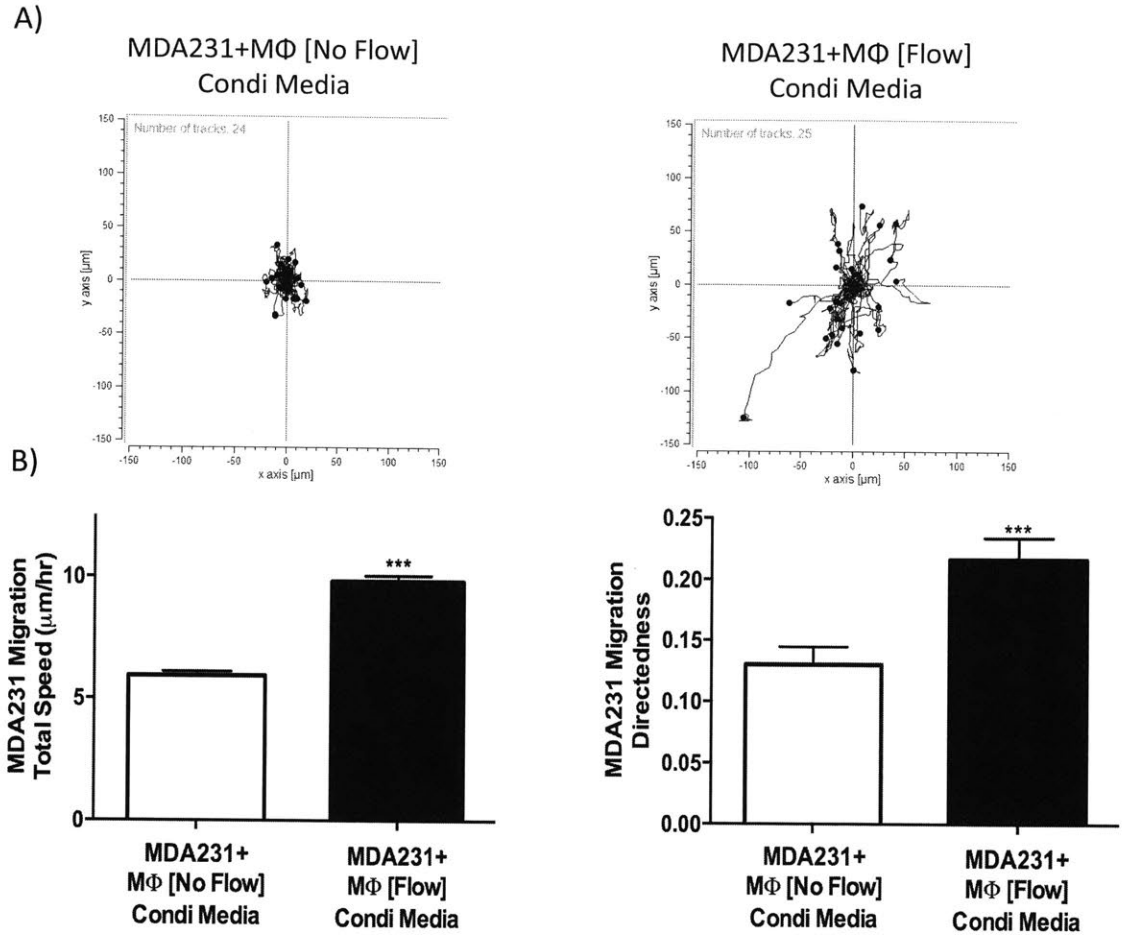

Fig. 4.17: IF enhances the ability of macrophages to promote cancer cell migration. (A) Representative cancer cell migration trajectories of MDA231 cancer cells treated with conditioned media collected from macrophages pre-treated with flow (MDA231+MΦ [Flow] Condi Media, right) and cancer cells treated with conditioned media from control macrophages (MDA231+MΦ [No Flow] Condi Media, left). **(B)** MDA231 cancer cells treated with conditioned media from IF-primed macrophages show a higher migration total speed (left) and directedness (right) than cells treated with conditioned media from control macrophages. Bars represent mean ± SEM of data from 45-100 cells (n=3; **: $p<0.01$; ***: $p<0.001$).

We then tested whether macrophages conditioned with IF have enhanced abilities to promote cancer cell migration. We treated MDA231 cancer cells seeded inside a 2.5 mg/mL collagen I ECM with conditioned media collected from Raw macrophages pre-treated with ~3 µm/s IF (Fig. 4.15B). We then tracked the movement of these cancer cells and quantified their migration total speed and directedness. We found that conditioned media collected from macrophages primed with IF resulted in higher cancer cell migration total speed and directedness than conditioned media collected from macrophages that were not pre-treated with flow (Fig. 4.17). Taken together, these results verify that IF promotes the pro-metastatic phenotypes of macrophages.

4.8 Discussion

Cells in the tumor microenvironment are constantly exposed to dynamic mechanical stimuli that influence cell behaviors and contribute to tumor progression (1, 30). Of particular importance is the role that tumor-associated interstitial flow (IF), which results from the buildup of interstitial fluid pressure inside the tumor tissue, plays in metastasis. Indeed, previous studies have shown that IF can direct cancer cell migration (4, 6), promote fibroblast activation (8), and induce endothelial monolayer sprouting (9, 10). However, the effects of this tumor-associated flow on macrophages, the most abundant immune cells in the tumor tissues and a key player in tumor progression (12, 15), have yet to be studied. Macrophages in the tumor microenvironment often adopt a pro-metastatic phenotype, suggesting that there may be therapeutic benefits in targeting these cells to reduce tumor metastasis. Therefore, it is important to understand how IF affects these immune cells to gain a deeper insight into the mechanobiology of the tumor microenvironment. In this study, we demonstrate, for the first time, that macrophages can sense and respond to IF.

We reveal that IF enhances the migration speed and directedness of macrophages in 3D ECM. Consistent with this observation, we found that IF increases the phosphorylation of FAK and Akt, kinases that are known to promote macrophage migration (24, 25, 31). We provide evidences that β1 integrin, a known mechanosensor on cancer cells, fibroblasts and endothelial cells (4, 8, 9), is involved in the flow-induced activation of these two kinases. Together, these results suggest that IF may induce macrophage movement by promoting integrin-mediated Akt and FAK activation. This is supported by the fact that integrin is involved in regulating macrophage migration and podosome formation (21, 32). Moreover, integrin activation can contribute to the auto-phosphorylation of FAK at Tyr397 and the downstream activation of Akt pathways (33, 34). Alternatively, the glycocalyx, which has been shown to interact with integrin and act as a flow sensor in smooth muscle cells (11), may be involved in flow-induced macrophage migration, as macrophages are major producers of syndecans, and glycocalyx plays a key role in macrophage migration (19, 22, 35).

We also demonstrate that IF can direct the migration of macrophages upstream. Migration against flow was previously reported for cancer cells and endothelial cells (5, 9, 10). In this study, we extend this observation to immune cells such as macrophages. Polacheck et al. have shown that IF promotes the migration of cancer cells against flow through flow-induced activation of β1 integrin located on the upstream side of cells (4). Besides this mechanotransduction pathway, IF-generated transcellular autocrine chemotactic gradients (autologous chemotaxis) have been shown to induce the migration of cells in the direction of flow (downstream) (6). However, we believe that autologous chemotaxis is unlikely to play a dominant role in this study, since we found that macrophages moved preferentially upstream, rather than downstream, in response to IF. In addition, the high cell seeding density used in this study (to mimic densely packed tumor tissues) created an unfavorable environment for the generation of this autocrine gradients, as the chemokines secreted by nearby cells can mask this gradient (5). Therefore, because integrin is involved in macrophage migration, we suspect that

localized activation of integrin at the upstream side of macrophages could account for the migration of macrophages against flow.

The observation that macrophages migrate against the direction of IF has significant implications in tumor metastasis. *In vivo*, macrophages tend to reside near the tumor margin (14, 16, 17). Since the interstitial flow rates are highest at this margin (1), IF-induced forces have potential to drastically affect macrophages that reside there. Additionally, interstitial fluid flows from the tumor core to tumor margin. Therefore, the observation that macrophages migrate against the flow suggests that IF, in addition to chemoattractants secreted by cancer cells (12, 36), can act as a stimulus to guide macrophage recruitment into the tumor. Because the infiltration of macrophages into tumors correlates with poor prognosis (14), this result strongly suggests that IF could promote metastasis though its ability to recruit macrophages.

Interestingly, we found that IF can induce the polarization of macrophages toward a pro-metastatic M2 phenotype as is evident from the up-regulation of M2 markers ArgI and TGFβ. We further demonstrate that this flow-induced M2 polarization leads to the enhanced abilities of macrophages to promote cancer cell migration and protrusion formation. It is well known that macrophage polarization can be induced by chemical stimuli (growth factors and chemokines) or physical confinement (13, 37). For instance, externally supplied cytokines such as IL-4 and IL-10 are known to induce the expression of M2 markers in macrophages. In contrast, LPS and IFNγ are used to initiate the production of macrophage M1 markers (38). Our results are the first to demonstrate that interstitial flow can polarize macrophages into M2 phenotype. Moreover, the finding that IF induces the production of TGFβ by macrophages is significant in the context of tumor progression since TGFβ can promote epithelial-to-mesenchymal transition (EMT) and cancer cell migration (39). Furthermore, TGFβ promotes immune suppression by inhibiting the proliferation and activation of cytotoxic T cells, NK cells, and dendritic cells while enhancing the generation of anti-inflammatory T_{reg} cells (40). Therefore, our results suggest that IF-induced TGFβ expression by macrophages could contribute to tumor progression by promoting tumor cell motility and the suppression of immune responses.

We also report that flow-induced M2 polarization is mediated by the activation of STAT3/6 pathway, leading us to conclude that this pathway is flow-sensitive in macrophages. It is well known that cytokines can activate STAT3/6 in macrophages (41, 42). Moreover, mechanical stretch has been reported to induce STAT3 phosphorylation in cardiomyocytes (43). However, this study is the first to report that forces produced by IF can mechanically activate STAT3/6 in macrophages. We further demonstrate that β1 integrin and Src, known mechanosensors in cancer cells and endothelial cells (10, 14), are involved in flow-induced STAT3/6 activation in macrophages. This result is supported by the fact that considerable crosstalk between STAT and integrin/Src pathways has been reported (28). For example, Src and Akt, which are activated by FAK downstream of β1 integrin, are known to influence the phosphorylation of STAT3 at multiple sites (44, 45). Therefore, our results strongly suggest that mechanotransduction pathways containing β1

integrin, Src, and STAT3/6 are involved in the flow-induced M2 polarization of macrophages.

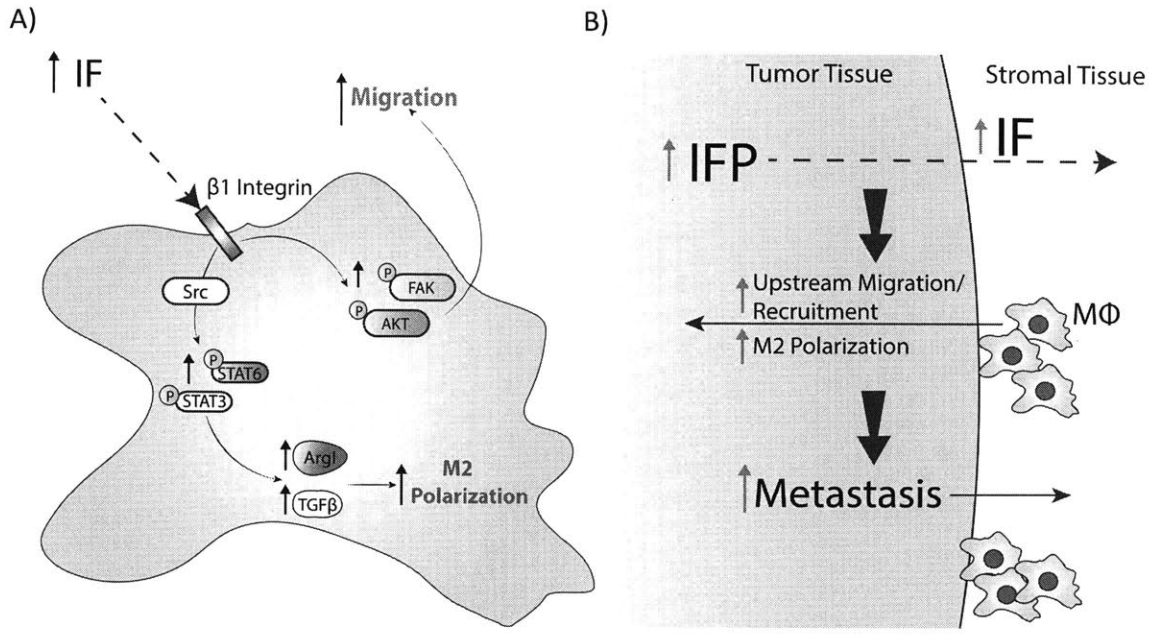

Fig. 4.18: Proposed models for the effects of IF on macrophages. (A) IF enhances macrophage migration via Akt/FAK activation and M2 polarization via Src/β1 integrin-mediated STAT3/6 activation. IF also directs macrophages to migrate upstream. **(B)** IF can promote metastasis by inducing macrophage upstream migration and M2 polarization. Tumor tissue has higher interstitial fluid pressure (IFP) than the surrounding stromal tissue, which drives an IF from tumor tissues to the stroma. Since IF induces upstream migration of macrophages, IF could promote macrophages that reside near the tumor boundary to infiltrate into tumor tissue and drive metastasis. IF could further promote metastasis by polarizing macrophages toward a pro-metastatic M2 phenotype.

In summary, we propose a new model whereby interstitial flow contributes to metastasis by promoting macrophage migration and M2 polarization. IF activates macrophage FAK and Akt, leading to an enhanced macrophage migration in 3D ECM. IF also induces the preferential migration of macrophages against the flow. Moreover, IF treatment, through β1 integrin/Src-mediated activation of STAT3/6, promotes macrophage transition to a pro-metastatic M2 phenotype evident by flow-induced ArgI/TGFβ expression and enhanced abilities to promote cancer cell motility (Fig. 4.18A). Since interstitial fluid flows from the tumor core to the tumor margin, macrophages could be directed by this flow to migrate upstream and infiltrate into tumor tissues. IF also promotes M2 polarization of macrophages, allowing them to produce cytokines, such as TGFβ, to promote EMT, immunosuppression, and metastasis (Fig. 4.18B). Finally, our findings also have implications in wound healing, as elevated IF often accompanies tissue inflammation (2). Our results suggest that IF could promote wound healing by polarizing macrophages at the inflamed site toward an M2 phenotype. Taken together, our study provides novel insights into the mechanobiology of macrophages and suggests that IF could play a key role in shaping the immune

environment. Therefore, we propose that the effects of IF on macrophages need to be considered in designing therapies to target macrophages in tumor and inflamed tissues, and a better understanding of the mechanotransduction pathways in macrophages could aid in the design of these immunotherapies.

4.9: References

1. Heldin C-H, Rubin K, Pietras K, Ostman A (2004) High interstitial fluid pressure - an obstacle in cancer therapy. *Nat Rev Cancer* 4(10):806–13.
2. Swartz MA, Lund AW (2012) Lymphatic and interstitial flow in the tumour microenvironment: linking mechanobiology with immunity. *Nat Rev Cancer* 12(3):210–9.
3. Hompland T, et al. (2012) Interstitial fluid pressure and associated lymph node metastasis revealed in tumors by dynamic contrast-enhanced MRI. *Cancer Res* 72(19):4899–908.
4. Polacheck WJ, German AE, Mammoto A, Ingber DE, Kamm RD (2014) Mechanotransduction of fluid stresses governs 3D cell migration. *Proc Natl Acad Sci U S A* 111(7):2447–52.
5. Polacheck WJ, Charest JL, Kamm RD (2011) Interstitial flow influences direction of tumor cell migration through competing mechanisms. *Proc Natl Acad Sci* 108(27):11115–11120.
6. Shields JD, et al. (2007) Autologous chemotaxis as a mechanism of tumor cell homing to lymphatics via interstitial flow and autocrine CCR7 signaling. *Cancer Cell* 11(6):526–38.
7. Haessler U, Teo JCM, Foretay D, Renaud P, Swartz M a (2012) Migration dynamics of breast cancer cells in a tunable 3D interstitial flow chamber. *Integr Biol (Camb)* 4(4):401–9.
8. Ng CP, Hinz B, Swartz M a (2005) Interstitial fluid flow induces myofibroblast differentiation and collagen alignment in vitro. *J Cell Sci* 118(Pt 20):4731–9.
9. Vickerman V, Kamm RD (2012) Mechanism of a flow-gated angiogenesis switch: early signaling events at cell-matrix and cell-cell junctions. *Integr Biol (Camb)* 4(8):863–74.
10. Song JW, Munn LL (2011) Fluid forces control endothelial sprouting. *Proc Natl Acad Sci U S A* 108(37):15342–7.
11. Shi Z-D, Wang H, Tarbell JM (2011) Heparan sulfate proteoglycans mediate interstitial flow mechanotransduction regulating MMP-13 expression and cell motility via FAK-ERK in 3D collagen. *PLoS One* 6(1):e15956.
12. Condeelis J, Pollard JW (2006) Macrophages: obligate partners for tumor cell migration, invasion, and metastasis. *Cell* 124(2):263–6.
13. Mantovani A, Sozzani S, Locati M, Allavena P, A S (2002) Macrophage polarization: tumor-associated macrophages as a paradigm for polarized M2 mononuclear phagocytes. *Trends Immunol* 23(11):549–555.
14. Leek RD, et al. (1996) Association of Macrophage Infiltration with Angiogenesis and Prognosis in Invasive Breast Carcinoma. *Cancer Res* 56(20):4625–4629.
15. Lewis CE, Pollard JW (2006) Distinct role of macrophages in different tumor microenvironments. *Cancer Res* 66(2):605–12.
16. Wyckoff JB, et al. (2007) Direct visualization of macrophage-assisted tumor cell intravasation in mammary tumors. *Cancer Res* 67(6):2649–56.
17. Ohno S, et al. (2004) Correlation of histological localization of tumor-associated macrophages with clinicopathological features in endometrial cancer. *Anticancer Res* 24(5C):3335–42.
18. Philippeaux M-M, et al. (2009) Culture and functional studies of mouse macrophages on native-like fibrillar type I collagen. *Eur J Cell Biol* 88(4):243–56.
19. Larabee JL, et al. (2011) Glycogen synthase kinase 3 activation is important for anthrax edema toxin-induced dendritic cell maturation and anthrax toxin receptor 2 expression in macrophages. *Infect Immun* 79(8):3302–8.
20. Abshire MY, Thomas KS, Owen KA, Bouton AH (2011) Macrophage motility requires distinct α5β1/FAK and α4β1/paxillin signaling events. *J Leukoc Biol* 89(2):251–257.
21. Dovas A, et al. (2009) Regulation of podosome dynamics by WASp phosphorylation: implication in matrix degradation and chemotaxis in macrophages. *J Cell Sci* 122(Pt 21):3873–82.
22. Asplund A, Ostergren-Lundén G, Camejo G, Stillemark-Billton P, Bondjers G (2009) Hypoxia increases macrophage motility, possibly by decreasing the heparan sulfate proteoglycan biosynthesis. *J Leukoc Biol* 86(2):381–8.
23. Berton G, Lowell C a (1999) Integrin signalling in neutrophils and macrophages. *Cell Signal* 11(9):621–35.
24. Miao L, Xin X, Xin H, Shen X, Zhu Y-Z (2016) Hydrogen Sulfide Recruits Macrophage Migration by Integrin β1-Src-FAK/Pyk2-Rac Pathway in Myocardial Infarction. *Sci Rep* 6:22363.

25. Yu H, Littlewood T, Bennett M (2015) Akt isoforms in vascular disease. *Vascul Pharmacol* 71:57–64.
26. Niemand C, et al. (2003) Activation of STAT3 by IL-6 and IL-10 in Primary Human Macrophages Is Differentially Modulated by Suppressor of Cytokine Signaling 3. *J Immunol* 170(6):3263–3272.
27. Wang N, Liang H, Zen K (2014) Molecular mechanisms that influence the macrophage m1-m2 polarization balance. *Front Immunol* 5:614.
28. Millward-Sadler SJ, Khan NS, Bracher MG, Wright MO, Salter DM (2006) Roles for the interleukin-4 receptor and associated JAK/STAT proteins in human articular chondrocyte mechanotransduction. *Osteoarthritis Cartilage* 14(10):991–1001.
29. Silva CM (2004) Role of STATs as downstream signal transducers in Src family kinase-mediated tumorigenesis. *Oncogene* 23(48):8017–8023.
30. Wirtz D, Konstantopoulos K, Searson PC (2011) The physics of cancer: the role of physical interactions and mechanical forces in metastasis. *Nat Rev Cancer* 11(7):512–22.
31. Zhang Y, et al. (2013) Kinase AKT controls innate immune cell development and function. *Immunology* 140(2):143–52.
32. Pradip D, Peng X, Durden DL (2003) Rac2 Specificity in Macrophage Integrin Signaling: Potential role for Syk kinase. *J Biol Chem* 278(43):41661–41669.
33. Mitra SK, Hanson DA, Schlaepfer DD (2005) Focal adhesion kinase: in command and control of cell motility. *Nat Rev Mol Cell Biol* 6(1):56–68.
34. Guo W, Giancotti FG (2004) Integrin signalling during tumour progression. *Nat Rev Mol Cell Biol* 5(10):816–26.
35. Angsana J, et al. (2015) Syndecan-1 modulates the motility and resolution responses of macrophages. *Arterioscler Thromb Vasc Biol* 35(2):332–40.
36. Quail DF, Joyce JA (2013) Microenvironmental regulation of tumor progression and metastasis. *Nat Med* 19(11):1423–37.
37. McWhorter FY, Wang T, Nguyen P, Chung T, Liu WF (2013) Modulation of macrophage phenotype by cell shape. *Proc Natl Acad Sci* 110(43):17253–17258.
38. Italiani P, Boraschi D (2014) From Monocytes to M1/M2 Macrophages: Phenotypical vs. Functional Differentiation. *Front Immunol* 5:514.
39. Lamouille S, Xu J, Derynck R (2014) Molecular mechanisms of epithelial-mesenchymal transition. *Nat Rev Mol Cell Biol* 15(3):178–96.
40. Wrzesinski SH, Wan YY, Flavell RA (2007) Transforming growth factor-beta and the immune response: implications for anticancer therapy. *Clin Cancer Res* 13(18 Pt 1):5262–70.
41. Jiang H, Harris MB, Rothman P (2000) IL-4/IL-13 signaling beyond JAK/STAT. *J Allergy Clin Immunol* 105(6):1063–1070.
42. Nakamura R, et al. (2015) IL10-driven STAT3 signalling in senescent macrophages promotes pathological eye angiogenesis. *Nat Commun* 6:7847.
43. Pan J, et al. (1999) Mechanical stretch activates the JAK/STAT pathway in rat cardiomyocytes. *Circ Res* 84(10):1127–36.
44. Zhu YP, Brown JR, Sag D, Zhang L, Suttles J (2015) Adenosine 5'-monophosphate-activated protein kinase regulates IL-10-mediated anti-inflammatory signaling pathways in macrophages. *J Immunol* 194(2):584–94.
45. Reddy EP, Korapati A, Chaturvedi P, Rane S (2000) IL-3 signaling and the role of Src kinases, JAKs and STATs: a covert liaison unveiled. *Oncogene* 19(21):2532–47.

Chapter 5: Conclusions, Implications, and Future Works

5.1: Conclusions

Cancer is a group of systemic diseases that are marked by uncontrollable growth and dissemination of abnormal, cancerous cells (1). Metastasis, the dissemination of cancer cells from the primary tumor site to a secondary one, accounts for the majority of cancer death (1–3). However, most current treatment strategies against metastasis remain unsuccessful. This is due to the fact that metastasis is a complex process that depends on both cancer cells themselves and the environment that surrounds them. Indeed, recent advances in tumor biology have revealed that tumor microenvironment at the primary tumor site is a crucial regulator of tumor metastasis. For examples, tumor-associated stromal cells (fibroblast and macrophages), ECM, and biophysical forces (elevated interstitial flow and altered ECM stiffness) have all been shown to contribute to cancer cell growth, invasion, or intravasation (4, 5). Hence, a successful anti-metastatic therapy will have to take into account the interaction between the tumor and its microenvironment. However, since the importance of tumor microenvironment has only recently been recognized, our knowledge of its effects on metastasis is still inadequate.

The migration behavior of cancer cell is a key determinant of tumor metastasis. It dictates how cancer cells break through basement membrane and invade the ECM-rich tissue surrounding the primary tumor. Recently, it has become clear that the overall dissemination of a population of cancer cells from a primary tumor site is influenced by the migration speed and persistence of each individual cancer cell (6). These characteristics of cancer cell migration, collectively called migration dynamics, can be modulated independently of one another by a single stimulus (7). Moreover, a stimulus can affect speed and persistence of migration differently when cells are cultured on 2D substrates compared to in 3D matrix. Collectively, these results highlight the importance of characterizing how a stimulus affects the dynamics of cancer cell migration (i.e. speed and persistence) in 3D ECM to gain a detailed, quantitative, and realistic understanding of metastasis.

Macrophages are one type of the most abundant stromal cells in the tumor microenvironment (8). These immune cells can quickly adopt different phenotypes (i.e. M1 pro-inflammatory phenotype vs. M2 anti-inflammatory phenotype) based on stimuli in their microenvironment. Various clinical data have revealed that the infiltration of M2 macrophages in tumor tissues correlates with poor prognosis in cases of breast cancer, prostate cancer, and melanoma (8, 9). Moreover, *in vivo* and *in vitro* studies have shown that macrophages enhance cancer cell intravasation (10, 11) and invasion through various signaling pathways (12, 13). However, the majority of these studies were carried out using transwell assays, which only yield an end-point readout of cell behaviors (14) and thereby provide little information on how macrophages affect different aspects of cancer cell migration, such as how fast or how persistently the cancer cell moves. **As such, the effects of macrophages on the dynamics (speed and persistence) of cancer cell**

migration in 3D ECM remain to be characterized. In addition to macrophages, the growth of solid tumors often results in an elevated interstitial fluid flow inside the tumor microenvironment. This flow, which originates from the tumor tissues and drains into the surrounding stroma, has been shown to influence the migratory behaviors of cancer cells and fibroblasts. **However, whether interstitial flow affects macrophages, a key tumor-associate immune cell type, is still unknown.** Therefore, this thesis aims to address these two gaps in our current knowledge of tumor microenvironment.

To study the effects of macrophages on the dynamics of cancer cell migration, we utilized a microfluidic 3D migration assay that allows us to perform real-time high-resolution tracking of cancer cell migration in a 3D ECM containing macrophages. This assay enables us to quantify the effects of macrophages on the speed and persistence of cancer cell migration in an environment that better mimic the *in vivo* tumor microenvironment than traditional *in vitro* transwell assay. We found that macrophages significantly enhance cancer cell migration speed and persistence in the 3D ECM by up-regulating cancer cell expression of matrix metalloproteases (MMPs). Moreover, we found that these enhancements in cancer cell migration are mediated by macrophage-secreted TNFα and TGFβ1 through two distinct pathways. Specifically, macrophage-released TGFβ1 enhances cancer cell migration speed through the induction of MT1-MMP expression in cancer cells. In contrast, macrophage-released TNFα and TGFβ1 synergistically promote cancer cell migration persistence through the induction of NF-κB-dependent MMP1 expression in cancer cells.

We also utilized microfluidic and transwell flow assays to investigate how tumor-associated IF (~3 um/s) affects macrophage migration and protein expression in 3D extracellular matrix (ECM). Using the microfluidic assay, we demonstrate that IF not only enhances macrophage migration, but also directs macrophages to move against the direction of flow (upstream). Surprisingly, we found that IF promotes macrophage expression of pro-metastatic M2 markers Arg I and TGF-β via integrin/Src-dependent STAT3/6 activation. Consistent with this flow-induced M2 polarization, macrophages primed with IF have an enhanced capability in promoting cancer cell migration. Since interstitial fluid flows from tumor core to the surrounding stroma, these results suggest that IF can promote metastasis by not only recruiting macrophages from stroma into tumor (since IF directs macrophage migration against flow), but also enhancing the M2 polarization of macrophages in the tumor microenvironment.

5.2: Implications

5.2.1: Cancer cell migration dynamics and their implication in therapy

Our study demonstrated, for the first time, that macrophages affect speed and persistence of cancer cell migration in 3D ECM via different pathways. Specifically, we found that macrophage-released TNFα and TGFβ1 synergistically enhance cancer cell migration persistence in 3D ECM, whereas increase in cancer cell migration speed is mainly attributed to TGFβ1 secreted by macrophages. Since both the speed and persistence of migration are important determinants of cancer cell invasiveness, these

results suggest that TNF α and TGF β 1 dual blockade could be a possible anti-metastatic strategy in solid tumors. We have already begun to explore the effectiveness of this therapeutic strategy. Specifically, we treated BALB/c mice bearing 4T1 breast tumors with anti-TNFα and/or anti-TGFβ1 blocking antibodies, and we evaluated the results of these treatment regimens on metastatic formation in lung. We found that mono-treatment of anti-TNFα or anti-TGFβ1 blocking antibody led to a noticeable, but not statistically significant, reduction in the formation of metastatic lesions in the lungs of the mice. However, co-treatment of both anti-TNFα and anti-TGFβ1 blocking antibodies led to a substantial and statistically significant reduction in the metastatic formation (Fig. 3.20). Therefore, this *in vivo* result points to the possibility that this treatment regimen could be useful in combating metastasis. However, additional *in vivo* studies are needed to fully characterize and develop this dual blockade therapy.

This study also broadens our current view of 3D migration by showing that MT1-MMP mainly controls migration speed while MMP1 primarily regulates migration persistence. This result raises an interesting possibility of controlling the migration behaviors of the cells (i.e. how fast and how persistently the cells migrate), as therapeutic and tissue engineering strategies, by modulating their MT1-MMP and MMP1 expressions. Since morphogenesis, angiogenesis, and wound healing critically (15–17) depend on cells' ability to breakdown ECM and migrate, regulating MMP expression, either by inhibiting the expression of specific MMP or introducing cells engineered with a pre-defined MMP expression profile (i.e. cell therapy), could be a useful strategy in controlling these processes.

5.2.2: Interstitial flow as a regulator of immune environment and its implication in immunotherapy

Our study reveals, for the first time, that macrophages can sense and react to interstitial flow. Specifically, we show that interstitial flow skews the polarization of macrophages toward an M2 phenotype. In addition, interstitial flow promotes macrophage migration and directs macrophage movement against the flow. These results broaden our current view on the tumor mechanobiology by suggesting that interstitial flow can promote metastasis by inducing macrophage M2 polarization, as well as macrophage infiltration into the tumor core. Since interstitial flow seems to play an important role in shaping the immune microenvironment in tumor, its effects on immune cells need to be considered in designing anti-tumor immunotherapy. For instance, our findings suggest that therapies that aim to re-educate macrophages toward an anti-tumor M1 phenotype (18) may be more effective when used in combination with therapies that reduce interstitial flow in tumors.

Finally, in this thesis, we have started to investigate the mechanisms of interstitial flow-induced M2 polarization and migration. We demonstrated that STAT3/6 activation, mediated by β1 integrin and Src, controls flow-induced M2 polarization. In contrast, interstitial flow promotes macrophage migration through the activation of FAK and Akt. Although we have shed light on the mechanisms that govern these flow responses, a more detailed mechanistic study is needed to completely understand these phenomena. Knowledge from this future study could be used to engineer macrophages (as a possible

immunotherapy) that can be promoted by elevated interstitial flow to infiltrate into tumor tissues while at same time maintaining an M1 anti-tumor phenotype.

5.3: Future Works

5.3.1: Synergistic responses of cancer cells to TNFα and TGFβ1 treatment.

As shown in Chapter 3, we found that TNFα and TGFβ1 co-treatment results in a synergistic induction of NF-κB nuclear translocation, leading to a synergistic increase in cancer cell MMP1 expression. The detailed mechanism behind this synergy is still unknown. We suspect this is the result of the convergence of TNFα and TGFβ1 pathways at TGF-β-activated kinase 1 (TAK1) (19). In TNFα pathway, TAK1 mediates the activation of NF-κB pathway upon the binding of TNFα to its receptor. Specifically, it phosphorylates IκB kinase (IKK), which when activated, phosphorylates the inhibitor of kappa B (IκBα). When IκBα is phosphorylated, it dissociates from NF-κB complex, allowing NF-κB to translocate into the nucleus. Recent report suggests that in addition to TNFα treatment, TGFβ1 stimulation can also induce TAK1 phosphorylation. Hence, it is possible that the synergistic response of cancer cells to TNFα and TGFβ1 co-treatment is mediated by TAK1. In addition, SMAD7 could also be involved in this synergistic response, since it is present in both TNFα and TGFβ1 pathways (19). In an effort to understand this synergism, a detailed computational study of the possible interactions between TNFα and TGFβ1 pathways is currently being performed in collaboration with Dr. Mohammad Zaman's lab at Boston University.

5.3.2: Differential controls of cell migration dynamics by different MMPs.

We discovered that MMP1 controls cancer cell migration persistence, while MT1-MMP mainly controls cancer cell migration speed. We hypothesize that this is due to the fact that MT1-MMP and MMP1 affect cell intrinsic and extrinsic properties of migration differently. MT1-MMP can influence cell intrinsic migration behaviors (activities of kinases and expression of integrin), as well as cell extrinsic matrix properties (ECM pore size). This is in contrast to MMP1, which primarily degrades collagen I matrix to alter the cell extrinsic properties. Since both intrinsic and extrinsic properties are known determinants of cell migration speed in 3D matrix (20, 21), MT1-MMP should be the primarily determinant of cell speed. In contrast, MMP1 is more efficient in degrading collagen I ECM and altering extrinsic matrix properties than MT1-MMP (22). Since cell extrinsic matrix properties seem to dominate over intrinsic property as the primary determinant of 3D migration persistence (20, 23), MMP1 should therefore be the major contributor to migration persistence. Needless to say, this hypothesis needs to be tested. Since it is difficult to perform *in vitro* experiments to validate this hypothesis, an *in silico* approach may be needed. We are currently seeking collaboration to build a computational model of cell migration that incorporates matrix degradation and cell intrinsic properties (kinase activities and syndecan shedding).

5.3.3: Interstitial flow's effects on macrophages: polarization subtypes, population heterogeneity, and mechanisms

In this thesis, we have demonstrated that interstitial flow induces the M2 polarization of macrophages. However, in recent years, it has become evident that subtypes of macrophages exist within the M2 classification. M2 macrophages can be further divided into M2a, M2b, or M2c subtypes. M2a macrophages are induced by IL-4 or IL-13. They are anti-inflammatory and promote cell migration. M2b macrophages, on the other hand, result from LPS and IL-1 stimulation. They secrete TNFα and VEGF, and they are considered immune-regulatory and pro-angiogenic. Finally, M2c macrophages are immunosuppressive. They are induced by TGFβ or IL-10 stimulation, and they secrete a large amount of TGFβ and CCL18 in response (24). Since these subtypes are functionally distinct, it will be interesting to investigate which types of M2 macrophages can result from the interstitial flow treatment. It is possible that flow treatment could induce subpopulations of macrophages to adopt different M2 phenotypes. This is supported by the fact that interstitial flow treatment induced the activation of both STAT3 and STAT6, which are transcription factors for M2a and M2c polarization, respectively. Moreover, from the histogram of macrophage upstream migration velocity (Fig. 4.6), we can clearly identify two subpopulations of cells with different migratory responses to flow treatment. Therefore, we hypothesize that interstitial flow treatment could induce a population heterogeneity in macrophage M2 polarization, with a subpopulation of cells adopting an M2a phenotype while the other adopting an M2c phenotype. Current efforts are focused on addressing this hypothesis.

As mentioned previously, the mechanisms of interstitial flow-induced M2 polarization still need to be fully characterized. As such, many un-answered questions remain. For example, even though we know that β1 integrin is involved in this mechanotransduction process, how exactly does integrin participate in the activation of STAT3 and 6 is still unknown. Moreover, whether other molecules, especially cytokine receptors, participate in flow-induced M2 polarization is yet to be elucidated. Finally, the involvement of cytoskeleton, a key regulator of cell mechanics (25), is unexplored. All these unanswered questions can be bases for future research.

5.4: References

1. Chambers AF, Groom AC, MacDonald IC (2002) Dissemination and growth of cancer cells in metastatic sites. *Nat Rev Cancer* 2(8):563–72.
2. Mehlen P, Puisieux A (2006) Metastasis: a question of life or death. *Nat Rev Cancer* 6(6):449–58.
3. Steeg PS (2006) Tumor metastasis: mechanistic insights and clinical challenges. *Nat Med* 12(8):895–904.
4. Joyce JA, Pollard JW (2009) Microenvironmental regulation of metastasis. *Nat Rev Cancer* 9(4):239–52.
5. Wirtz D, Konstantopoulos K, Searson PC (2011) The physics of cancer: the role of physical interactions and mechanical forces in metastasis. *Nat Rev Cancer* 11(7):512–22.
6. Maheshwari G, Lauffenburger D a (1998) Deconstructing (and reconstructing) cell migration. *Microsc Res Tech* 43(5):358–68.
7. Haessler U, Teo JCM, Foretay D, Renaud P, Swartz M a (2012) Migration dynamics of breast cancer cells in a tunable 3D interstitial flow chamber. *Integr Biol (Camb)* 4(4):401–9.
8. Lewis CE, Pollard JW (2006) Distinct role of macrophages in different tumor microenvironments. *Cancer Res* 66(2):605–12.
9. Chen P, et al. (2011) Tumor-associated macrophages promote angiogenesis and melanoma growth via adrenomedullin in a paracrine and autocrine manner. *Clin Cancer Res* 17(23):7230–9.
10. Wyckoff JB, et al. (2007) Direct visualization of macrophage-assisted tumor cell intravasation in mammary tumors. *Cancer Res* 67(6):2649–56.
11. Zervantonakis IK, et al. (2012) Three-dimensional microfluidic model for tumor cell intravasation and endothelial barrier function. *Proc Natl Acad Sci* 109(34):13515–13520.
12. Patsialou A, et al. (2009) Invasion of human breast cancer cells in vivo requires both paracrine and autocrine loops involving the colony-stimulating factor-1 receptor. *Cancer Res* 69(24):9498–506.
13. Goswami S, et al. (2005) Macrophages promote the invasion of breast carcinoma cells via a colony-stimulating factor-1/epidermal growth factor paracrine loop. *Cancer Res* 65(12):5278–83.
14. Polacheck WJ, Zervantonakis IK, Kamm RD (2013) Tumor cell migration in complex microenvironments. *Cell Mol Life Sci* 70(8):1335–56.
15. Armstrong DG, Jude EB (2002) The role of matrix metalloproteinases in wound healing. *J Am Podiatr Med Assoc* 92(1):12–8.
16. Rundhaug JE Matrix metalloproteinases and angiogenesis. *J Cell Mol Med* 9(2):267–85.
17. Simian M, et al. (2001) The interplay of matrix metalloproteinases, morphogens and growth factors is necessary for branching of mammary epithelial cells. *Development* 128(16).
18. Pyonteck SM, et al. (2013) CSF-1R inhibition alters macrophage polarization and blocks glioma progression. *Nat Med* 19(10):1264–1272.
19. Freudlsperger C, et al. (2013) TGF-β and NF-κB signal pathway cross-talk is mediated through TAK1 and SMAD7 in a subset of head and neck cancers. *Oncogene* 32(12):1549–1559.
20. Kim H-D, et al. (2008) Epidermal growth factor-induced enhancement of glioblastoma cell migration in 3D arises from an intrinsic increase in speed but an extrinsic matrix- and proteolysis-dependent increase in persistence. *Mol Biol Cell* 19(10):4249–59.
21. Wolf K, et al. (2013) Physical limits of cell migration: control by ECM space and nuclear deformation and tuning by proteolysis and traction force. *J Cell Biol* 201(7):1069–84.
22. Imai K (1997) Membrane Type 1Matrix Metalloproteinase Digests Interstitial Collagens and Other Extracellular Matrix Macromolecules. *J Biol Chem* 272(4):2446–2451.
23. Wu P-H, Giri A, Sun SX, Wirtz D (2014) Three-dimensional cell migration does not follow a random walk. *Proc Natl Acad Sci U S A* 111(11):3949–54.
24. Gensel JC, Zhang B (2015) Macrophage activation and its role in repair and pathology after spinal cord injury. *Brain Res* 1619:1–11.
25. Fletcher DA, Mullins RD (2010) Cell mechanics and the cytoskeleton. *Nature* 463(7280):485–92.

Appendix A: Supplementary Materials and Methods for Chapter 3

Reagents used in Microfluidic 3D cell migration assay

As appropriate, 100 μM GM6001 (Sigma), 2 μg/mL anti-mouse TNFα antibody (R&D), 10 μg/mL anti-mouse TGFβ1 antibody (Thermo), 200 μg/mL anti-MMP-1 antibody (R&D, Clone#36665), 30 μg/mL anti-MT1-MMP (Abcam, Clone#LEM-2/63.1), 2 μg/mL goat IgG isotype control (R&D), 10 μg/mL rabbit IgG isotype control (Thermo), 200 μg/mL mouse IgG isotype control (R&D), 5 or 10 ng/mL TNFα (Peprotech), 5 or 10 ng/mL TGFβ1 (Peprotech), or 0.5 μg/mL of MMP1 (Peprotech) was added to the cell culture media and the gel.

2D Cell Migration Assay

100,000 of GFP-expressing MDA-MB-231 breast cancer cells were seeded with 750,000 of Raw 264.7 macrophages on a 35 mm MatTek dish (MatTek Corp.). After overnight incubation in a humidified incubator operating at 37 °C and 5% CO_2, the co-culture was transferred to a fluorescent microscope (Zeiss) fitted with an environmental chamber operating at 37 °C and 5% CO_2. Time-lapse microscopy was used to record cancer cell movement on the 2D glass substrate. Fluorescent and phase-contrast images were taken every 15 min. for 18 hrs. Image J (NIH) was used to track the movement of the MDA231 cancer cells, and Ibidi Chemotaxis and Migration software (Ibidi) was used to quantify the total speed and directedness of cancer cell migration. Total speed and directedness are defined as before.

Immunofluorescent staining, confocal microscopy, and DQ-Collagen I Release Assay

4% para-formaldehyde was perfused into the microfluidic device to fix the cells in the collagen I ECM. Confocal microscopy images of the cells were taken with confocal microscope fitted with a camera (Olympus). Cells were stained with rhodamine-phalloidin and DAPI (Invitrogen) to visualize the actin and nucleus. Confocal reflectance images were taken at high magnification to visualize collagen I fibers surrounding the cells. The lack of collagen I fibers surrounding the cells indicates microtrack resulting from ECM degradation. The ability of cells to degrade collagen I ECM was assessed using fluorescein conjugated DQ-Collagen I according to manufactures' protocol (Invitrogen).

ELISA

75,000 MDA-MB-231 cancer cells or Raw 264.7 macrophages were cultured for 3 days. The conditioned media were subsequently collected and immediately frozen at -70 °C. The concentrations of mouse TNFα and mouse TGFβ1 in the conditioned media of Raw 264.7 cells, as well as the concentrations of human TNFα and human TGFβ1 in

the conditioned media of MDA231 cells, were determined using ELISA (enzyme-linked immunosorbant assay) kits (R&D).

Cancer cell-macrophage co-culture for western blot analysis

To assess the effects of macrophages on cancer cell expression of MT1-MMP and MMP1, MDA-MB-231 breast cancer cells, PC3 prostate cancer cells, or MDA-MB-435S melanoma cells were co-cultured with Raw 264.7 macrophages in a transwell system. Briefly, 100,000 cancer cells were seeded in the wells of six-well plates (Falcon). Separately, 100,000 Raw 264.7 macrophages were seeded in the transwell inserts (Falcon). After overnight incubation in a humidified incubator operating at 37 °C and 5% CO_2, the transwell inserts containing macrophages were washed and placed in the wells containing cancer cells. The cancer cells and macrophages were co-cultured for 48 hrs, after which the transwell inserts containing macrophages were discard, and cancer cell lysates were collected for western blot analysis. In some experiments, both cancer cells and macrophages were cultured in 2.5 mg/mL rat-tail collagen I ECM (BD Bioscience). As appropriate, the co-cultures were treated with 2 μg/mL anti-mouse TNFα antibody (R&D), 10 μg/mL anti-mouse TGFβ1 antibody (Thermo), 2 μg/mL goat IgG isotype control (R&D), or 10 μg/mL rabbit IgG isotype control (Thermo).

Treatment of cancer cells for western blot analysis

MDA-MB-231 and MDA-MB-435S cancer cells were treated with conditioned media collected from Raw 264.7 macrophages. Briefly, 1,375,000 Raw 264.7 macrophages were cultured and the conditioned media was collected. 500,000 of cancer cells were treated with the conditioned media from macrophages for 48 hrs, and cancer cell lysates were collected for western blot analysis. In some experiments, both cancer cells and macrophages were cultured in 2.5 mg/mL rat-tail collagen I ECM (BD Bioscience) as before.

To assess the effects of TNFα and TGFβ1 on cancer cell expression of MT1-MMP and MMP1, 50,000 MDA-MB-231, PC3, or MDA-MB-435S cancer cells were treated with 5-10 ng/mL of TNFα and/or 5-10 ng/mL of TGFβ1 for 24-48 hrs. The cancer cell lysates were collected for qRT-PCR and western blot analyses. To assess the effects of TNFα and TGFβ1 on cancer cell secretion of MMP1, 50,000 MDA231 cells were cultured in DMEM supplemented with bovine serum albumin (BSA, Sigma) instead of FBS. After 48 hrs of treatment with TNFα and/or TGFβ1, the conditioned media was collected for western blot analysis. In some experiments, cancer cells were cultured in 2.5 mg/mL rat-tail collagen I ECM (BD Bioscience).

Protein isolation and western blot analysis

In some experiments, the cellular lysates were extracted from cells cultured inside a collagen I ECM. To extract lysates from these samples, the collagen gel containing the cells was transferred to an Eppendorf tube. RIPA buffer containing protease inhibitors was added, and the cell-gel mixture was mechanically homogenized using a 1-mL

syringe. The samples were incubated on ice for at least 30 mins, after which the lysates in the supernatant were separated from the ECM via a centrifuge.

The nitrocellulose membranes were probed with mouse anti-MMP1 antibody (R&D, clone#36665) at 1:250, rabbit anti-MT1-MMP antibody (Cell Signaling, clone#D1E4) at 1:500, rabbit anti-NF-κB p65 antibody (Millipore) at 1:2000, rabbit anti-β actin antibody (Sigma) at 1:20,000, mouse anti-β actin antibody (Thermo, clone#BA3R) at 1:20,000, mouse anti-GAPDH antibody (Thermo, clone#GA1R) at 1:20,000, or mouse anti-Lamin B1 antibody (Invitrogen, clone#L-5) at 1:500. Following the primary antibody incubation, the membranes were incubated with appropriate secondary antibodies conjugated to horseradish peroxidase (Cell Signaling). The immunoreactive bands were detected with ECL Chemiluminescent substrate (Invitrogen). Densitometry analysis was performed using Alpha Innotech software (Alpha Innotech) to quantify western blot data. β-actin, GAPDH, or Lamin B1 was used as loading control. The nuclear fraction and the cytoplasmic fraction of the cells were extracted using NE-PER Nuclear and Cytoplasmic Extraction Reagents (Thermo) according to manufacturer's protocol.

Total RNA extraction and mRNA detection

The sequences of primers used were as follows: MMP-1-F CATGCTTTTCAACCAGGCCC; MMP-1-R GTCCAAGAGAATGGCCGAGT; MT1-MMP-F GTGGTCTCGGACCATGTCTC; MT1-MMP-R AGCCATATTGCTGTAGCCAGG; GAPDH-F CCACATCGCTCAGACACCAT; and GAPDH-R ACCAGAGTTAAAAGCAGCCCT.

In vivo metastasis assay

Spontaneous metastasis formation was assayed by transplanting 4T1 murine mammary carcinoma cells (ATCC) into the mammary fat pad of 7-week-old female BALB/C mice (Taconic). Mice were anesthetized through inhalation of 3% isoflurane, followed by IP injection of 100 μl of 12 μg/ml buprenorphine for analgesia. A small incision was made in the right flank, and 2.5 x 10^5 cells in 25 μl of HBSS were injected into the right number four fat pad. Mice received three additional IP injections of 100 μl of 12 μg/ml buprenorphine at 12-hr intervals following the surgery. Twice weekly, each mouse was given 100 μl IP injections of PBS (vehicle control), 250 μg anti-TNF-α antibody (Bio X Cell), 250 μg anti-TGF-β1 antibody (Bio X Cell), or 250 μg each of both antibodies. After four weeks, the animals were sacrificed and the lungs were inflated and fixed in 3.8% (wt/vol) formaldehyde for 24 hrs, then embedded in paraffin and sectioned. Area of the metastatic lesion in lungs was quantified using Image J (NIH) following H&E staining. This area was normalized to the total area of the lung to calculate % metastatic burden. All animal care and experimental procedures were performed according to approved institutional guidelines and protocols.

Appendix B: Supplementary Materials and Methods for Chapter 4

Reagents used for transwell flow assay

When appropriate, macrophages in the transwell chambers were treated with 5 μM ruxolitinib (Invivogen), 20 μM PP2 (Abcam), 15 μg/mL anti-mouse β1 integrin antibody (Clone#HMb1-1, ebioscience), 15 μg/mL IgG isotype control antibody (Clone#299Arm, ebioscience), or dimethyl sulfoxide (DMSO, Sigma).

Immunofluorescent staining and confocal microscopy

4% para-formaldehyde (PFA, EMS) was perfused into the microfluidic devices to fix the cells in the collagen I ECM. To visualize the nucleus, the cells were stained with DAPI (diamidino-2-phenylindole, Sigma). The cells were also stained with Alexa-fluor 488 conjugated phalloidin (Invitrogen) to visualize actin. Confocal microscopy images of the cells were taken with Olympus confocal microscope fitted with a camera.

The confocal images were analyzed to quantify the distribution of the actin inside the macrophages as describe previously (2). Mid-plane of the cell was selected for image analysis. The image of the cell was divided at the centroid using an Image J script. The average fluorescent intensities of the actin at the upstream $<I_{up}>$ and downstream $<I_{down}>$ sides of the cell were calculated. The actin distribution score (ADS) for each cell was quantified using the following formula:

$$ADS = \frac{< I_{up} > - < I_{down} >}{\frac{< I_{up} > + < I_{down} >}{2}}$$

Additionally, the same confocal images were analyzed to quantify the distribution of the protrusion as describe in previous studies (2). The image of the cell was divided at the centroid as before. The perimeters of the upstream side (P_{up}) and the downstream side (P_{down}) were quantified using Image J. The protrusion distribution score (PDS) of each cell was calculated as:

$$PDS = \frac{P_{up} - P_{down}}{\frac{P_{up} + P_{down}}{2}}$$

To test the effects of IF on the macrophage viability, Raw macrophages were first treated with IF (~3 μm/s) for 48 hrs in the microfluidic device. Cell viability was subsequently assessed using live/dead viability kit (Invitrogen) according to the manufacturer's protocol.

Protein isolation and western blot analysis

Protein was extracted from the cells in the transwell flow chamber. Collagen I gel containing cells was washed two times with ice-cold 1X PBS and transferred into an Eppendorf tube. RIPA buffer (Cell Signaling) containing protease inhibitor (Sigma) and PMSF (Cell Signaling) was used to extract the cell lysates. A syringe was used to homogenize the gel to facilitate lysate extraction. We quantified the total protein concentration using BCA protein assay kit (Pierce) according to manufacturer's protocol. Equal amount of the total protein (30 μg-60 μg) was resolved on 4-12% NuPAGE electrophoresis gels (Invitrogen) and subsequently transferred onto nitrocellulose membranes (BioRad). The membranes were probed with rabbit anti-arginase I antibody (Thermo) at 1:1000, rabbit anti-TGFβ antibody (Cell Signaling) at 1:1000, mouse anti-iNOS antibody (Cell Signaling) at 1:500, rabbit anti-phospho STAT3 (Serine 727) antibody (Cell Signaling) at 1:600, rabbit anti-phospho STAT3 (Tyrosine 705) antibody (Cell Signaling, Clone#D3A7) at 1:600, rabbit anti-phospho Akt (Serine 473) antibody (Cell Signaling) at 1:1000, rabbit anti-phospho FAK (Tyrosine 397) antibody (Cell Signaling) at 1:1000, rabbit anti-phospho STAT6 (Tyrosine 641) antibody (Abcam) at 1:1000, rabbit anti-phospho STAT1 (Tyrosine 701) antibody (Cell Signaling, Clone#D4A7) at 1:500, mouse anti-STAT3 antibody (Cell Signaling, Clone#124H6) at 1:1000, rabbit anti-STAT6 antibody (Cell Signaling, Clone#D3H4) at 1:1000, mouse anti-Akt antibody (Cell Signaling, Clone#40D4) at 1:1000, rabbit anti-FAK antibody (Cell Signaling) at 1:1000, rabbit anti-STAT1 antibody (Cell Signaling) at 1:1000, mouse anti-β actin antibody (Thermo, clone#BA3R) at 1:20,000, or mouse anti-GAPDH antibody (Thermo, clone#GA1R) at 1:20,000. After the primary antibody incubation, the membranes were incubated with appropriate secondary antibodies conjugated to horseradish peroxidase (Cell Signaling). ECL Chemiluminescent substrate (Invitrogen) was used to detect the immunoreactive band. Densitometry analysis, performed using Alpha Innotech (Alpha Innotech) software, was used to quantify western blot images. β-actin or GAPDH was used as loading control. When appropriate, stripping buffer (Thermo) was used to allow for the re-probing of nitrocellulose membranes.

Cancer cell morphology and migration experiment

800,000 cells/mL of Raw 264.7 were first seeded in a 2.5 mg/mL collagen I gel and then pretreated with IF for 48 hrs using transwell flow chamber. After the flow treatment, the transwell insert containing the macrophages was transferred into a well containing 200,000-300,000 cells/mL of MDA231, MDA435, or Du145 cancer cells so that the macrophages can be co-cultured with cancer cells. After 24-hr co-culture, cancer cells were fixed using 4% PFA and stained with DAPI and Alexa-fluor 488 conjugated phalloidin (Invitrogen). Phase-contrast and fluorescent images of cancer cells were taken using a fluorescent microscope (Nikon) fitted with a camera. The aspect ratio and circularity of cancer cells were quantified using ImageJ (NIH) to assess the morphology of the cells.

800,000 cells/mL of Raw 264.7 were pretreated with IF for 48 hrs using the Transwell flow chamber. After the flow treatment, conditioned media were collected from the transwell. Meanwhile, $1x10^6$ cells/mL of MDA231 GFP cells were seeded inside a 2.5 mg/mL collagen I ECM within a microfluidic device. These MDA231 cells

were treated with the conditioned media from macrophages, and their migration was monitored using a fluorescent microscope (Zeiss) fitted with an environmental chamber operating at 5% CO_2 and 37 °C. Image J (NIH) was used to track cancer cell migration to produce cell trajectory plots. Ibidi Chemotaxis and Migration software (Ibidi) was used to calculate cell migration metrics such as total speed (total distance travelled divided by migration time) and directedness (ratio between the displacement of the cells and distance that cell travelled).

Appendix C: Cell Passage Protocol

Cell should be passaged when they reach 80-90% confluence. It is best to have cells adhered to the plate for 3 days between the passage.

1. Precoat the culture dish with collagen solution for at least 30 min (If HUVECs or HMVECs are used).
2. After 30 min, aspirate the collagen solution, wash the culture dish once with PBS and replace with GM (10 mL for T75 flask). Place in the incubator to warm up. (If HUVECs or HMVECs are used).
3. Meanwhile, warm up media, PBS, and trypsin used for cell passage.
4. Aspirate media from the cells.
5. Add 10 mL of PBS to each T75 flask (5 mL to each T25 flask). Swirl flask to rinse cells. Remove PBS.
6. Add 3 mL of trypsin to each T75 flask (1 mL to each T25 flask). Lay horizontally in the incubator for 5-10 mins.
7. Check via microscope to see if cells have detached.
8. Add 3 to 7 mL of media to each T75 flask to neutralize the trypsin, mix the solution up/down. Pipet trypsin/GM/cell solution from flask into centrifuge tubes. Centrifuge for 5 minutes at 1200 rpm. (4 mL to each T25 flask)
9. Aspirate supernatant off cell pellets in each centrifuge tube.
10. Resuspend cells in desirable amount of growth media depending on the splitting ratio. For new T75 flask, each flask requires 5 mL of resuspension. Resuspend cells by up and down pipetting for at least 10 times.
11. Transfer the cell solution to new flasks.
12. Check under microscope. Label flasks with name, cell type, date, and passage number. Return them to incubator.